Introduction to Molecular Electronics

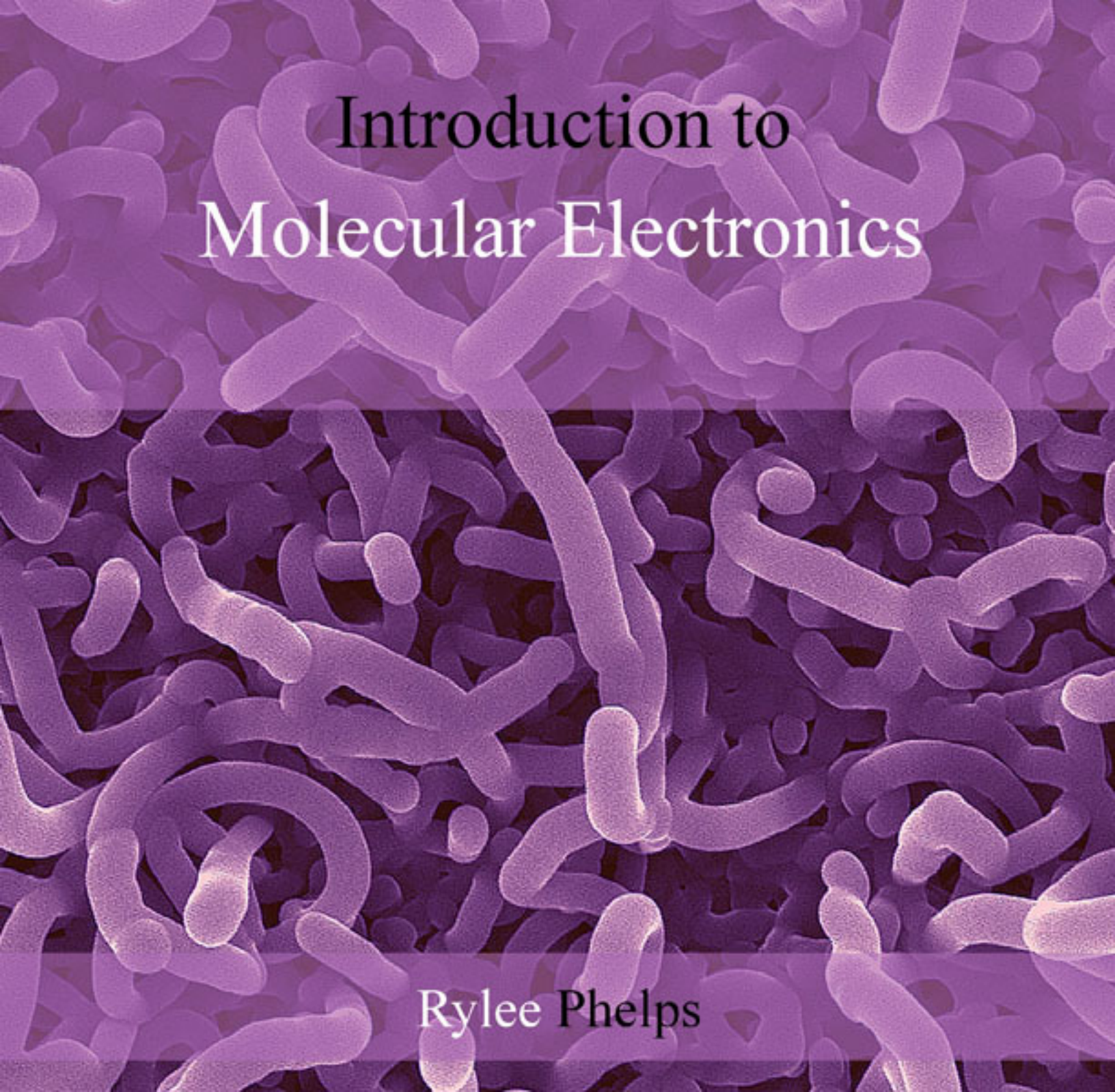

Rylee Phelps

First Edition, 2011

ISBN 978-93-81157-24-4

Published by:
The English Press
4735/22 Prakashdeep Bldg,
Ansari Road, Darya Ganj,
Delhi - 110002
Email: info@wtbooks.com

Table of Contents

Chapter- 1

Introduction to Molecular Electronics

Molecular electronics (sometimes called *moletronics*) involves the study and application of molecular building blocks for the fabrication of electronic components. This includes both passive and active electronic components. Molecular electronics is a branch of nanotechology.

An interdisciplinary pursuit, molecular electronics spans physics, chemistry, and materials science. The unifying feature is the use of molecular building blocks for the fabrication of electronic components. This includes both passive (e.g. resistive wires) and active components such as transistors and molecular-scale switches. Due to the prospect of size reduction in electronics offered by molecular-level control of properties, molecular electronics has aroused much excitement both in science fiction and among scientists. Molecular electronics provides means to extend Moore's Law beyond the foreseen limits of small-scale conventional silicon integrated circuits.

Molecular electronics is split into two related but separate subdisciplines: *molecular materials for electronics* utilizes the properties of the molecules to affect the bulk properties of a material, while *molecular scale electronics* focuses on single-molecule applications.

Concept genesis and theory

In their 1940's discussion of so-called "donor-acceptor" complexes, Robert Mulliken and Albert Szent-Gyorgi advanced the concept of charge transfer in molecules. They subsequently further refined the study of both charge transfer and energy transfer in molecules. Likewise, a 1974 paper from Mark Ratner and Ari Aviram [1] illustrated a theoretical molecular rectifier. In 1988, Aviram described in detail a theoretical single-molecule field-effect transistor. Further concepts were proposed by Forrest Carter of the Naval Research Laboratory, including single-molecule logic gates.

These were all theoretical constructs and not concrete devices. The *direct* measurement of the electronic characteristics of individual molecules awaited the development of methods for making molecular-scale electrical contacts. This was no easy task. Thus, the

first experiment directly-measuring the conductance of a single molecule was only reported in 1997 by Mark Reed and co-workers. Since then, this branch of the field has progressed rapidly. Likewise, as it has become possible to measure such properties directly, the theoretical predictions of the early workers have been substantially confirmed.

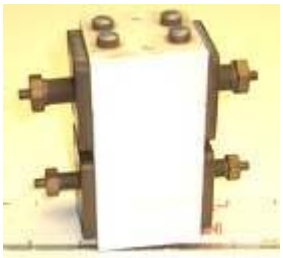

Voltage-controlled switch, a molecular electronic device from 1974. From Smithsonian Chip collection

However, while mostly operating in the quantum realm of less than 100 nanometers, "molecular" electronic processes can collectively manifest on a macro scale. Examples include quantum tunneling, negative resistance, phonon-assisted hopping, polarons, and the like. Thus, macro-scale active organic electronic devices were described decades before molecular-scale ones. E.g., in 1974, John McGinness and his coworkers described the putative "first experimental demonstration of an operating molecular electronic device". This was a voltage-controlled switch. As its active element, this device used DOPA melanin, an oxidized mixed polymer of polyacetylene, polypyrrole, and polyaniline. The "ON" state of this switch exhibited almost metallic conductivity.

Since the 1970s, scientists have developed an entire panoply of new materials and devices. These findings have opened the door to plastic electronics and optoelectronics, which are beginning to find commercial application.

Charge transfer complexes

The first highly-conductive organic compounds were the charge transfer complexes. In 1954, researchers at Bell Labs and elsewhere reported organic charge transfer complexes with resistivities as low as 8 ohms-cm. In the early 1970s, salts of tetrathiafulvalene were shown to exhibit almost metallic conductivity, while superconductivity was demonstrated in 1980. Broad research on charge transfer salts continues today.

Conducting polymers

The linear-backbone "polymer blacks" (polyacetylene, polypyrrole, and polyaniline) and their copolymers are the main class of conductive polymers. Historically, these are known as melanins. In 1963 Australians DE Weiss and coworkers reported iodine-doped oxidized polypyrrole blacks with resistivities as low as 1 ohm/cm. Subsequent papers reported resistances as low as 0.03 Ohm/cm. With the notable exception of Charge

transfer complexes (some of which are even superconductors), organic molecules were previously considered insulators or at best weakly conducting semiconductors.

Over a decade later in 1977, Shirakawa, Heeger, and MacDiarmid reported equivalent high conductivity in rather similarly oxidized and iodine-doped polyacetylene. They later received the 2000 Nobel prize in chemistry "for the discovery and development of conductive polymers". The Nobel citation made no reference to Weiss *et al.'s* similar earlier work.

C_{60} and carbon nanotubes

From graphite to C_{60}

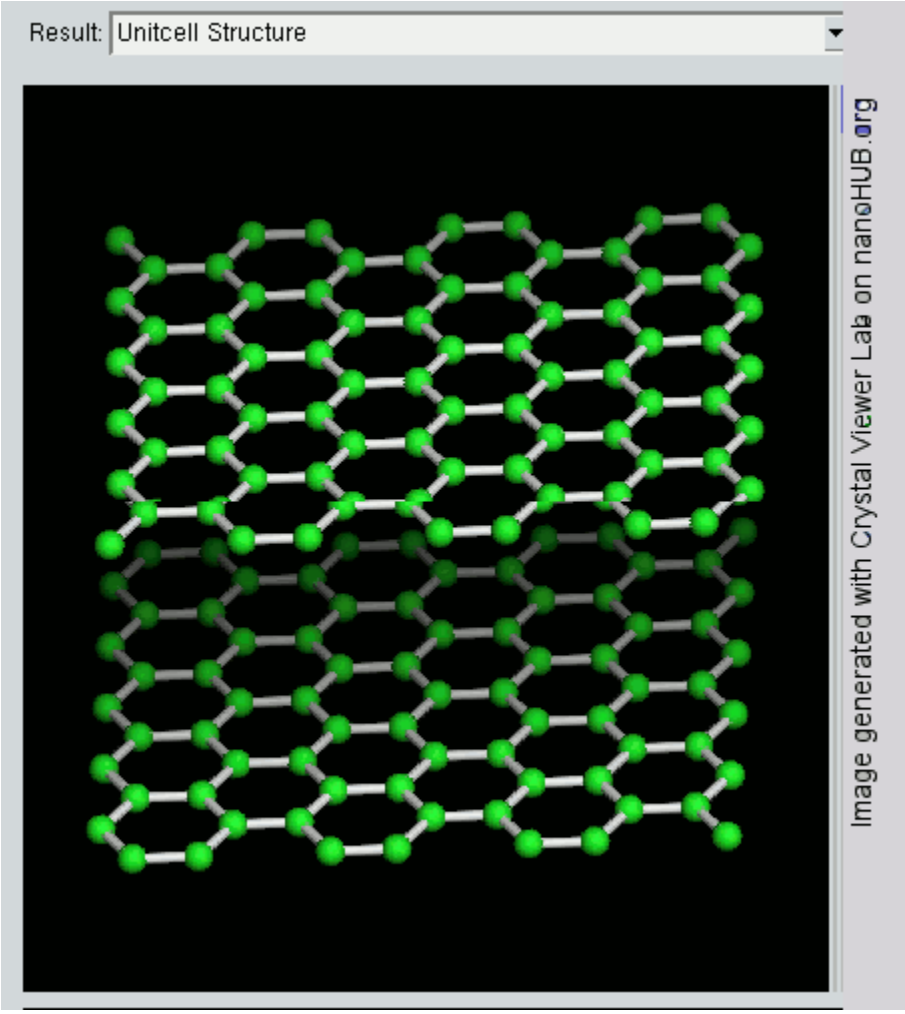

Rotating view of a graphite crystal (2 graphene layers)

In polymers, classical organic molecules are composed of both carbon and hydrogen (and

sometimes additional compounds such as nitrogen, chlorine or sulphur). They are obtained from petrol and can often be synthesized in large amounts. Most of these molecules are insulating when their length exceeds a few nanometers. However, naturally occurring carbon is conducting. In particular, graphite (recovered from coal or encountered naturally) is conducting. From a theoretical point of view, graphite is a semi-metal, a category in between metals and semi-conductors. It has a layered structure, each sheet being one atom thick. Between each sheet, the interactions are weak enough to allow an easy manual cleavage.

Tailoring the graphite sheet to obtain well defined nanometer-sized objects remains a challenge. However, by the close of the twentieth century, chemists were exploring methods to fabricate extremely small graphitic objects that could be considered single molecules. After studying the interstellar conditions under which carbon is known to form clusters, Richard Smalley's group (Rice University, Texas) set up an experiment in which graphite was vaporized using laser irradiation. Mass spectrometry revealed that clusters containing specific "magic numbers" of atoms were stable, in particular those clusters of 60 atoms. Harry Kroto, an English chemist who assisted in the experiment, suggested a possible geometry for these clusters - atoms covalently bound with the exact symmetry of a soccer ball. Coined buckminsterfullerenes, buckyballs or C_{60}, the clusters retained some properties of graphite, such as conductivity. These objects were rapidly envisioned as possible building blocks for molecular electronics.

Carbon nanotubes

Carbon nanotube

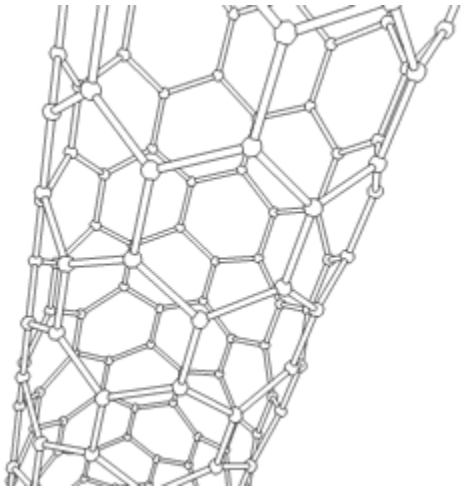

Carbon nanotubes (**CNTs**; also known as **buckytubes**), not to be confused with Carbon Fiber, are allotropes of carbon with a cylindrical nanostructure. Nanotubes have been constructed with length-to-diameter ratio of up to 132,000,000:1, significantly larger than any other material. These cylindrical carbon molecules have novel properties, making

them potentially useful in many applications in nanotechnology, electronics, optics, and other fields of materials science, as well as potential uses in architectural fields. They may also have applications in the construction of body armor. They exhibit extraordinary strength and unique electrical properties, and are efficient thermal conductors.

Nanotubes are members of the fullerene structural family, which also includes the spherical buckyballs. The ends of a nanotube may be capped with a hemisphere of the buckyball structure. Their name is derived from their size, since the diameter of a nanotube is on the order of a few nanometers (approximately 1/50,000th of the width of a human hair), while they can be up to 18 centimeters in length (as of 2010). Nanotubes are categorized as single-walled nanotubes (SWNTs) and multi-walled nanotubes (MWNTs).

Applied quantum chemistry, specifically, orbital hybridization best describes chemical bonding in nanotubes. The chemical bonding of nanotubes is composed entirely of sp^2 bonds, similar to those of graphite. These bonds, which are stronger than the sp^3 bonds found in alkanes, provide nanotubules with their unique strength. Moreover, nanotubes naturally align themselves into "ropes" held together by van der Waals forces.

Most single-walled nanotubes (SWNT) have a diameter of close to 1 nanometer, with a tube length that can be many millions of times longer. The structure of a SWNT can be conceptualized by wrapping a one-atom-thick layer of graphite called graphene into a seamless cylinder. The way the graphene sheet is wrapped is represented by a pair of indices (n,m) called the chiral vector. The integers n and m denote the number of unit vectors along two directions in the honeycomb crystal lattice of graphene. If $m = 0$, the nanotubes are called "zigzag". If $n = m$, the nanotubes are called "armchair". Otherwise, they are called "chiral". The diameter of a nanotube can be calculated from its (n,m) indices as follows

$$d = \frac{a}{\pi}\sqrt{(n^2 + nm + m^2)}.$$

where $a = 0.246$ nm.

Single-walled nanotubes are an important variety of carbon nanotube because they exhibit electric properties that are not shared by the multi-walled carbon nanotube (MWNT) variants. In particular, their band gap can vary from zero to about 2 eV and their electrical conductivity can show metallic or semiconducting behavior, whereas MWNTs are zero-gap metals. Single-walled nanotubes are the most likely candidate for miniaturizing electronics beyond the micro electromechanical scale currently used in electronics. The most basic building block of these systems is the electric wire, and SWNTs can be excellent conductors. One useful application of SWNTs is in the development of the first intramolecular field effect transistors (FET). Production of the first intramolecular logic gate using SWNT FETs has recently become possible as well. To create a logic gate you must have both a p-FET and an n-FET. Because SWNTs are p-FETs when exposed to oxygen and n-FETs otherwise, it is possible to protect half of an SWNT from oxygen exposure, while exposing the other half to oxygen. This results in a

single SWNT that acts as a NOT logic gate with both p and n-type FETs within the same molecule.

Single-walled nanotubes are dropping precipitously in price, from around $1500 per gram as of 2000 to retail prices of around $50 per gram of as-produced 40–60% by weight SWNTs as of March 2010.

Multi-walled

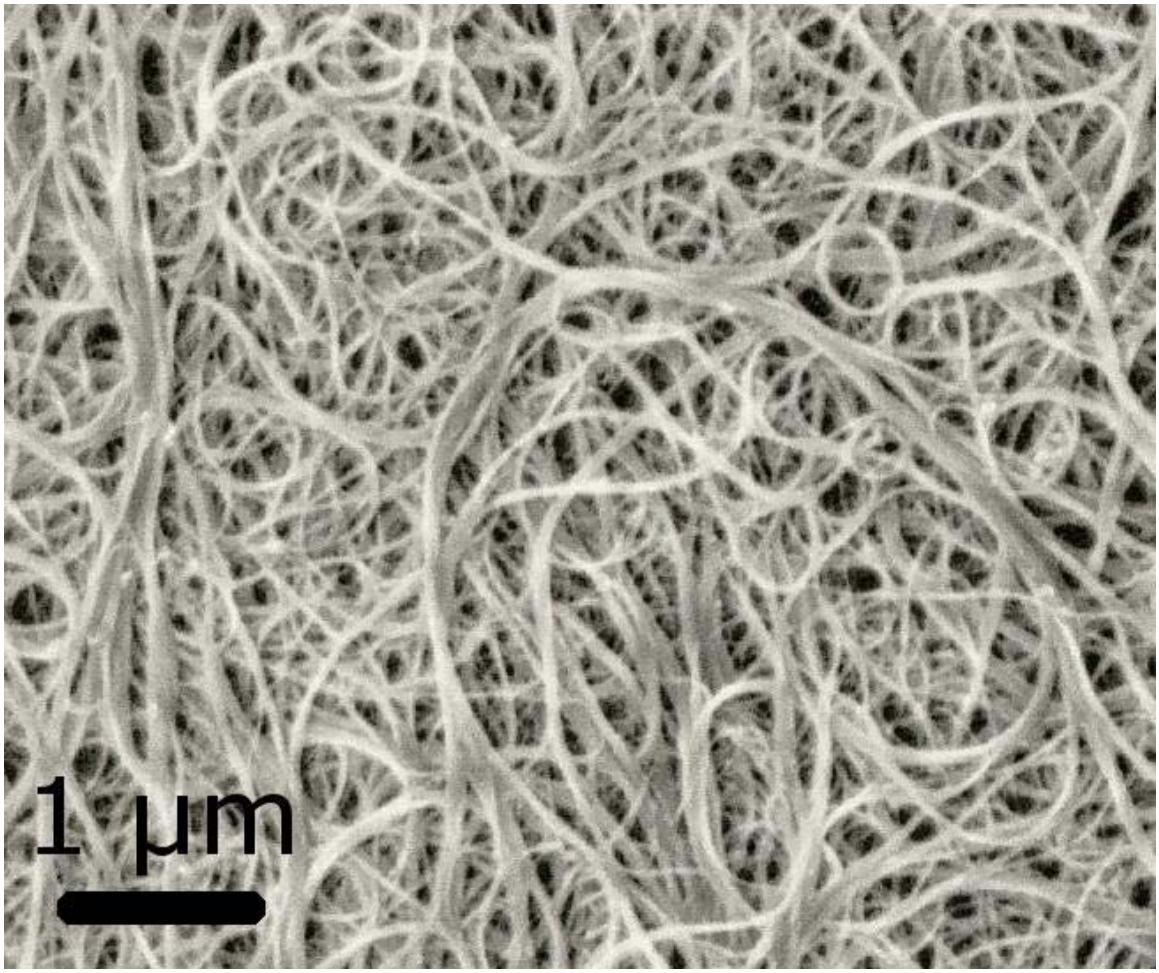

SEM image of carbon nanotubes bundles.

Multi-walled nanotubes (MWNT) consist of multiple rolled layers (concentric tubes) of graphite. There are two models which can be used to describe the structures of multi-walled nanotubes. In the *Russian Doll* model, sheets of graphite are arranged in concentric cylinders, e.g. a (0,8) single-walled nanotube (SWNT) within a larger (0,17) single-walled nanotube. In the *Parchment* model, a single sheet of graphite is rolled in around itself, resembling a scroll of parchment or a rolled newspaper. The interlayer distance in multi-walled nanotubes is close to the distance between graphene layers in graphite, approximately 3.4 Å.

The special place of double-walled carbon nanotubes (DWNT) must be emphasized here because their morphology and properties are similar to SWNT but their resistance to chemicals is significantly improved. This is especially important when functionalization is required (this means grafting of chemical functions at the surface of the nanotubes) to add new properties to the CNT. In the case of SWNT, covalent functionalization will break some C=C double bonds, leaving "holes" in the structure on the nanotube and thus modifying both its mechanical and electrical properties. In the case of DWNT, only the outer wall is modified. DWNT synthesis on the gram-scale was first proposed in 2003 by the CCVD technique, from the selective reduction of oxide solutions in methane and hydrogen.

Torus

A stable nanobud structure

In theory, a nanotorus is a carbon nanotube bent into a torus (doughnut shape). Nanotori are predicted to have many unique properties, such as magnetic moments 1000 times larger than previously expected for certain specific radii. Properties such as magnetic moment, thermal stability, etc. vary widely depending on radius of the torus and radius of the tube.

Nanobud

Carbon nanobuds are a newly created material combining two previously discovered allotropes of carbon: carbon nanotubes and fullerenes. In this new material, fullerene-like "buds" are covalently bonded to the outer sidewalls of the underlying carbon nanotube. This hybrid material has useful properties of both fullerenes and carbon nanotubes. In particular, they have been found to be exceptionally good field emitters. In composite materials, the attached fullerene molecules may function as molecular anchors preventing slipping of the nanotubes, thus improving the composite’s mechanical properties.

Cup stacked carbon nanotubes

Cup-stacked carbon nanotubes (CSCNTs) differ from other quasi-1D carbon structures, which normally behave as quasi-metallic conductors of electrons. CSCNTs exhibit semiconducting behaviors due to the stacking microstructure of graphene layers.

Extreme carbon nanotubes

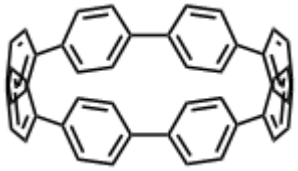

Cycloparaphenylene

The observation of the *longest* carbon nanotubes (18.5 cm long) was reported in 2009. These nanotubles were grown on Si substrates using an improved chemical vapor deposition (CVD) method and represent electrically uniform arrays of single-walled carbon nanotubes.

The *shortest* carbon nanotube is the organic compound cycloparaphenylene which was synthesized in early 2009.

The *thinnest* carbon nanotube is armchair (2,2) CNT with a diameter of 3 Å. This nanotube was grown inside a multi-walled carbon nanotube. Assigning of carbon nanotube type was done by combination of high-resolution transmission electron microscopy (HRTEM), Raman spectroscopy and density functional theory (DFT) calculations.

The *thinnest freestanding* single-walled carbon nanotube is about 4.3 Å in diameter. Researchers suggested that it can be either (5,1) or (4,2) SWCNT, but exact type of carbon nanotube remains questionable. (3,3), (4,3) and (5,1) carbon nanotubes (all about 4 Å in diameter) were unambiguously identified using more precise aberration-corrected high-resolution transmission electron microscopy. However, they were found inside of double-walled carbon nanotubes.

Properties

Strength

Carbon nanotubes are the strongest and stiffest materials yet discovered in terms of tensile strength and elastic modulus respectively. This strength results from the covalent sp^2 bonds formed between the individual carbon atoms. In 2000, a multi-walled carbon nanotube was tested to have a tensile strength of 63 gigapascals (GPa). (This, for illustration, translates into the ability to endure tension of a weight equivalent to 6422 kg on a cable with cross-section of 1 mm^2.) Since carbon nanotubes have a low density for a solid of 1.3 to 1.4 $g \cdot cm^{-3}$, its specific strength of up to 48,000 $kN \cdot m \cdot kg^{-1}$ is the best of known materials, compared to high-carbon steel's 154 $kN \cdot m \cdot kg^{-1}$.

Under excessive tensile strain, the tubes will undergo plastic deformation, which means the deformation is permanent. This deformation begins at strains of approximately 5%

and can increase the maximum strain the tubes undergo before fracture by releasing strain energy.

CNTs are not nearly as strong under compression. Because of their hollow structure and high aspect ratio, they tend to undergo buckling when placed under compressive, torsional or bending stress.

Comparison of mechanical properties

Material	Young's modulus (TPa)	Tensile strength (GPa)	Elongation at break (%)
SWNT	~1 (from 1 to 5)	13–53[E]	16
Armchair SWNT	0.94[T]	126.2[T]	23.1
Zigzag SWNT	0.94[T]	94.5[T]	15.6–17.5
Chiral SWNT	0.92		
MWNT	0.27[E]–0.8[E]–0.95[E]	11[E]–63[E]–150[E]	
Stainless steel	0.186[E]–0.214[E]	0.38[E]–1.55[E]	15–50
Kevlar–29&149	0.06[E]–0.18[E]	3.6[E]–3.8[E]	~2

[E]Experimental observation; [T]Theoretical prediction

The above discussion referred to axial properties of the nanotube, whereas simple geometrical considerations suggest that carbon nanotubes should be much softer in the radial direction than along the tube axis. Indeed, TEM observation of radial elasticity suggested that even the van der Waals forces can deform two adjacent nanotubes. Nanoindentation experiments, performed by several groups on multiwalled carbon nanotubes, indicated Young's modulus of the order of several GPa confirming that CNTs are indeed rather soft in the radial direction.

Hardness

Diamond is considered to be the hardest material. Under conditions of high temperature and high pressure, graphite transforms into diamond. One study succeeded in the synthesis of a super-hard material by compressing SWNTs to above 24 GPa at *room temperature*. The hardness of this material was measured with a nanoindenter as 62–152 GPa. The hardness of reference diamond and boron nitride samples was 150 and 62 GPa, respectively. The bulk modulus of compressed SWNTs was 462–546 GPa, surpassing the value of 420 GPa for diamond.

Kinetic

Multi-walled nanotubes are multiple concentric nanotubes precisely nested within one another. These exhibit a striking telescoping property whereby an inner nanotube core

may slide, almost without friction, within its outer nanotube shell, thus creating an atomically perfect linear or rotational bearing. This is one of the first true examples of molecular nanotechnology, the precise positioning of atoms to create useful machines. Already, this property has been utilized to create the world's smallest rotational motor. Future applications such as a gigahertz mechanical oscillator are also envisaged.

Electrical

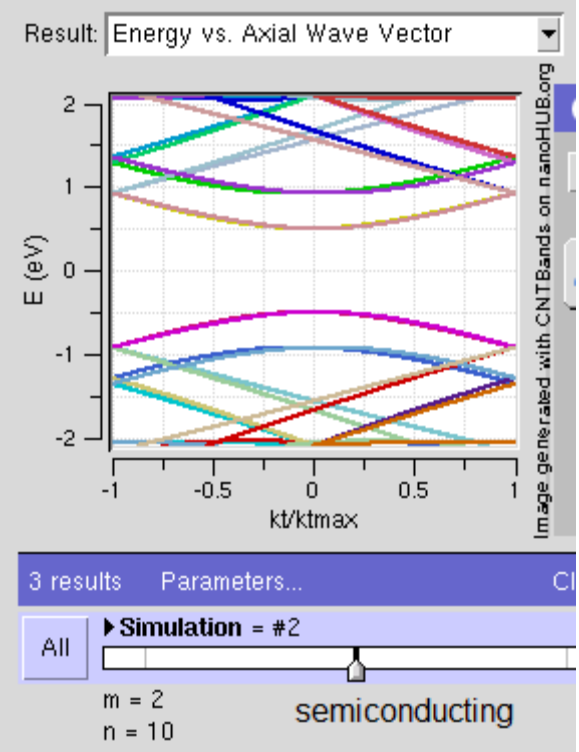

Band structures computed using tight binding approximation for (6,0) CNT (zigzag, metallic) (10,2) CNT (semiconducting) and (10,10) CNT (armchair, metallic).

Because of the symmetry and unique electronic structure of graphene, the structure of a nanotube strongly affects its electrical properties. For a given (n,m) nanotube, if $n = m$, the nanotube is metallic; if $n - m$ is a multiple of 3, then the nanotube is semiconducting with a very small band gap, otherwise the nanotube is a moderate semiconductor. Thus all armchair ($n = m$) nanotubes are metallic, and nanotubes (6,4), (9,1), etc. are semiconducting.

However, this rule has exceptions, because curvature effects in small diameter carbon nanotubes can influence strongly electrical properties. Thus, a (5,0) SWCNT that should be semiconducting in fact is metallic according to the calculations. Likewise, *vice versa*--zigzag and chiral SWCNTs with small diameters that should be metallic have finite gap (armchair nanotubes remain metallic). In theory, metallic nanotubes can carry an electric current density of 4×10^9 A/cm^2 which is more than 1,000 times greater than metals such as copper.

Multiwalled carbon nanotubes with interconnected inner shells show superconductivity with a relatively high transition temperature $T_c = 12$ K. In contrast, the T_c value is an order of magnitude lower for ropes of single-walled carbon nanotubes or for MWNTs with usual, non-interconnected shells.

Optical

Thermal

All nanotubes are expected to be very good thermal conductors along the tube, exhibiting a property known as "ballistic conduction", but good insulators laterally to the tube axis. Measurements show that a SWNT has a room-temperature thermal conductivity along its axis of about 3500 $W \cdot m^{-1} \cdot K^{-1}$; compare this to copper, a metal well-known for its good thermal conductivity, which transmits 385 $W \cdot m^{-1} \cdot K^{-1}$. A SWNT has a room-temperature thermal conductivity across its axis (in the radial direction) of about 1.52 $W \cdot m^{-1} \cdot K^{-1}$, which is about as thermally conductive as soil. The temperature stability of carbon nanotubes is estimated to be up to 2800 °C in vacuum and about 750 °C in air.

Defects

As with any material, the existence of a crystallographic defect affects the material properties. Defects can occur in the form of atomic vacancies. High levels of such defects can lower the tensile strength by up to 85%. Another form of carbon nanotube defect is the Stone Wales defect, which creates a pentagon and heptagon pair by rearrangement of the bonds. Because of the very small structure of CNTs, the tensile strength of the tube is dependent on its weakest segment in a similar manner to a chain, where the strength of the weakest link becomes the maximum strength of the chain.

Crystallographic defects also affect the tube's electrical properties. A common result is lowered conductivity through the defective region of the tube. A defect in armchair-type tubes (which can conduct electricity) can cause the surrounding region to become semiconducting, and single monoatomic vacancies induce magnetic properties.

Crystallographic defects strongly affect the tube's thermal properties. Such defects lead to phonon scattering, which in turn increases the relaxation rate of the phonons. This reduces the mean free path and reduces the thermal conductivity of nanotube structures. Phonon transport simulations indicate that substitutional defects such as nitrogen or boron will primarily lead to scattering of high-frequency optical phonons. However, larger-scale defects such as Stone Wales defects cause phonon scattering over a wide range of frequencies, leading to a greater reduction in thermal conductivity.

One-dimensional transport

Because of the nanoscale dimensions, electrons propagate only along the tube's axis and electron transport involves many quantum effects. Because of this, carbon nanotubes are frequently referred to as “one-dimensional”.

Toxicity

Determining the toxicity of carbon nanotubes has been one of the most pressing questions in nanotechnology. Unfortunately, such research has only just begun. Thus, the data are still fragmentary and subject to criticism. Preliminary results highlight the difficulties in evaluating the toxicity of this heterogeneous material. Parameters such as structure, size distribution, surface area, surface chemistry, surface charge, and agglomeration state as well as purity of the samples, have considerable impact on the reactivity of carbon nanotubes. However, available data clearly show that, under some conditions, nanotubes can cross membrane barriers, which suggests that if raw materials reach the organs they can induce harmful effects such as inflammatory and fibrotic reactions.

A study led by Alexandra Porter from the University of Cambridge shows that CNTs can enter human cells and accumulate in the cytoplasm, causing cell death.

Results of rodent studies collectively show that regardless of the process by which CNTs were synthesized and the types and amounts of metals they contained, CNTs were capable of producing inflammation, epithelioid granulomas (microscopic nodules), fibrosis, and biochemical/toxicological changes in the lungs. Comparative toxicity studies in which mice were given equal weights of test materials showed that SWCNTs were more toxic than quartz, which is considered a serious occupational health hazard when chronically inhaled. As a control, ultrafine carbon black was shown to produce minimal lung responses.

The needle-like fiber shape of CNTs, similar to asbestos fibers, raises fears that widespread use of carbon nanotubes may lead to mesothelioma, cancer of the lining of the lungs often caused by exposure to asbestos. A recently-published pilot study supports this prediction. Scientists exposed the mesothelial lining of the body cavity of mice, as a surrogate for the mesothelial lining of the chest cavity, to long multiwalled carbon nanotubes and observed asbestos-like, length-dependent, pathogenic behavior which included inflammation and formation of lesions known as granulomas. Authors of the study conclude:

> "This is of considerable importance, because research and business communities continue to invest heavily in carbon nanotubes for a wide range of products under the assumption that they are no more hazardous than graphite. Our results suggest the need for further research and great caution before introducing such products into the market if long-term harm is to be avoided."

According to co-author Dr. Andrew Maynard:

> "This study is exactly the kind of strategic, highly focused research needed to ensure the safe and responsible development of nanotechnology. It looks at a specific nanoscale material expected to have widespread commercial applications and asks specific questions about a specific health hazard. Even though scientists have been raising concerns about the safety of long, thin carbon nanotubes for

over a decade, none of the research needs in the current U.S. federal nanotechnology environment, health and safety risk research strategy address this question."

Although further research is required, results presented today clearly demonstrate that, under certain conditions, especially those involving chronic exposure, carbon nanotubes can pose a serious risk to human health.

Synthesis

Powder of carbon nanotubes

Techniques have been developed to produce nanotubes in sizeable quantities, including arc discharge, laser ablation, high pressure carbon monoxide (HiPco), and chemical vapor deposition (CVD). Most of these processes take place in vacuum or with process gases. CVD growth of CNTs can occur in vacuum or at atmospheric pressure. Large quantities of nanotubes can be synthesized by these methods; advances in catalysis and continuous growth processes are making CNTs more commercially viable.

Arc discharge

Nanotubes were observed in 1991 in the carbon soot of graphite electrodes during an arc discharge, by using a current of 100 amps, that was intended to produce fullerenes. However the first macroscopic production of carbon nanotubes was made in 1992 by two researchers at NEC's Fundamental Research Laboratory. The method used was the same as in 1991. During this process, the carbon contained in the negative electrode sublimates because of the high discharge temperatures. Because nanotubes were initially discovered using this technique, it has been the most widely-used method of nanotube synthesis.

The yield for this method is up to 30 percent by weight and it produces both single- and multi-walled nanotubes with lengths of up to 50 micrometers with few structural defects.

Laser ablation

In the laser ablation process, a pulsed laser vaporizes a graphite target in a high-temperature reactor while an inert gas is bled into the chamber. Nanotubes develop on the cooler surfaces of the reactor as the vaporized carbon condenses. A water-cooled surface may be included in the system to collect the nanotubes.

This process was developed by Dr. Richard Smalley and co-workers at Rice University, who at the time of the discovery of carbon nanotubes, were blasting metals with a laser to produce various metal molecules. When they heard of the existence of nanotubes they replaced the metals with graphite to create multi-walled carbon nanotubes. Later that year the team used a composite of graphite and metal catalyst particles (the best yield was from a cobalt and nickel mixture) to synthesize single-walled carbon nanotubes.

The laser ablation method yields around 70% and produces primarily single-walled carbon nanotubes with a controllable diameter determined by the reaction temperature. However, it is more expensive than either arc discharge or chemical vapor deposition.

Chemical vapor deposition (CVD)

Nanotubes being grown by plasma enhanced chemical vapor deposition

The catalytic vapor phase deposition of carbon was first reported in 1959, but it was not until 1993 that carbon nanotubes were formed by this process. In 2007, researchers at the University of Cincinnati (UC) developed a process to grow aligned carbon nanotube arrays of 18 mm length on a FirstNano ET3000 carbon nanotube growth system.

During CVD, a substrate is prepared with a layer of metal catalyst particles, most commonly nickel, cobalt, iron, or a combination. The metal nanoparticles can also be produced by other ways, including reduction of oxides or oxides solid solutions. The diameters of the nanotubes that are to be grown are related to the size of the metal particles. This can be controlled by patterned (or masked) deposition of the metal, annealing, or by plasma etching of a metal layer. The substrate is heated to approximately

700°C. To initiate the growth of nanotubes, two gases are bled into the reactor: a process gas (such as ammonia, nitrogen or hydrogen) and a carbon-containing gas (such as acetylene, ethylene, ethanol or methane). Nanotubes grow at the sites of the metal catalyst; the carbon-containing gas is broken apart at the surface of the catalyst particle, and the carbon is transported to the edges of the particle, where it forms the nanotubes. This mechanism is still being studied. The catalyst particles can stay at the tips of the growing nanotube during the growth process, or remain at the nanotube base, depending on the adhesion between the catalyst particle and the substrate. Thermal catalytic decomposition of hydrocarbon has become an active area of research and can be a promising route for the bulk production of CNTs. Fluidised bed reactor is the most widely used reactor for CNT preparation. Scale-up of the reactor is the major challenge.

CVD is a common method for the commercial production of carbon nanotubes. For this purpose, the metal nanoparticles are mixed with a catalyst support such as MgO or Al_2O_3 to increase the surface area for higher yield of the catalytic reaction of the carbon feedstock with the metal particles. One issue in this synthesis route is the removal of the catalyst support via an acid treatment, which sometimes could destroy the original structure of the carbon nanotubes. However, alternative catalyst supports that are soluble in water have proven effective for nanotube growth.

If a plasma is generated by the application of a strong electric field during the growth process (plasma enhanced chemical vapor deposition*), then the nanotube growth will follow the direction of the electric field. By adjusting the geometry of the reactor it is possible to synthesize vertically aligned carbon nanotubes (i.e., perpendicular to the substrate), a morphology that has been of interest to researchers interested in the electron emission from nanotubes. Without the plasma, the resulting nanotubes are often randomly oriented. Under certain reaction conditions, even in the absence of a plasma, closely spaced nanotubes will maintain a vertical growth direction resulting in a dense array of tubes resembling a carpet or forest.

Of the various means for nanotube synthesis, CVD shows the most promise for industrial-scale deposition, because of its price/unit ratio, and because CVD is capable of growing nanotubes directly on a desired substrate, whereas the nanotubes must be collected in the other growth techniques. The growth sites are controllable by careful deposition of the catalyst. In 2007, a team from Meijo University demonstrated a high-efficiency CVD technique for growing carbon nanotubes from camphor. Researchers at Rice University, until recently led by the late Richard Smalley, have concentrated upon finding methods to produce large, pure amounts of particular types of nanotubes. Their approach grows long fibers from many small seeds cut from a single nanotube; all of the resulting fibers were found to be of the same diameter as the original nanotube and are expected to be of the same type as the original nanotube.

Super-growth CVD

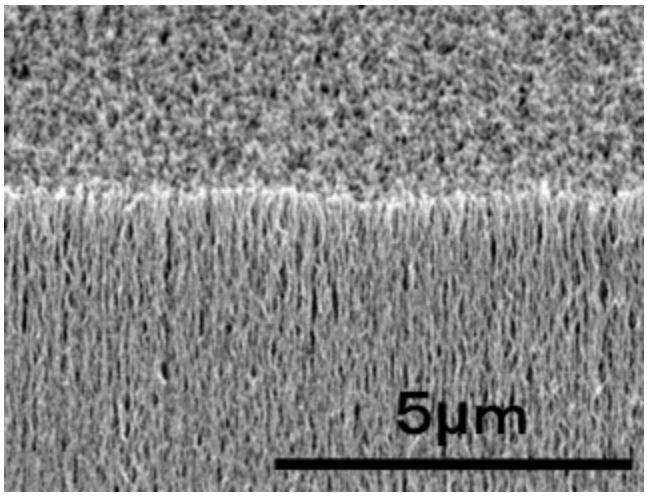

SEM photo of SWNT forests produced by super-growth

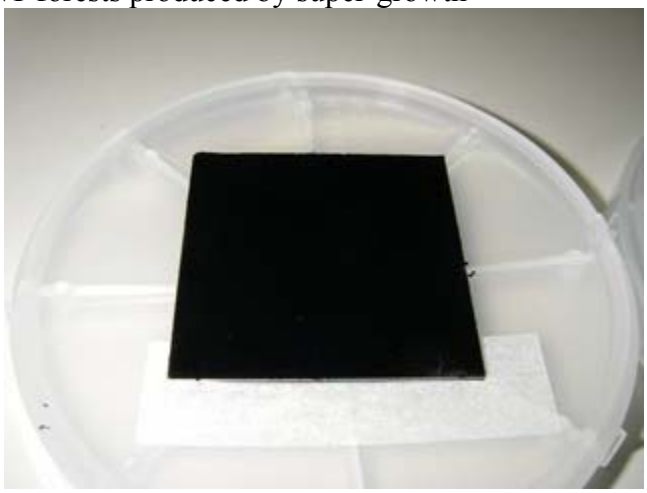

A small SWNT sample produced by super-growth

Super-growth CVD (water-assisted chemical vapour deposition) process was developed by Kenji Hata, Sumio Iijima and co-workers at AIST, Japan. In this process, the activity and lifetime of the catalyst are enhanced by addition of water into the CVD reactor. Dense millimeter-tall nanotube "forests", aligned normal to the substrate, were produced. The forests growth rate could be expressed, as

$$H(t) = \beta\tau_o(1 - e^{-t/\tau_o}).$$

In this equation, β is the initial growth rate and τ_o is the characteristic catalyst lifetime.

Their specific surface exceeds 1,000 m^2/g (capped) or 2,200 m^2/g (uncapped), surpassing the value of 400–1,000 m^2/g for HiPco samples. The synthesis efficiency is about 100 times higher than for the laser ablation method. The time required to make SWNT forests of the height of 2.5 mm by this method was 10 minutes in 2004. Those SWNT forests can be easily separated from the catalyst, yielding clean SWNT material (purity >99.98%)

without further purification. For comparison, the as-grown HiPco CNTs contain about 5-35% of metal impurities; it is therefore purified through dispersion and centrifugation that damages the nanotubes. The super-growth process avoids this problem. Patterned highly organized single-walled nanotube structures were successfully fabricated using the super-growth technique.

The mass density of super-growth CNTs is about 0.037 g/cm^3. It is much lower than that of conventional CNT powders (~1.34 g/cm^3), probably because the latter contain metals and amorphous carbon.

The super-growth method is basically a variation of CVD. Therefore, it is possible to grow material containing SWNT, DWNTs and MWNTs, and to alter their ratios by tuning the growth conditions. Their ratios change by the thinness of the catalyst. Many MWNTs are included so that the diameter of the tube is wide.

The vertically aligned nanotube forests originate from a "zipping effect" when they are immersed in a solvent and dried. The zipping effect is caused by the surface tension of the solvent and the van der Waals forces between the carbon nanotubes. It aligns the nanotubes into a dense material, which can be formed in various shapes, such as sheets and bars, by applying weak compression during the process. Densification increases the Vickers hardness by about 70 times and density is 0.55 g/cm^3. The packed carbon nanotubes are more than 1 mm long and have a carbon purity of 99.9% or higher; they also retain the desirable alignment properties of the nanotubes forest.

Natural, incidental, and controlled flame environments

Fullerenes and carbon nanotubes are not necessarily products of high-tech laboratories; they are commonly formed in such mundane places as ordinary flames, produced by burning methane, ethylene, and benzene, and they have been found in soot from both indoor and outdoor air. However, these naturally occurring varieties can be highly irregular in size and quality because the environment in which they are produced is often highly uncontrolled. Thus, although they can be used in some applications, they can lack in the high degree of uniformity necessary to satisfy the many needs of both research and industry. Recent efforts have focused on producing more uniform carbon nanotubes in controlled flame environments. Such methods have promise for large-scale, low-cost nanotube synthesis, though they must compete with rapidly developing large scale CVD production.

Application related issues

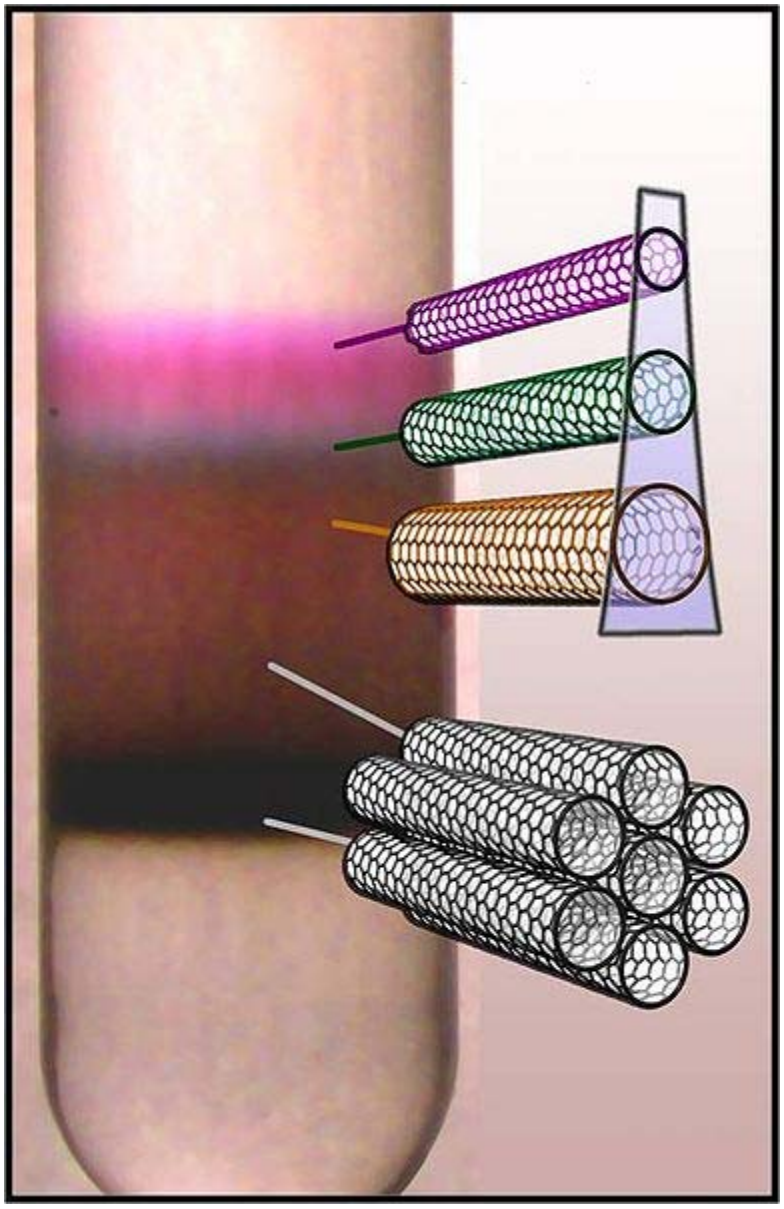

Centrifuge tube with a solution of carbon nanotubes, which were sorted by diameter using density-gradient ultracentrifugation.

Many electronic applications of carbon nanotubes crucially rely on techniques of selectively producing either semiconducting or metallic CNTs, preferably of a certain chirality. Several methods of separating semiconducting and metallic CNTs are known, but most of them are not yet suitable for large-scale technological processes. The most efficient method relies on density-gradient ultracentrifugation which separates surfactant-wrapped nanotubes by the minute difference in their density. This density difference often translates into difference in the nanotube diameter and (semi)conducting properties. Another method of separation uses a sequence of freezing, thawing, and compression of SWNTs embedded in agarose gel. This process results in a solution containing 70% metallic SWNTs and leaves a gel containing 95% semiconducting SWNTs. The diluted

solutions separated by this method show various colors. Moreover, SWNTs can be separated by the column chromatography method. Yield is 95% in semiconductor type SWNT and 90% in metallic type SWNT.

In addition to separation of semiconducting and metallic SWNTs, it is possible to sort SWNTs by length, diameter, and chirality. The highest resolution length sorting, with length variation of <10%, has thus far been achieved by size exclusion chromatography (SEC) of DNA-dispersed carbon nanotubes (DNA-SWNT). SWNT diameter separation has been achieved by density-gradient ultracentrifugation (DGU) using surfactant-dispersed SWNTs and by ion-exchange chromatography (IEC) for DNA-SWNT. Purification of individual chiralities has also been demonstrated with IEC of DNA-SWNT: specific short DNA oligomers can be used to isolate individual SWNT chiralities. Thus far, 12 chiralities have been isolated at purities ranging from 70% for (8,3) and (9,5) SWNTs to 90% for (6,5), (7,5) and (10,5)SWNTs. There have been successful efforts to integrate these purified nanotubes into devices, e. g. FETs.

An alternative to separation is development of a selective growth of semiconducting or metallic CNTs. Recently, a new CVD recipe was announced which involves a combination of ethanol and methanol gases and quartz substrates resulting in horizontally aligned arrays of 95–98% semiconducting nanotubes.

Nanotubes are usually grown on nanoparticles of magnetic metal (Fe, Co), which facilitates production of electronic (spintronic) devices. In particular control of current through a field-effect transistor by magnetic field has been demonstrated in such a single-tube nanostructure.

Current applications

Current use and application of nanotubes has mostly been limited to the use of bulk nanotubes, which is a mass of rather unorganized fragments of nanotubes. Bulk nanotube materials may never achieve a tensile strength similar to that of individual tubes, but such composites may nevertheless yield strengths sufficient for many applications. Bulk carbon nanotubes have already been used as composite fibers in polymers to improve the mechanical, thermal and electrical properties of the bulk product.

Easton-Bell Sports, Inc. have been in partnership with Zyvex Performance Materials, using CNT technology in a number of their bicycle components—including flat and riser handlebars, cranks, forks, seatposts, stems and aero bars.

Zyvex Performance Materials has also built a 54' maritime vessel, the Piranha Unmanned Surface Vessel, as a technology demonstrator for what is possible using CNT technology. CNTs help improve the structural performance of the vessel, resulting in a lightweight 8,000lb boat.

Amroy Europe Oy manufactures Hybtonite carbon nanoepoxy resins where carbon nanotubes have been chemically bond to epoxy, resulting composite material that is 20%

to 30% stronger than other composite materials. It has been used for wind turbines, marine paints and variety of sports gear such as skis, ice hockey sticks, baseball bats, hunting arrows and surfboards.

Potential applications

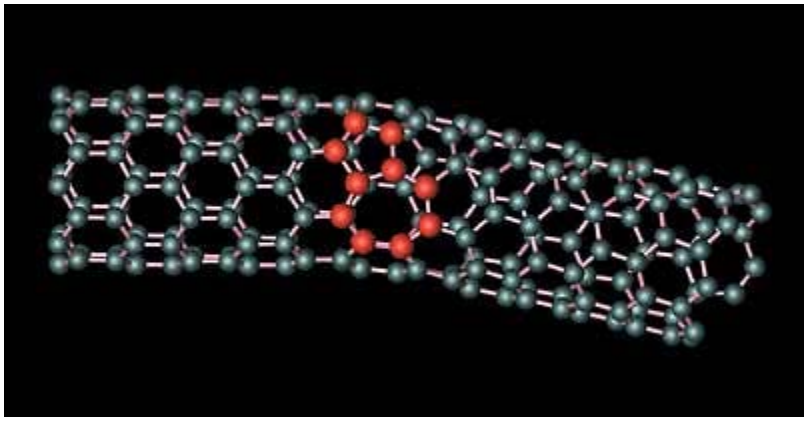

The joining of two carbon nanotubes with different electrical properties to form a diode has been proposed . L Chico et al. Phys Rev Lett 76, 971 (1996)

The strength and flexibility of carbon nanotubes makes them of potential use in controlling other nanoscale structures, which suggests they will have an important role in nanotechnology engineering. The highest tensile strength of an individual multi-walled carbon nanotube has been tested to be is 63 GPa. Carbon nanotubes were found in Damascus steel from the 17th century, possibly helping to account for the legendary strength of the swords made of it.

Structural

Because of the carbon nanotube's superior mechanical properties, many structures have been proposed ranging from everyday items like clothes and sports gear to combat jackets and space elevators. However, the space elevator will require further efforts in refining carbon nanotube technology, as the practical tensile strength of carbon nanotubes can still be greatly improved.

For perspective, outstanding breakthroughs have already been made. Pioneering work led by Ray H. Baughman at the NanoTech Institute has shown that single and multi-walled nanotubes can produce materials with toughness unmatched in the man-made and natural worlds.

Because of the high mechanical strength of carbon nanotubes, research is being made into weaving them into clothes to create stab-proof and bulletproof clothing. The nanotubes would effectively stop the bullet from penetrating the body, although the bullet's kinetic energy would likely cause broken bones and internal bleeding.

In electrical circuits

Nanotube-based transistors, also known as carbon nanotube field-effect transistors (CNFETs), have been made that operate at room temperature and that are capable of digital switching using a single electron. However, one major obstacle to realization of nanotubes has been the lack of technology for mass production. In 2001 IBM researchers demonstrated how metallic nanotubes can be destroyed, leaving semiconducting ones behind for use as transistors. Their process is called "constructive destruction" which includes the automatic destruction of defective nanotubes on the wafer. This process, however, only gives control over the electrical properties on a statistical scale.

The potential of carbon nanotubes was demonstrated in 2003 when room-temperature ballistic transistors with ohmic metal contacts and high-k gate dielectric were reported, showing 20–30x higher ON current than state-of-the-art Si MOSFETs. This presented an important advance in the field as CNT was shown to potentially outperform Si. At the time, a major challenge was ohmic metal contact formation. In this regard, palladium, which is a high work function metal was shown to exhibit Schottky barrier-free contacts to semiconducting nanotubes with diameters >1.7 nm.

The first nanotube integrated memory circuit was made in 2004. One of the main challenges has been regulating the conductivity of nanotubes. Depending on subtle surface features a nanotube may act as a plain conductor or as a semiconductor. A fully automated method has however been developed to remove non-semiconductor tubes.

Another way to make carbon nanotube transistors has been to use random networks of them. By doing so one averages all of their electrical differences and one can produce devices in large scale at the wafer level. This approach was first patented by Nanomix Inc.(date of original application June 2002). It was first published in the academic literature by the United States Naval Research Laboratory in 2003 through independent research work. This approach also enabled Nanomix to make the first transistor on a flexible and transparent substrate.

Large structures of carbon nanotubes can be used for thermal management of electronic circuits. An approximately 1 mm–thick carbon nanotube layer was used as a special material to fabricate coolers, this materials has very low density, ~20 times lower weight than a similar copper structure, while the cooling properties are similar for the two materials.

Overall, incorporating carbon nanotubes as transistors into logic-gate circuits with densities comparable to modern CMOS technology has not yet been demonstrated.

As paper batteries

A paper battery is a battery engineered to use a paper-thin sheet of cellulose (which is the major constituent of regular paper, among other things) infused with aligned carbon nanotubes. The nanotubes act as electrodes; allowing the storage devices to conduct

electricity. The battery, which functions as both a lithium-ion battery and a supercapacitor, can provide a long, steady power output comparable to a conventional battery, as well as a supercapacitor's quick burst of high energy—and while a conventional battery contains a number of separate components, the paper battery integrates all of the battery components in a single structure, making it more energy efficient.

Solar cells

Solar cells developed at the New Jersey Institute of Technology use a carbon nanotube complex, formed by a mixture of carbon nanotubes and carbon buckyballs (known as fullerenes) to form snake-like structures. Buckyballs trap electrons, although they can't make electrons flow. Add sunlight to excite the polymers, and the buckyballs will grab the electrons. Nanotubes, behaving like copper wires, will then be able to make the electrons or current flow.

Ultracapacitors

MIT Laboratory for Electromagnetic and Electronic Systems uses nanotubes to improve ultracapacitors. The activated charcoal used in conventional ultracapacitors has many small hollow spaces of various size, which create together a large surface to store electric charge. But as charge is quantized into elementary charges, i.e. electrons, and each such elementary charge needs a minimum space, a significant fraction of the electrode surface is not available for storage because the hollow spaces are not compatible with the charge's requirements. With a nanotube electrode the spaces may be tailored to size—few too large or too small—and consequently the capacity should be increased considerably.

Other applications

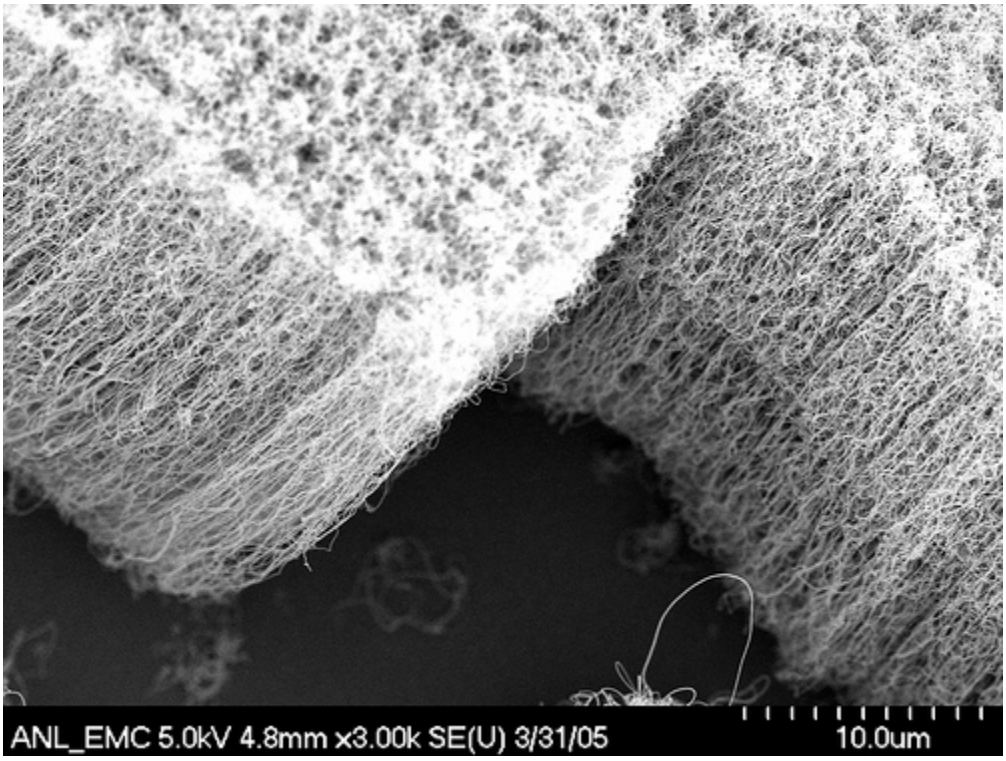

Aligned nanotubes are preferred for many applications.

Carbon nanotubes have been implemented in nanoelectromechanical systems, including mechanical memory elements (NRAM being developed by Nantero Inc.) and nanoscale electric motors.

In May 2005, Nanomix Inc placed on the market a hydrogen sensor which integrated carbon nanotubes on a silicon platform. Since then Nanomix has been patenting many such sensor applications such as in the field of carbon dioxide, nitrous oxide, glucose, DNA detection, etc.

Research at University of California, Riverside has shown that carbon nanotubes are suitable scaffold materials for osteoblast proliferation and bone formation.

Eikos Inc of Franklin, Massachusetts and Unidym Inc. of Silicon Valley, California are developing transparent, electrically conductive films of carbon nanotubes to replace indium tin oxide (ITO). Carbon nanotube films are substantially more mechanically robust than ITO films, making them ideal for high-reliability touchscreens and flexible displays. Printable water-based inks of carbon nanotubes are desired to enable the production of these films to replace ITO. Nanotube films show promise for use in displays for computers, cell phones, PDAs, and ATMs.

A nanoradio, a radio receiver consisting of a single nanotube, was demonstrated in 2007. In 2008 it was shown that a sheet of nanotubes can operate as a loudspeaker if an

alternating current is applied. The sound is not produced through vibration but thermoacoustically.

A flywheel made of carbon nanotubes could be spun at extremely high velocity on a floating magnetic axis in a vacuum, and potentially store energy at a density approaching that of conventional fossil fuels. Since energy can be added to and removed from flywheels very efficiently in the form of electricity, this might offer a way of storing electricity, making the electrical grid more efficient and variable power suppliers (like wind turbines) more useful in meeting energy needs. The practicality of this depends heavily upon the cost of making massive, unbroken nanotube structures, and their failure rate under stress.

Ultra-short SWNTs (US-tubes) have been used as nanoscaled capsules for delivering MRI contrast agents in vivo.

Nitrogen-doped carbon nanotubes may replace platinum catalysts used to reduce oxygen in fuel cells. A forest of vertically-aligned nanotubes can reduce oxygen in alkaline solution more effectively than platinum, which has been used in such applications since the 1960s. The nanotubes have the added benefit of not being subject to carbon monoxide poisoning.

Discovery

A 2006 editorial written by Marc Monthioux and Vladimir Kuznetsov in the journal *Carbon* described the interesting and often misstated origin of the carbon nanotube. A large percentage of academic and popular literature attributes the discovery of hollow, nanometer-size tubes composed of graphitic carbon to Sumio Iijima of NEC in 1991.

In 1952 L. V. Radushkevich and V. M. Lukyanovich published clear images of 50 nanometer diameter tubes made of carbon in the Soviet *Journal of Physical Chemistry*. This discovery was largely unnoticed, as the article was published in the Russian language, and Western scientists' access to Soviet press was limited during the Cold War. It is likely that carbon nanotubes were produced before this date, but the invention of the transmission electron microscope (TEM) allowed direct visualization of these structures.

Carbon nanotubes have been produced and observed under a variety of conditions prior to 1991. A paper by Oberlin, Endo, and Koyama published in 1976 clearly showed hollow carbon fibers with nanometer-scale diameters using a vapor-growth technique. Additionally, the authors show a TEM image of a nanotube consisting of a single wall of graphene. Later, Endo has referred to this image as a single-walled nanotube.

In 1979 John Abrahamson presented evidence of carbon nanotubes at the 14th Biennial Conference of Carbon at Pennsylvania State University. The conference paper described carbon nanotubes as carbon fibers which were produced on carbon anodes during arc discharge. A characterization of these fibers was given as well as hypotheses for their growth in a nitrogen atmosphere at low pressures.

In 1981 a group of Soviet scientists published the results of chemical and structural characterization of carbon nanoparticles produced by a thermocatalytical disproportionation of carbon monoxide. Using TEM images and XRD patterns, the authors suggested that their “carbon multi-layer tubular crystals” were formed by rolling graphene layers into cylinders. They speculated that by rolling graphene layers into a cylinder, many different arrangements of graphene hexagonal nets are possible. They suggested two possibilities of such arrangements: circular arrangement (armchair nanotube) and a spiral, helical arrangement (chiral tube).

In 1987, Howard G. Tennett of Hyperion Catalysis was issued a U.S. patent for the production of "cylindrical discrete carbon fibrils" with a "constant diameter between about 3.5 and about 70 nanometers..., length 10^2 times the diameter, and an outer region of multiple essentially continuous layers of ordered carbon atoms and a distinct inner core...."

Iijima's discovery of multi-walled carbon nanotubes in the insoluble material of arc-burned graphite rods in 1991 and Mintmire, Dunlap, and White's independent prediction that if single-walled carbon nanotubes could be made, then they would exhibit remarkable conducting properties helped create the initial buzz that is now associated with carbon nanotubes. Nanotube research accelerated greatly following the independent discoveries by Bethune at IBM and Iijima at NEC of *single-walled* carbon nanotubes and methods to specifically produce them by adding transition-metal catalysts to the carbon in an arc discharge. The arc discharge technique was well-known to produce the famed Buckminster fullerene on a preparative scale, and these results appeared to extend the run of accidental discoveries relating to fullerenes. The original observation of fullerenes in mass spectrometry was not anticipated, and the first mass-production technique by Krätschmer and Huffman was used for several years before realizing that it produced fullerenes.

The discovery of nanotubes remains a contentious issue. Many believe that Iijima's report in 1991 is of particular importance because it brought carbon nanotubes into the awareness of the scientific community as a whole.

Theory of molecular electronics

Molecular electronics operates in the quantum realm of distances less than 100 nanometers. The theory of single molecule devices is particularly interesting since the system under consideration is an open quantum system in nonequilibrium (driven by voltage).

In the low bias voltage regime, the nonequilibrium nature of the molecular junction can be ignored, and the current-voltage characteristics of the device can be calculated using the equilibrium electronic structure of the system. However, in stronger bias regimes a more sophisticated treatment is required, as there is no longer a variational principle. In the elastic tunneling case (where the passing electron does not exchange energy with the

system), the formalism of Rolf Landauer can be used to calculate the transmission through the system as a function of bias voltage, and hence the current.

In inelastic tunneling, an elegant formalism based on the non-equilibrium Green's functions of Leo Kadanoff and Gordon Baym, and independently by Leonid Keldysh was put forth by Ned Wingreen and Yigal Meir. This Meir-Wingreen formulation has been used to great success in the molecular electronics community to examine the more difficult and interesting cases where the transient electron exchanges energy with the molecular system (for example through electron-phonon coupling or electronic excitations).

Recent progress

Recent progress in nanotechnology and nanoscience has facilitated both experimental and theoretical study of molecular electronics. In particular, the development of the scanning tunneling microscope (STM) and later the atomic force microscope (AFM) have facilitated manipulation of single-molecule electronics. In addition, theoretical advances in molecular electronics have facilitated further understanding of non-adibatic charge transfer events at electrode-electrolyte interfaces.

The first measurement of the conductance of a single molecule was realised in 1994 by C. Joachim and J. K. Gimzewski and published in 1995. This was the conclusion of 10 years of research started at IBM TJ Watson, using the scanning tunnelling microscope tip apex to switch a single molecule as already explored by A. Aviram, C. Joachim and M. Pomerantz at the end of the 80's. The trick was to use an UHV Scanning Tunneling microscope to allow the tip apex to gently touch the top of a single C_{60} molecule adsorbed on a Au(110) surface. A resistance of 55 MOhms was recorded together with a low voltage linear I-V. The contact was certified by recording the I-z current distance characteristic, which allows the measurement of the deformation of the C_{60} cage under contact. This first experiment was followed by the reported result using a mechanical break junction approach to connect two gold electrodes to a sulfur-terminated molecular wire by Mark Reed and James Tour.

A single-molecule amplifier was implemented by C. Joachim and J.K. Gimzewski in IBM Zurich. This experiment involving a single C_{60} molecule demonstrated that a single C_{60} molecule can provide gain in a circuit just by playing with through C_{60} intramolecular quantum interference effects.

A collaboration of researchers at HP and UCLA, led by James Heath, Fraser Stoddart, R. Stanley Williams, and Philip Kuekes, has developed molecular electronics based on rotaxanes and catenanes.

Work is also being done on the use of single-wall carbon nanotubes as field-effect transistors. Most of this work is being done by IBM.

Until recently entirely theoretical, the Aviram-Ratner model for a unimolecular rectifier has been unambiguously-confirmed in experiments by a group led by Geoffrey J. Ashwell at Bangor University, UK. Many rectifying molecules have so far been identified, and the number and efficiency of these systems is expanding rapidly.

Supramolecular electronics is a new field that tackles electronics at a supramolecular level.

An important issue in molecular electronics is the determination of the resistance of a single molecule (both theoretical and experimental). For example, Bumm, et al. used STM to analyze a single molecular switch in a self-assembled monolayer to determine how conductive such a molecule can be. Another problem faced by this field is the difficulty of performing direct characterization since imaging at the molecular scale is often difficult in many experimental devices.

Chapter- 2

Single Molecular Electronics

Single molecule electronics is a branch of molecular electronics that uses single molecules as electronic components. Because single molecules constitute the smallest stable structures imaginable this miniaturization is the ultimate goal for shrinking electrical circuits.

Concepts

In **single molecule electronics**, the bulk material is replaced by single molecules. That is, instead of creating structures by removing or applying material after a pattern scaffold, the atoms are put together in a chemistry lab. This way billions of billions of copies are made simultaneously (typically more than 10^{20} molecules are made at once) while the composition of molecules are controlled down to the last atom. The molecules utilized have properties that resemble traditional electronic components such as a wire, transistor or rectifier.

The miniaturization down to single molecules brings the scale down to a regime where quantum effects are important. As opposed to the case in conventional electronic components, where electrons can be filled in or drawn out more or less like a continuous flow of charge, the transfer of a single electron alters the system significantly. This means that when an electron has been transferred from the source electrode to the molecule, the molecule gets charged up and makes it much harder for the next one to transfer. The significant amount of energy due to charging has to be taken into account when making calculations about the electronic properties of the setup and is highly sensitive to distances to conducting surfaces nearby.

Because of the small size of the molecules, quantum mechanics put severe restraints on the states (or orbitals) the electrons can be in on the molecule. These states determine the energy and spatial distribution that an electron can have and hence the electronic properties of the setup. Unfortunately, even though the molecules seem small and simple

when drawn schematically, the possible electronic states can only be deduced approximately and this limits the predictability of the molecular electronic properties.

Further, connecting single molecules reliably to a larger scale circuit has proven to be a great challenge and constitute a significant hindrance to commercialization.

History

Conventionally, the electronics are made up of bulk material. Ever since its invention in 1958 the performance and complexity of integrated circuits has been growing exponentially (a trend also known as Moore's law) and has forced the feature sizes of the embedded components to shrink accordingly. As the structures become smaller the sensitivity for deviations increases and in a few generations, when the minimum feature sizes reaches 13 nm, the composition of the devices will have to be controlled to a precision of a few atoms in order for the devices to work. With the bulk approach having inherent limitations in addition to becoming increasingly demanding and expensive, the idea was born that the components could instead be built up atom for atom in a chemistry lab (bottom up) as opposed to carving them out of bulk material (top down). This idea is the reasoning behind molecular electronics with the ultimate miniaturization being components contained in single molecules.

The concept of molecular electronics was first published in 1974 when Aviram and Ratner suggested an organic molecule that could work as a rectifier . Having both huge commercial and fundamental interest much effort was put into proving its feasibility and 16 years later in 1990 the first demonstration of an intrinsic molecular rectifier was realized by Ashwell and coworkers for a thin film of molecules. It wasn't until 1997 that the first measurements on the conductance of a single molecule were published and then found to be fraudulent .

Examples

Common for molecules utilized in molecular electronics is that the structures contain a lot of alternating double and single bonds. The reason for this is that such a pattern delocalizes the molecular orbitals making it possible for electrons to move freely over the conjugated area.

Wires

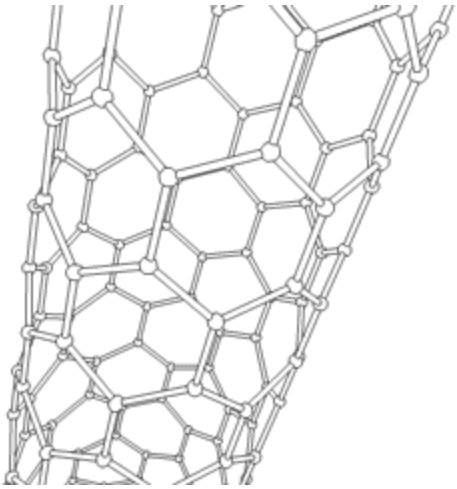

This image of a rotating carbon nanotube shows its 3D structure.

The sole purpose of molecular wires is to electrically connect different parts of a molecular electrical circuit. As the assembly of these and their connection to a macroscopic circuit is still to be mastered, the focus of research in single molecule electronics is primarily on the functionalized molecules: molecular wires are characterized by containing no functional groups and are hence composed of plain repetitions of a conjugated building block. Among these are the carbon nanotubes that are quite large compared to the other suggestions but have shown very promising electrical properties.

The main problem with the molecular wires is to obtain good electrical contact with the electrodes so that the electrons can move freely in and out of the wire.

Transistors

Single molecule transistors are fundamentally different than the ones known from bulk electronics. The gate in a conventional (field-emission) transistor determines the conductance between the source and drain electrode by controlling the density of charge carriers between them, whereas the gate in a single molecule transistor controls the feasibility of a single electron to jump on and off the molecule by modifying the energy of the molecular orbitals. One of the effects of this difference is that the single molecule transistor is almost binary: it is either ON or OFF. This opposes its bulk counterparts which have quadratic responses to gate voltage.

It is the quantization of charge into electrons that is responsible for the markedly different behavior compared to bulk electronics. Because of the size of a single molecule, the charging due to a single electron is significant and provides a mean to turn the transistor ON or OFF. For this to work, the electronic orbitals on the transistor molecule cannot be too well integrated with the orbitals on the electrodes. If they are, an electron cannot be said to be located on the molecule or the electrodes and the molecule will function as a wire.

A popular group of molecules, that can work as the semiconducting channel material in a molecular transistor, is the oligopolyphenylenevinylenes (OPVs) that works by the Coulomb blockade mechanism when placed between the source and drain electrode in an appropriate way . Fullerenes work by the same mechanism and have also been commonly utilized.

Semiconducting carbon nanotubes have also been demonstrated to work as channel material but although molecular, these molecules are sufficiently large to behave almost as bulk semiconductors.

The size of the molecules and the low temperature the measurements are being conducted at makes the quantum mechanical states well defined. It is therefore being researched if the quantum mechanical properties can be used for more advanced purposes than simple transistors (e.g. spintronics).

Physicists at the University of Arizona, in collaboration with chemists from the University of Madrid, have designed a single molecule transistor using a ring-shaped molecule similar to benzene. Physicists at Canada's National Institute for Nanotechnology have designed a single-molecule transistor using styrene. Both groups expect (their designs have yet to be experimentally verified) their respective devices to function at room temperature, and to be controlled by a single electron.

Rectifiers (diodes)

Molecular rectifiers are mimics of their bulk counterparts and have an asymmetric construction so that the molecule can accept electrons in one end but not the other. The molecules have an electron donor (D) in one end and an electron acceptor (A) in the other. This way, the unstable state D^+ - A^- will be more readily made than D^- - A^+. The result is that an electric current can be drawn through the molecule if the electrons are added through the acceptor end, but not so easily if the reverse is attempted. An example of a molecular rectifier was made by Geoffrey J. Ashwell's Ph.D. students.

Techniques

One of the biggest problems with measuring on single molecules is to establish reproducible electrical contact with only one molecule and doing so without shortcutting the electrodes. Because the current photolithographic technology is unable to produce electrode gaps small enough to contact both ends of the molecules tested (in the order of nanometers) alternative strategies is put into use.

Molecular gaps

One way to produce electrodes with a molecular sized gap between them is break junctions, in which a thin electrode is stretched until it breaks. Another is electromigration. Here a current is lead through a thin wire until it melts and the atoms

migrate to produce the gap. Further, the reach of conventional photolithography can be enhanced by chemically etching or depositing metal on the electrodes.

Probably the easiest way to conduct measurements on several molecules is to use the tip of a scanning tunneling microscope (STM) to contact molecules adhered at the other end to a metal substrate. The connection obtained this way is, however, not stable enough to conduct the advanced measurements possible with the above techniques.

Anchoring

A popular way to anchor molecules to the electrodes is to make use of sulfurs' high affinity to gold. In these setups, the molecules are synthesized so that sulfur atoms are placed strategically to function as crocodile clips connecting the molecules to the gold electrodes. Though useful, the anchoring is non-specific and thus anchors the molecules randomly to all gold surfaces. Further, the contact resistance is highly dependent on the precise atomic geometry around the site of anchoring and thereby inherently compromises the reproducibility of the connection.

To circumvent the latter issue, experiments has shown that fullerenes could be a good candidate for use instead of sulfur because of the large conjugated π-system that can electrically contact many more atoms at once than a single atom of sulfur.

Problems

Artifacts

When trying to measure electronic characteristics of molecules, artificial phenomena can occur that can be hard to distinguish from truly molecular behavior . Before they were discovered these artifacts have mistakenly been published as being features pertaining to the molecules in question.

Applying a voltage drop in the order of volts across a nanometer sized junction results in a very strong electrical field. The field can cause metal atoms to migrate and eventually close the gap by a thin filament which can be broken again when carrying a current. The two levels of conductance imitate molecular switching between a conductive and an isolating state of a molecule.

Another encountered artifact is when the electrodes undergo chemical reactions due to the high field strength in the gap. When the bias is reversed the reaction will cause hysteresis in the measurements that can be interpreted as being of molecular origin.

A metallic grain between the electrodes can act as a single electron transistor by the mechanism described above thus resembling the characteristics of a molecular transistor. This artifact is especially common with nanogaps produced by the electromigration technique.

Commercialization

One of the biggest hindrances for single molecule electronics to be commercially exploited is the lack of techniques to connect a molecular sized circuit to bulk electrodes in a way that gives reproducible results. At the current state, the difficulty of connecting single molecules vastly outweighs any possible performance increase that could be gained from such shrinkage. The picture becomes even worse if the molecules are to have a certain spatial orientation and/or have multiple poles to connect.

Also problematic is the fact that some measurements on single molecules are carried out in cryogenic temperatures (close to absolute zero) which is very energy consuming. This is done in order to reduce the signal noise to a degree where the faint currents of single molecules can be measured.

Perspectives

Single molecule electronics is an emerging field, and entire electronic circuits consisting exclusively of molecular sized compounds are still very far from being realized. However, the continuous demand for more computing power together with the inherent limitations of the present day lithographic methods make the transition seem unavoidable.

Currently, the focus is on discovering molecules with interesting properties and on finding ways to obtaining reliable and reproducible contacts between the molecular components and the bulk material of the electrodes.

Chapter- 3

Charge-Transfer Complex

A **charge-transfer complex** (**CT complex**) or **electron-donor-acceptor complex** is an association of two or more molecules, or of different parts of one very large molecule, in which a fraction of electronic charge is transferred between the molecular entities. The resulting electrostatic attraction provides a stabilizing force for the molecular complex. The source molecule from which the charge is transferred is called the electron donor and the receiving species is called the electron acceptor.

The nature of the attraction in a charge-transfer complex is not a stable chemical bond, and is much weaker than covalent forces. The attraction is created by an electronic transition into an excited electronic state, and is best characterized as a weak electron resonance. The excitation energy of this resonance occurs very frequently in the visible region of the electro-magnetic spectrum, which produces the usually intense color characteristic for these complexes. These optical absorption bands are often referred to as *charge-transfer bands* (CT bands). Optical spectroscopy is a powerful technique to characterize charge-transfer bands.

Charge-transfer complexes exist in many types of molecules, inorganic as well as organic, and in all phases of matter, i.e. in solids, liquids, and even gases. A well-known example is the blue charge-transfer band exhibited by iodine when combined with starch.

In inorganic chemistry, most charge-transfer complexes involve electron transfer between metal atoms and ligands. The charge-transfer bands in transition metal complexes result from movement of electrons between molecular orbitals (MO) that are predominantly metal in character and those that are predominantly ligand in character. If the electron moves from the MO with ligand like character to the metal like one, the complex is called ligand-to-metal charge-transfer (LMCT) complex. If the electron moves from the MO with metal like character to the ligand-like one, the complex is called a metal-to-ligand charge-transfer (MLCT) complex. Thus, a MLCT results in oxidation of the metal center whereas a LMCT results in the reduction of the metal center. Resonance Raman

Spectroscopy is also a powerful technique to assign and characterize charge-transfer bands in these complexes.

Donor-acceptor association equilibrium

Charge-transfer complexes are formed by weak association of molecules or molecular subgroups, one acting as an electron donor and another as an electron acceptor. The association does not constitute a strong covalent bond and is subject to significant temperature, concentration, and host (e.g., solvent) dependencies.

The charge-transfer association occurs in a chemical equilibrium with the independent donor (D) and acceptor (A) molecules:

$$D + A \rightleftharpoons DA$$

Quantum mechanically, this is described as a resonance between the non-bonded state |D, A> and the dative state $|D^+...A^->$. The formation of the dative state is an electronic transition giving rise to the colorful absorption bands.

The intensity of charge-transfer bands in the absorbance spectrum is strongly dependent upon the degree (equilibrium constant) of this association reaction. Methods have been developed to determine the equilibrium constant for these complexes in solution by measuring the intensity of absorption bands as a function of the concentration of donor and acceptor components in solution. The methods were first described for the association of iodine dissolved in aromatic hydrocarbons. The procedure is called the Benesi-Hildebrand method, named after the authors of the study.

Charge-transfer transition energy

The color of charge-transfer bands, i.e., the charge-transfer transition energy, is characteristic of the specific type of donor and acceptor entities.

The electron donating power of a donor molecule is measured by its ionization potential which is the energy required to remove an electron from the highest occupied molecular orbital. The electron accepting power of the electron acceptor is determined by its electron affinity which is the energy released when filling the lowest unoccupied molecular orbital.

The overall energy balance (ΔE) is the energy gained in a spontaneous charge transfer. It is determined by the difference between the acceptor's electron affinity (E_A) and the donor's ionization potential (E_I), adjusted by the resulting electrostatic attraction (J) between donor and acceptor:

$$\Delta E = E_A - E_I + J$$

The positioning of the characteristic CT bands in the electromagnetic spectrum is directly related to this energy difference and the balance of resonance contributions of non-bonded and dative states in the resonance equilibrium.

Identification of CT bands

Charge-transfer complexes are identified by

- *Color*: The color of CT complexes is reflective of the relative energy balance resulting from the transfer of electronic charge from donor to acceptor.
- *Solvatochromism*: In solution, the transition energy and therefore the complex color varies with variation in solvent permittivity, indicating variations in shifts of electron density as a result of the transition. This distinguishes it from the $\pi^* \leftarrow \pi$ transitions on the ligand.
- *Intensity*: CT absorptions bands are intense and often lie in the ultraviolet or visible portion of the spectrum. For inorganic complexes, the typical molar absorptivities, ε, are about 50000 L mol^{-1} cm^{-1}, that are three orders of magnitude higher than typical ε of 20 L mol^{-1} cm^{-1} or lower, for d-d transitions (transition from t_2g to e_g). This is because the CT transitions are spin-allowed and Laporte-allowed. However, d-d transitions are only spin-allowed; they are Laporte-forbidden.

Inorganic charge-transfer complexes

Charge-transfer occurs often in inorganic ligand chemistry involving metals. Depending on the direction of charge transfer they are either classified as ligand-to-metal (LMCT) or metal-to-ligand (MLCT) charge transfer.

Ligand-to-metal charge transfer

LMCT complexes arise from transfer of electrons from MO with ligand like character to those with metal like character. This type of transfer is predominant if complexes have ligands with relatively high energy lone pairs (example S or Se) or if the metal has low lying empty orbitals. Many such complexes have metals in high oxidation states (even d^0). These conditions imply that the acceptor level is available and low in energy.

Consider a d^6 octahedral complex (example $IrBr_6^{3-}$). The t_2g levels are filled as shown in Figure 1. Consequently an intense absorption is observed around 250 nm corresponding to a transition from ligand σ MO to the empty e_g MO. However, in $IrBr_6^{2-}$ that is a d^5 complex two absorptions, one near 600 nm and another near 270 nm, are observed. This is because two transitions are possible, one to t_{2g} (that can now accommodate one more electron) and another to e_g. The 600 nm band corresponds to transition to the t_{2g} MO and the 270 nm band to the e_g MO.

Figure 1. MO diagram showing ligand to metal charge transfer for a d^6 octahedral complex Another thing to note is that CT bands might also arise from transfer of electrons from nonbonding orbitals of the ligand to the e_g MO.

Trend of LMCT energies

Oxidation Number

+7 MnO_4^- < TcO_4^- < ReO_4^-
+6 CrO_4^{2-} < MoO_4^{2-} < WO_4^{2-}
+5 VO_4^{3-} < NbO_4^{3-} < TaO_4^{3-}

The energies of transitions correlate with the order of the electrochemical series. The metal ions that are most easily reduced correspond to the lowest energy transitions. The above trend is consistent with transfer of electrons from the ligand to the metal, thus resulting in a reduction of metal ions by the ligand.

Examples include:

1. MnO_4^- : The permanganate ion having tetrahedral geometry is intensely purple due to strong absorption involving charge transfer from MO derived primarily from filled oxygen p orbitals to empty MO derived from manganese(VII).
2. CdS: The color of artist's pigment cadmium yellow is due to transition from Cd^{2+} (5s) ← $S^{2-}(\pi)$.
3. HgS: it is red due to Hg^{2+} (6s) ← $S^{2-}(\pi)$ transition.
4. Fe Oxides: they are red and yellow due to transition from Fe (3d) ← $O^{2-}(\pi)$.

Metal-to-ligand charge transfer

Metal-to-ligand charge-transfer (MLCT) complexes arise from transfer of electrons from MO with metal like character to those with ligand like character. This is most commonly observed in complexes with ligands having low-lying π^* orbitals especially aromatic ligands. The transition will occur at low energy if the metal ion has a low oxidation number for its d orbitals will relatively be high in energy.

Examples of such ligands taking part in MLCT include 2,2'-bipyridine (bipy), 1,10-phenanthroline (phen), CO, CN^- and SCN^-. Examples of these complexes include:

1. Tris(2,2'-bipyridyl)ruthenium(II) : This orange colored complex is being studied as the excited state resulting from this charge transfer has a lifetime of microseconds and the complex is a versatile photochemical redox reagent.
2. $W(CO)_4$(phen)
3. $Fe(CO)_3$(bipy)

Photoreactivity of MLCT excited states

The photoreactivity of MLCT complexes result from the nature of the oxidized metal and the reduced ligand. Though the states of traditional MLCT complexes like $Ru(bipy)_3^{2+}$ and $Re(bipy)(CO)_3Cl$ were intrinsically not reactive, several MLCT complexes have been synthesized that are characterized by reactive MLCT states.

Vogler and Kunkely considered the MLCT complex to be an isomer of the ground state which contains an oxidized metal and reduced ligand. Thus various reactions like electrophilic attack and radical reactions on the reduced ligand, oxidative addition at the metal center due to the reduced ligand, and outer sphere charge-transfer reactions can be attributed to states arising from MLCT transitions. MLCT states' reactivity often depends on the oxidation of the metal. Subsequent processes include associative ligand substitution, exciplex formation and cleavage of metal---metal bonds.

Color of charge-transfer complexes

Many metal complexes are colored due to d-d electronic transitions. Visible light of the correct wavelength is absorbed, promoting a lower d-electron to a higher excited state. This absorption of light causes color. These colors are usually quite faint, though. This is because of two selection rules:

The spin rule: $\Delta S = 0$

On promotion, the electron should not experience a change in spin. Electronic transitions which experience a change in spin are said to be *spin forbidden*.

Laporte's rule: $\Delta l = \pm 1$

d-d transitions for complexes which have a center of symmetry are forbidden - *symmetry forbidden* or *Laporte forbidden*.

Charge-transfer complexes do not experience d-d transitions. Thus, these rules do not apply and the absorptions are generally very intense.

For example, the classic example of a charge-transfer complex is that between iodine and starch to form an intense purple color. This has widespread use as a rough screen for counterfeit currency. Unlike most paper, the paper used in US currency is not sized with starch. Thus, formation of this purple color on application of an iodine solution indicates a counterfeit.

Other examples

Hexaphenylbenzenes like **H** (fig. 3) lend themselves extremely well to forming charge-transfer complexes. Cyclic voltammetry for **H** displays 4 well separated maxima corresponding to H^+ right up to H^{4+} with the first ionization at $E_{1/2}$ of only 0.51 eV. oxidation of these arenes by for instance dodecamethylcarboranyl (**B**) to the blue crystal solid H^+B^- complex is therefore easy.

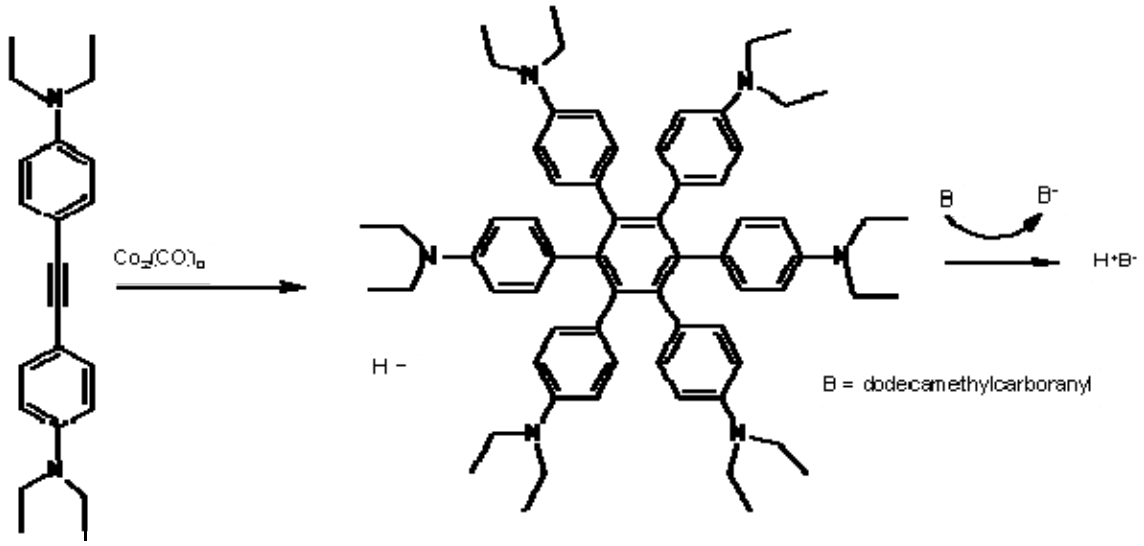

Fig. 3 Synthesis of H^+B^- complex: Alkyne trimerisation of bisubstituted alkyne with dicobalt octacarbonyl, delocalization is favored with activating groups such as a di(ethylamino) group

The phenyl groups are all positioned in an angle of around 45° with respect to the central aromatic ring and the positive charge in the radical cation is therefore through space delocalised through the 6 benzene rings in the shape of a toroid. The complex has 5 absorption bands in the near infrared region which can be assigned to specific electronic transitions with the aid of deconvolution and the Mulliken-Hush theory.

Electrical conductivity

In 1954 researchers at Bell Laboratories and elsewhere reported charge-transfer complexes with resistivities as low as 8 ohms·cm in combinations of perylene with iodine or bromine. In 1962, the well-known acceptor tetracyanoquinodimethane (TCNQ) was reported. Tetrathiafulvalene (TTF) was synthesized in 1970 and found to be a strong electron donor. In 1973 it was discovered that a combination of these components formed a strong charge-transfer complex, henceforth referred to as TTF-TCNQ. The complex is formed in solution and may be crystallized into a well-formed crystalline solid. The solid shows almost metallic electrical conductance and was the first discovered purely organic conductor. In a TTF-TCNQ crystal, TTF and TCNQ molecules are arranged independently in separate parallel-aligned stacks and an electron transfer occurs from donor (TTF) to acceptor (TCNQ) stacks. Hence, electrons and electron holes are separated and concentrated in the stacks and can traverse in a one-dimensional direction along the TCNQ and TTF columns, respectively, when an electric potential is applied to the ends of a crystal in the stack direction.

The first organic molecule that forms a superconductor was discovered in 1980. Tetramethyl-tetraselenafulvalene-phosphorus hexafloride ($TMTSF_2PF_6$), a semi-conductor at ambient conditions, shows superconductivity at low temperature (critical temperature) and high pressure: 0.9 K and 12 kbar. Since 1980, many organic

superconductors have been synthesized, and the critical temperature has been raised to over 100 K as of 2001 . Unfortunately, critical current densities in these complexes are very small.

CT complexation involved in diseases

In humans, elevated systemic levels of transition-series metals, electron-donors, etc. are associated with specific disease symptoms. These include psychosis, movement disorders, pigmentary abnormalities, and deafness. This may involve charge-transfer complexes with the Melanin in the midbrain, skin, and the stria vascularis of the inner ear.

Chapter- 4

Conductive Polymer

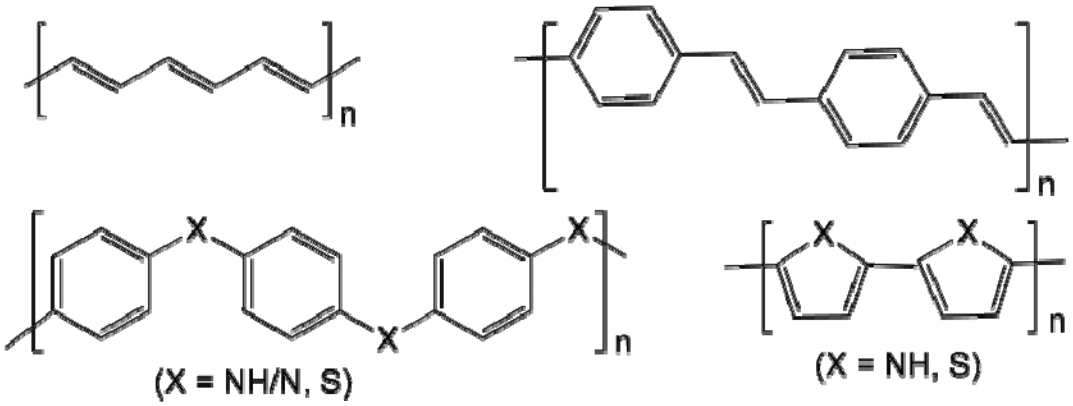

Conductive polymers or more precisely **intrinsically conducting polymers** (ICPs) are organic polymers that conduct electricity. Such compounds may have metallic conductivity or be semiconductors. The biggest advantage of conductive polymers is their processability. Conductive polymers are also plastics, which are organic polymers. Therefore, they can combine the mechanical properties (flexibility, toughness, malleability, elasticity, etc.) of plastics with high electrical conductivity. These properties can be fine-tuned using the methods of organic synthesis.

Correlation of chemical structure and electrical conductivity

In traditional polymers such as polyethylenes, the valence electrons are bound in sp^3 hybridized covalent bonds. Such "sigma-bonding electrons" have low mobility and do not contribute to the electrical conductivity of the material. The situation is completely different in conjugated materials. Conducting polymers have backbones of contiguous sp^2 hybridized carbon centers. One valence electron on each center resides in a p_z orbital, which is orthogonal to the other three sigma-bonds. The electrons in these delocalized orbitals have high mobility when the material is "doped" by oxidation, which removes some of these delocalized electrons. Thus the conjugated p-orbitals form a one-

dimensional electronic band, and the electrons within this band become mobile when it is partially emptied. The band structures of conductive polymers can easily be calculated with a tight binding model. In principle, these same materials can be doped by reduction, which adds electrons to an otherwise unfilled band. In practice, most organic conductors are doped oxidatively to give p-type materials. The redox doping of organic conductors is analogous to the doping of silicon semiconductors, whereby a small fraction silicon atoms are replaced by electron-rich (e.g., phosphorus) or electron-poor (e.g. boron) atoms to create n-type and p-type semiconductors, respectively.

Although typically "doping" conductive polymers involves oxidizing or reducing the material, conductive organic polymers associated with a protic solvent may also be "self-doped."

The most notable difference between conductive polymers and inorganic semiconductors is the mobility, which until very recently was dramatically lower in conductive polymers than their inorganic counterparts. This difference is diminishing with the invention of new polymers and the development of new processing techniques. Low charge carrier mobility is related to structural disorder. In fact, as with inorganic amorphous semiconductors, conduction in such relatively disordered materials is mostly a function of "mobility gaps" with phonon-assisted hopping, polaron-assisted tunneling, etc., between localized states. Recently, it has been reported that Quantum Decoherence on localized electron states might be the fundamental mechanism behind electron transport in conductive polymers.

The conjugated polymers in their undoped, pristine state are semiconductors or insulators. As such, the energy gap can be > 2 eV, which is too great for thermally activated conduction. Therefore, undoped conjugated polymers, such as polythiophenes, polyacetylenes only have a low electrical conductivity of around 10^{-10} to 10^{-8} S/cm. Even at a very low level of doping (< 1%), electrical conductivity increases several orders of magnitude up to values of around 0.1 S/cm. Subsequent doping of the conducting polymers will result in a saturation of the conductivity at values around 0.1–10 kS/cm for different polymers. Highest values reported up to now are for the conductivity of stretch oriented polyacetylene with confirmed values of about 80 kS/cm. Although the pi-electrons in polyactetylene are delocalized along the chain, pristine polyacetylene is not a metal. Polyacetylene has alternating single and double bonds which have lengths of 1.44 and 1.36 Å, respectively. Upon doping, the bond alteration is diminished in conductivity increases. Non-doping increases in conductivity can also be accomplished in a field effect transistor (organic FET or OFET) and by irradiation. Some materials also exhibit negative differential resistance and voltage-controlled "switching" analogous to that seen in inorganic amorphous semiconductors.

Classes of materials

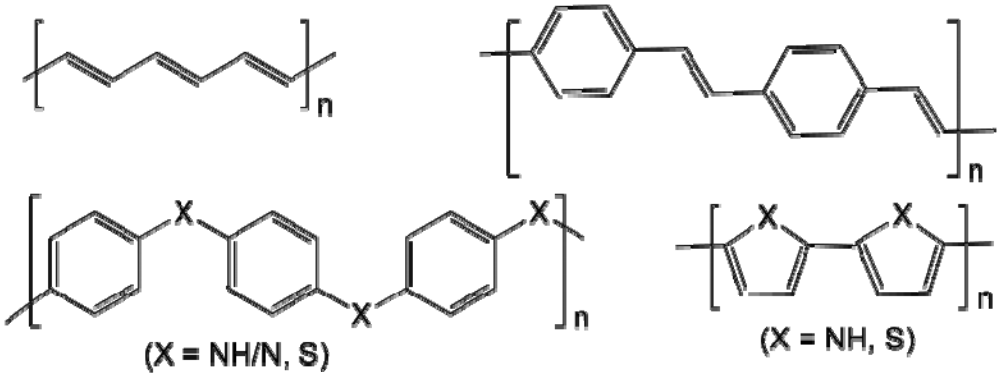

Structures of various conductive organic polymers. Clockwise; polyacetylene, polyphenylenevinylene, polypyrrole (X = NH), and polythiophene (X = S), polyaniline (X = N, NH) and polyphenylene sulfide (X = S).

The following table presents some organic conductive polymers according to their composition. **The well-studied classes are written in bold** and *the less well studied ones are in italic*.

The main chain contains	**No heteroatom**	**NH or NR**	**S**
Aromatic cycles	*Poly(fluorene)s, polypyrenes, polyazulenes, polynaphthalenes*	The N is in the aromatic cycle: **poly(pyrrole)s (PPY)**, *polycarbazoles, polyindoles, polyazepines*... The N is outside the aromatic cycle: **polyanilines (PANI)**	The S is in the aromatic cycle: **poly(thiophene)s (PT)**... The S is outside the aromatic cycle: **poly(p-phenylene sulfide) (PPS)**
Double bonds	**Poly(acetylene)s (PAC)**		
Aromatic cycles and double bonds	**Poly(p-phenylene vinylene) (PPV)**		

PPV and its soluble derivatives have emerged as the prototypical electroluminescent semiconducting polymers. Today, poly(3-alkylthiophenes) are the archetypical materials for solar cells and transistors.

Synthesis of conductive polymers

Many methods for the synthesis of conductive polymers have been developed. Most conductive polymers are prepared by oxidative coupling of monocyclic precursors. Such reactions entail dehydrogenation:

$$n\ H–[X]–H \rightarrow H–[X]_n–H + 2(n–1)\ H^+ + 2(n–1)\ e^–$$

One challenge is usually the low solubility of the polymer. This has been addressed by some researchers through the formation of nanostructures and surfactant stabilized conducting polymer dispersions in water. These include polyaniline nanofibers and PEDOT:PSS. These materials have lower molecular weights than that of some materials previously explored in the literature. However, in some cases, the molecular weight need not be high to achieve the desired properties.

Properties and applications

Conductive polymers enjoy few large-scale applications due to their poor processability. They have been known to have promise in antistatic materials and they have been incorporated into commercial displays and batteries, but there have had limitations due to the manufacturing costs, material inconsistencies, toxicity, poor solubility in solvents, and inability to directly melt process. Literature suggests they're also promising in organic solar cells, printing electronic circuits, organic light-emitting diodes, actuators, electrochromism, supercapacitors, biosensors, flexible transparent displays, electromagnetic shielding and possibly replacement for the popular transparent conductor indium tin oxide. Conducting polymers are rapidly gaining attraction in new applications with increasingly processable materials with better electrical and physical properties and lower costs. The new nanostructured forms of conducting polymers particularly, provide fresh air to this field with their higher surface area and better dispersability.

Electroluminescence

Electroluminescence is light emission stimulated by electrical current. In organic compounds, electroluminescence has been known since the early 1950s, when Bernanose and coworkers first produced electroluminescence in crystalline thin films of acridine orange and quinacrine. In 1960, researchers at Dow Chemical developed AC-driven electroluminescent cells using doping. In some cases, similar light emission is observed when a voltage is applied to a thin layer of a conductive organic polymer film. While electroluminescence was originally mostly of academic interest, the increased conductivity of modern conductive polymers means enough power can be put through the device at low voltages to generate practical amounts of light. This property has led to the development of flat panel displays using Organic LEDs, solar panels, and optical amplifiers.

Barriers to applications

Since most conductive polymers require oxidative doping, the properties of the resulting state are crucial. Such materials are often salt-like, which diminishes their solubility in

organic solvents and hence their processability. Furthermore, the charged organic backbone is often unstable towards atmospheric moisture. Compared to metals, organic conductors can be expensive requiring multi-step synthesis. The poor processability for many polymers requires the introduction of solubilizing substituents, which can further complicate the synthesis.

History

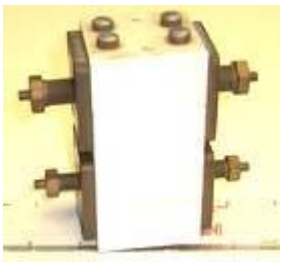

voltage-controlled switch, an organic polymer electronic device from 1974. Now in the Smithsonian Chip collection.

There are multiple reviews of the history of the field. The first report on polyaniline goes back to the discovery of aniline. In the mid-19th century, Letheby reported the electrochemical and chemical oxidation products of aniline in acidic media, noting that reduced form was colourless but the oxidized forms were deep blue. In the early 20th century, German chemists named several compounds "aniline black" and "pyrrole black" and used them industrially. Classically, such polymer "blacks", their parent compound polyacetylene, and their co-polymers were called "Melanins".

The first highly-conductive polymers were mixtures of plastics with embedded conducting particles (metal powders, carbon black...) or coated plastics. For example, page 52 of the December 26, 1949, issue of LIFE magazine shows a light bulb in a circuit without wires. The conductor was Markite, a clear pyrolyzed inorganic silica. The conductivity of Markite ranges from as low as distilled water to as high as mercury.

In the 1950s, researchers reported that polycyclic aromatic compounds formed semi-conducting charge-transfer complex salts with halogens. This indicated that organic compounds could carry current. While organic conductors were previously intermittently discussed, the field was particularly energized by the prediction of superconductivity following the discovery of BCS theory.

As for "pure" conductive organic polymers—in 1963, Bolto and co-workers reported conductivity in iodine-doped polypyrroles. This Australian group eventually claimed to reach resistivities as low as 0.03 ohm·cm with other conductive organic polymers. This resistivity is roughly equivalent to present-day efforts.

Subsequently, DeSurville and coworkers reported high conductivity in a polyaniline. Similarly, in 1980, Diaz and Logan reported films of polyaniline that could serve as electrodes.

Similarly, much early work on the physics and chemistry of conductive polymers was done under the melanin rubrick. This was because of the medical relevance of this material. For example, in the 1960s Blois *et al.* showed semiconduction in melanins, as well as further defining their physical structures and properties Nicolaus *et al.* further defined the conductive polymer structures. Classically, all polyacetylenes, polypyrroles and polyanilines are melanins, "The most simple melanin can be considered the acetylene-black from which it is possible to derive all the others.. Substitution does not qualitatively influence the physical properties like conductivity, colour, EPR, which remain unaltered."

In 1974, McGinness and coworkers described an "active" organic-polymer electronic device, a voltage-controlled bistable switch. This device used DOPA-melanin, a well-characterized self-doping copolymer of polyaniline, polypyrrole, and polyacetylene. The "ON" state of this device exhibited low conductivity with switching, with as much as five orders of magnitude shifts in current. Their material also exhibited classic negative differential resistance.

In 1977, Alan J. Heeger, Alan MacDiarmid and Hideki Shirakawa reported similar high conductivity in oxidized iodine-doped polyacetylene. This research earned them the 2000 Nobel prize in Chemistry *"For the discovery and development of conductive polymers."* Some reviewers have questioned the Nobel citation's *discovery* assignment. Thus, Inzelt notes that, while the Nobelists deserve credit for publicising and popularizing the field, conductive polymers were " *..produced, studied and even applied* " well before their work.

Trends

Most recent emphasis is on organic light emitting diodes and organic polymer solar cells. The Organic Electronics Association is an international platform to promote applications of organic semiconductors. Conductive polymer products with embedded and improved electromagnetic interference (EMI) and electrostatic discharge (ESD) protection have led to both prototypes and products. For example, Polymer Electronics Research Center at University of Auckland is developing a range of novel DNA sensor technologies based on conducting polymers, photoluminescent polymers and inorganic nanocrystals (quantum dots) for simple, rapid and sensitive gene detection. Typical conductive polymers must be "doped" to produce high conductivity. To date, there remains to be discovered an organic polymer that is *intrinsically* electrically conducting.

Chapter- 5

Negative Resistance

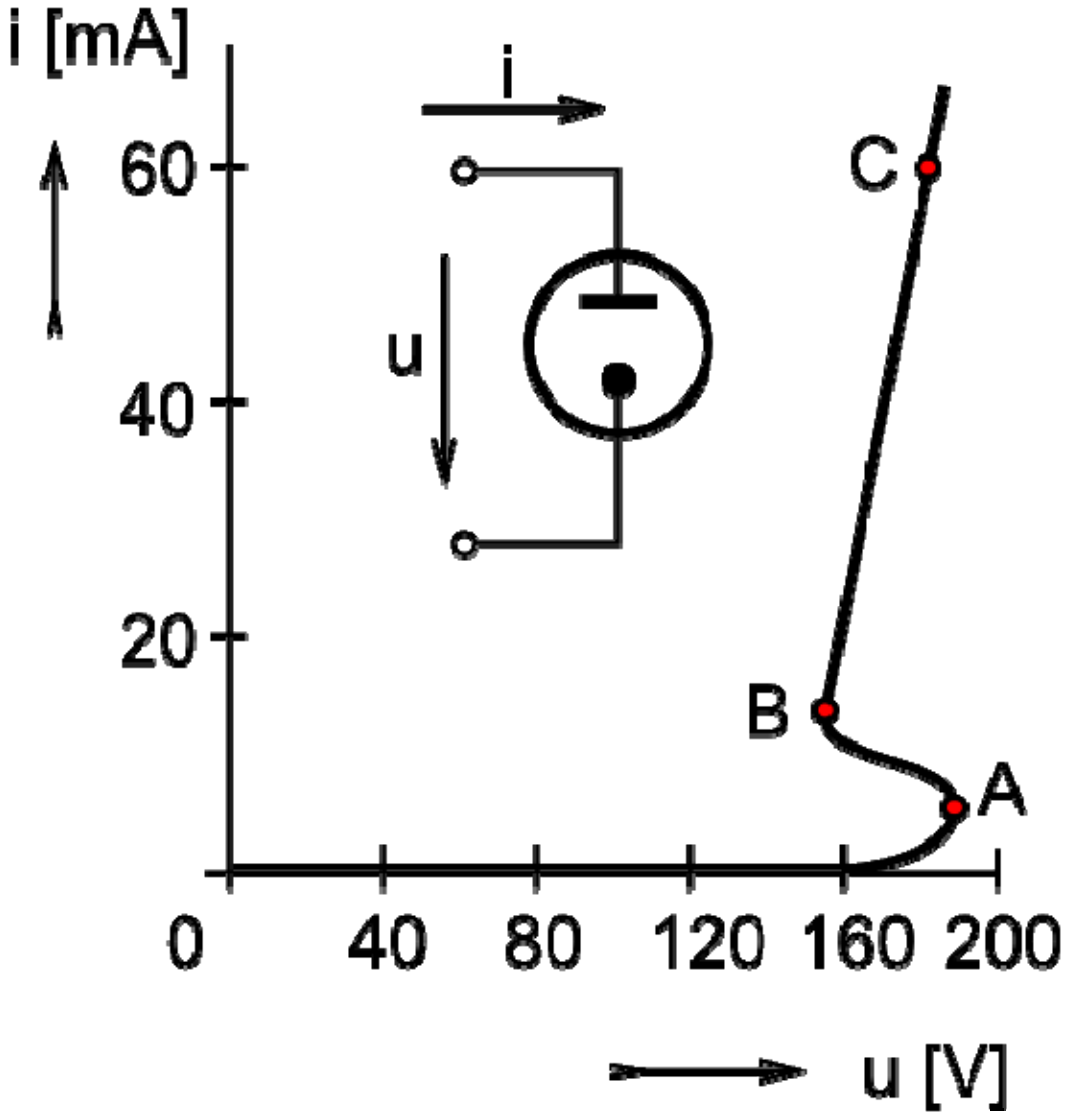

A neon lamp exhibits S-shaped negative differential resistance in A–B section of its IV curve where an increase in the current results in a decreased voltage; total resistance is still positive.

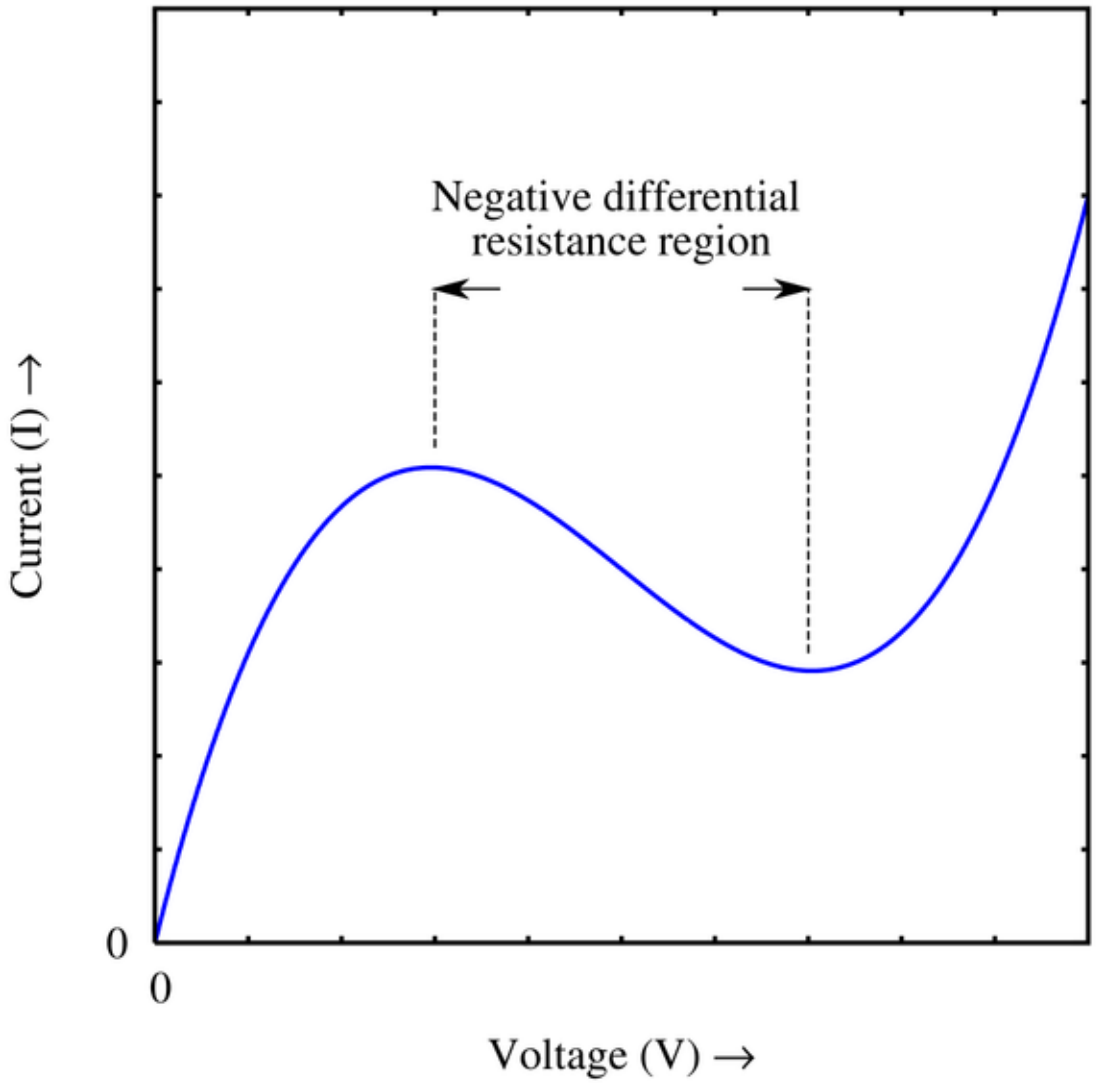

A tunnel diode exhibits N-shaped negative differential resistance in the middle region of its IV curve where an increase in the voltage results in a decreased current; total resistance is still positive.

Negative resistance is a property of some electric circuits where current through and voltage across the same port change in opposite directions. This is in contrast to a simple ohmic resistor, where current and voltage change in the same direction under the same conditions. Negative resistors are theoretical and do not exist as a discrete component. However, some types of diodes (e.g., tunnel diodes) can be built that exhibit negative resistance in some part of their operating range. Such a differential negative resistance can be illustrated with a resonant tunneling diode. Similarly, some chalcogenide glasses,

organic semiconductors, and conductive polymers exhibit a similar region of negative resistance as a bulk property of the material.

Properties

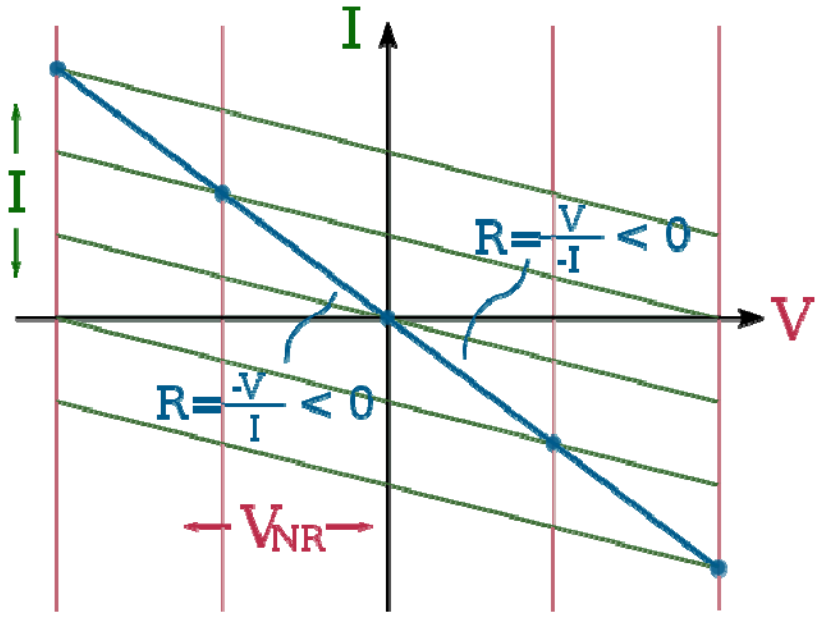

Figure 2: The IV curve of a theoretical negative resistor

Fig. 2 shows a graph of a negative resistor, showing the negative slope. In contrast to this, a resistor will have a positive slope. Tunnel diodes and Gunn diodes exhibit a negative resistance region in their IV (current - voltage) curve. They have two terminals like a resistor; but are not linear devices. Unijunction transistors also have negative resistance properties when a circuit is built using other components.

For negative resistance to be present there must be active components in the circuit providing a source of energy. This is because current through a negative resistance implies a source of energy just as current through positive resistance implies that energy is being dissipated. A resistor produces voltage that is proportional to the current through it according to Ohm's law. The IV curve of a true negative resistor has a negative slope and passes through the origin of the coordinate system (the curve can only enter the 2nd and 4th quadrants if energy is being supplied). This is to be compared with devices such as the tunnel diode where the negative slope portion of the curve does not pass through the origin. Clearly, there is no source of energy in a two terminal diode.

History

In early research it was noticed that arc discharge devices and some vacuum tube devices such as the dynatron exhibit negative differential resistance effects. Practical and economic devices only became available with solid state technology. The typical true negative impedance circuit—the negative impedance converter -- is due to John G. Linvill (1953) and the popular element with negative differential resistance—the tunnel diode -- is due to Leo Esaki (1958).

Implementations

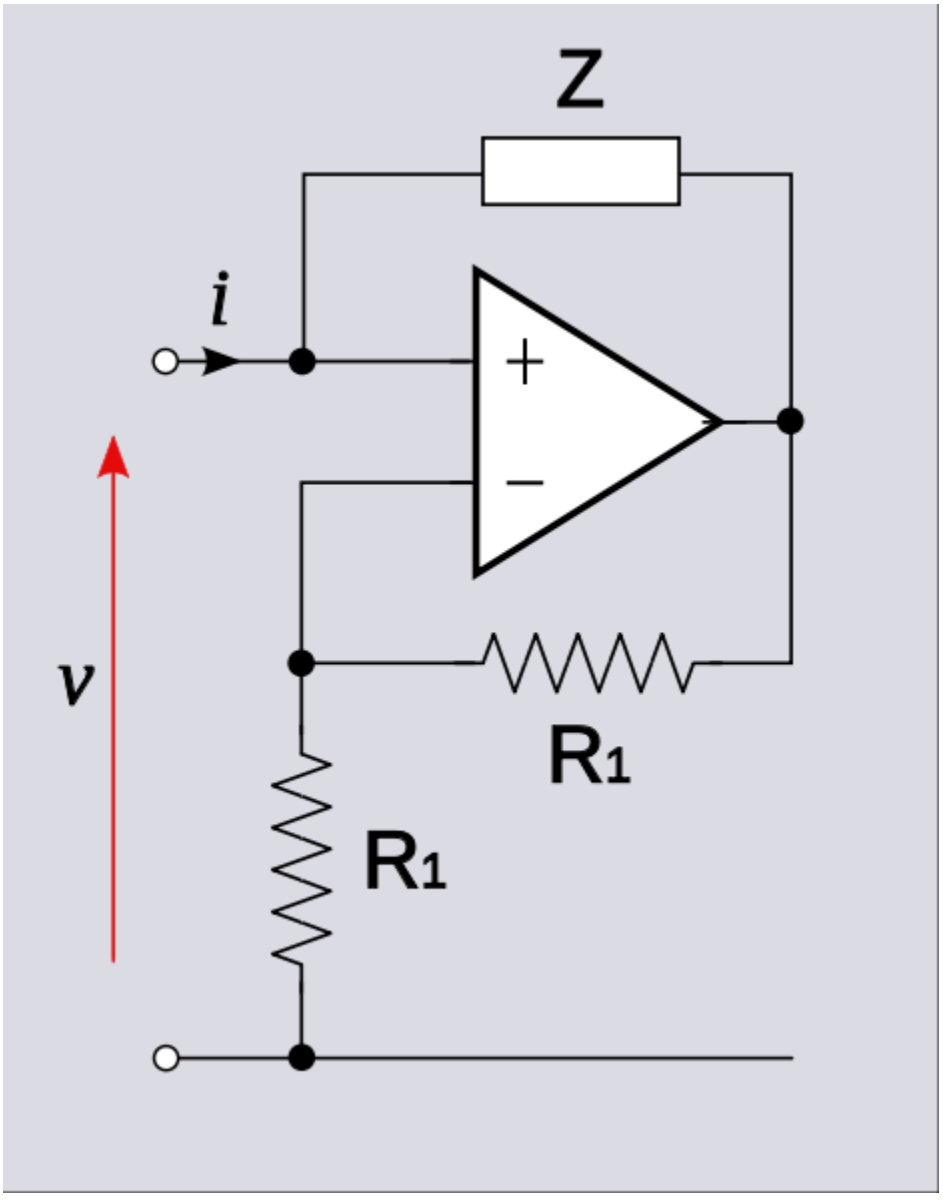

Figure 3: Negative impedance circuit with $Z_{\text{in}} \triangleq \frac{v}{i} = -Z$

Diodes

Tunnel diodes are heavily doped semiconductor junctions that have an "N" shaped transfer curve. A vacuum tube can also be made to exhibit negative resistance.. Other negative resistance diodes have been built that have an "S" shaped transfer curve. When biased so that the operating point is in the negative resistance region, these devices can be used as an Amplifier. These devices can also be biased so that they will switch between two states very quickly, as the applied voltage changes.

Operational Amplifiers

The negative resistance circuit shown in Figure 3 is an opamp implementation of the negative impedance converter (see below). The two resistors R1 and the op amp constitute a negative feedback non-inverting amplifier with gain A = 2. In the case $Z = R$, the input resistance (for an ideal opamp) is given by;

$$R_{\text{in}} = -Z = -R$$

The input port of the circuit can be connected into another network as if it were a negative resistance component.

In the general case Z can be selected to produce negative capacitances or negative inductances.

Applications

Oscillators

All feedback oscillators imply the presence of negative resistance. There are many such topologies, including the Dynatron oscillator, Colpitts oscillator, Hartley oscillator, Wien bridge oscillator, and some types of relaxation oscillators. If the feedback loop is broken and the input impedance examined it will be found to include negative resistance. Negative resistance characteristics of Gunn diodes are often used in microwave frequencies as well.

Amplifiers

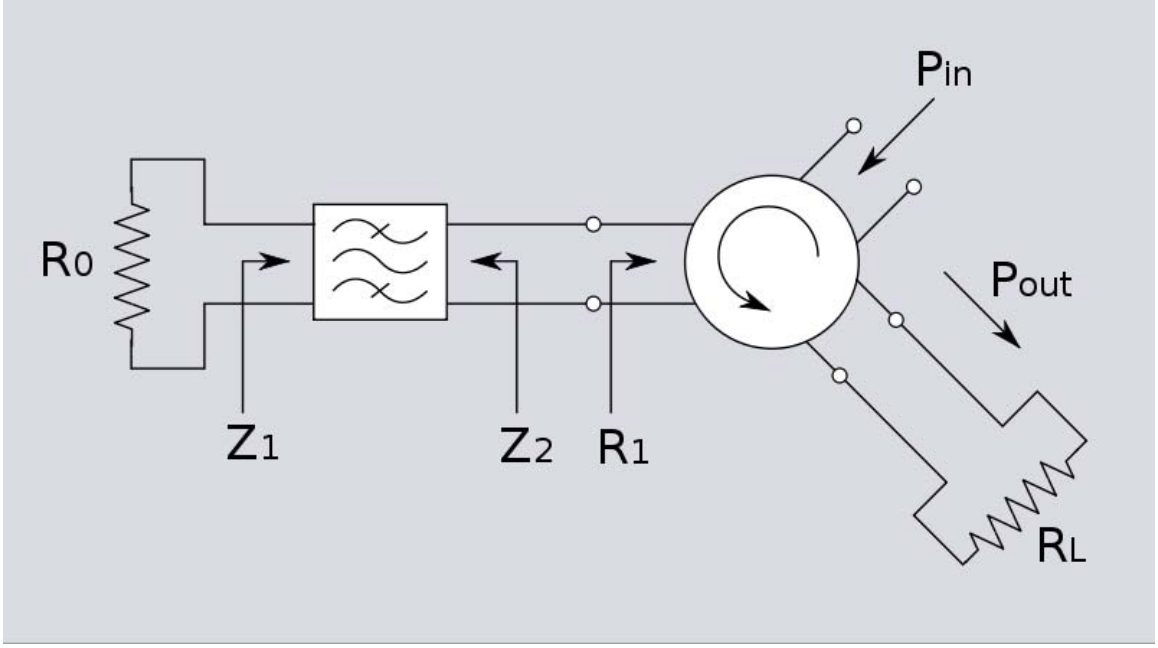

Figure 4: Negative resistance microwave amplifier using a circulator

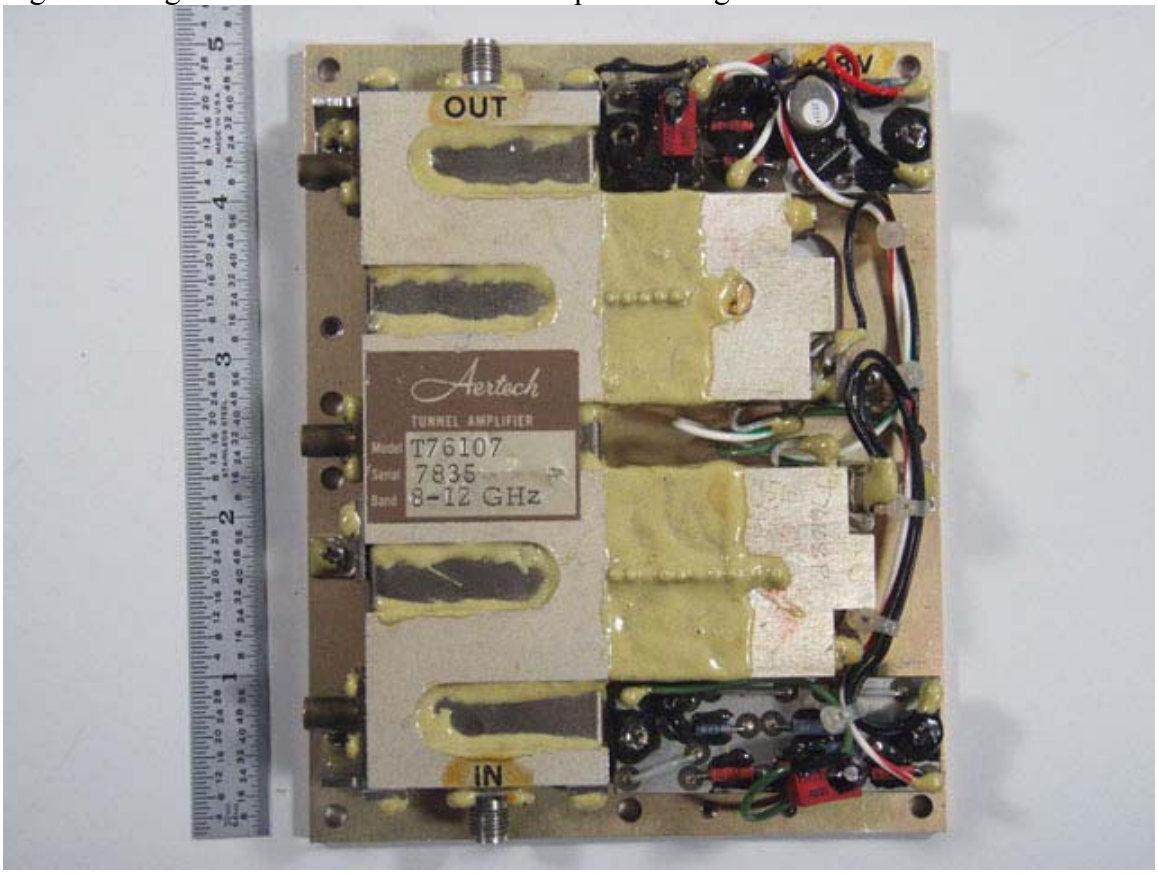

Figure 5: 8 - 12 GHz tunnel diode amplifier, circa 1970

A device exhibiting negative resistance can be used to amplify a signal and this is an especially useful technique at microwave frequencies. Such devices do not present as pure negative resistance at these frequencies (in the case of the tunnel diode a large parallel capacitance is also present) and a matching filter is usually required. The reactive components of the device's equivalent circuit can be absorbed into the filter design so the circuit can be represented as a pure resistance followed by a bandpass filter. The output of this arrangement is fed into one port of a three-port circulator. The other two ports constitute the input and output of the amplifier with the direction of circulation as shown in the diagram. Treating R_0 as being positive, the reflection coefficients at the two ends of the filter are given by;

$$\Gamma_1 = \frac{Z_1 - R_0}{Z_1 + R_0} \text{and,} \quad \Gamma_2 = \frac{Z_2 - R_1}{Z_2 + R_1}$$

Since the filter has no resistive elements, there is no dissipation and the magnitudes of the two reflection coefficients must be equal,

$$|\Gamma_1| = |\Gamma_2|$$

The input power entering the cirulator is directed at the matching filter, is reflected at both the input and output of the filter and a portion finally arrives at the load. This portion is given by;

$$\frac{P_{\text{out}}}{P_{\text{in}}} = |\Gamma_1|^2$$

For a well matched filter, the reflection coefficients will be very small in the passband and very little power will reach the load. On the other hand if R_0 is replaced by a negative resistance such that,

$$R_0' = -R_0 \text{then,}$$
$$\Gamma_1' = \frac{Z_1 + R_0}{Z_1 - R_0} \text{and,}$$
$$|\Gamma_1'| = |\Gamma_2'| = \frac{1}{|\Gamma_1|}$$

Now the reflection coefficients are very large and more power is reaching the load than was injected in the input port. The net result of terminating one port in a negative resistance is amplification between the remaining two ports.

Mixers and frequency converters

The highly non-linear characteristics of tunnel diodes makes them useful as frequency mixers. The conversion gain of a tunnel diode mixer can be as high as 20 dB if it is biased to operate in the negative resistance region.

Antenna design

Another concept of negative resistance exists in the domain of radio frequency antenna design. This is also known as negative impedance. It is not uncommon for an antenna containing multiple driven elements to exhibit apparent negative impedance in one or more of the driven elements.

Impedance cancellation

Negative impedances can be used to cancel the effects of positive impedances, for example, by eliminating the internal resistance of a voltage source or making the internal resistance of a current source infinite. This property is used in telephony line repeaters and in circuits such as the Howlan

Chapter- 6

Organic Light-Emitting Diode

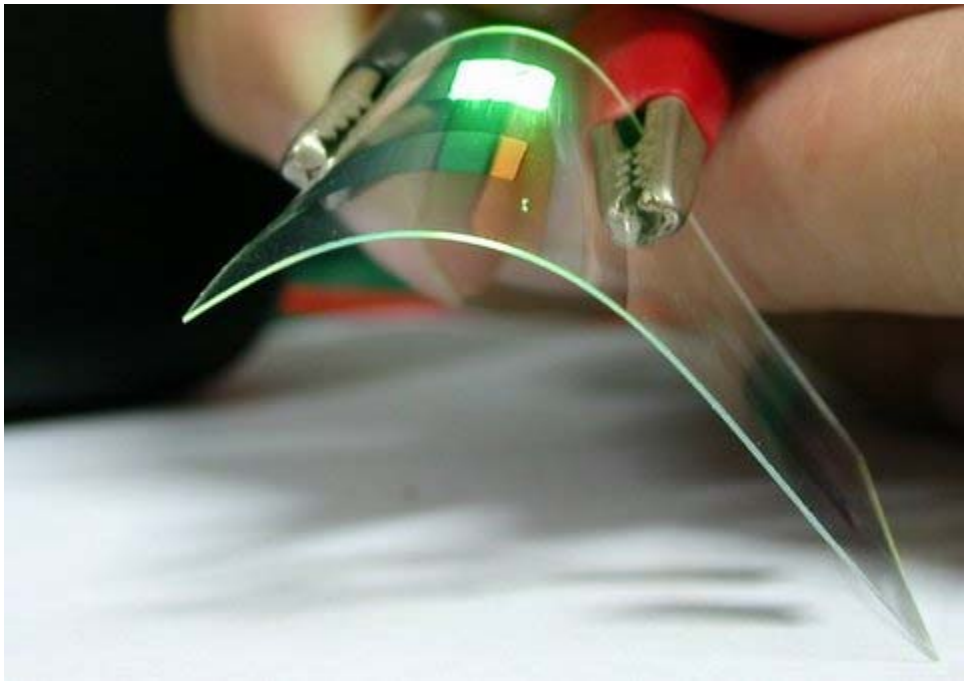

Demonstration of a flexible OLED device

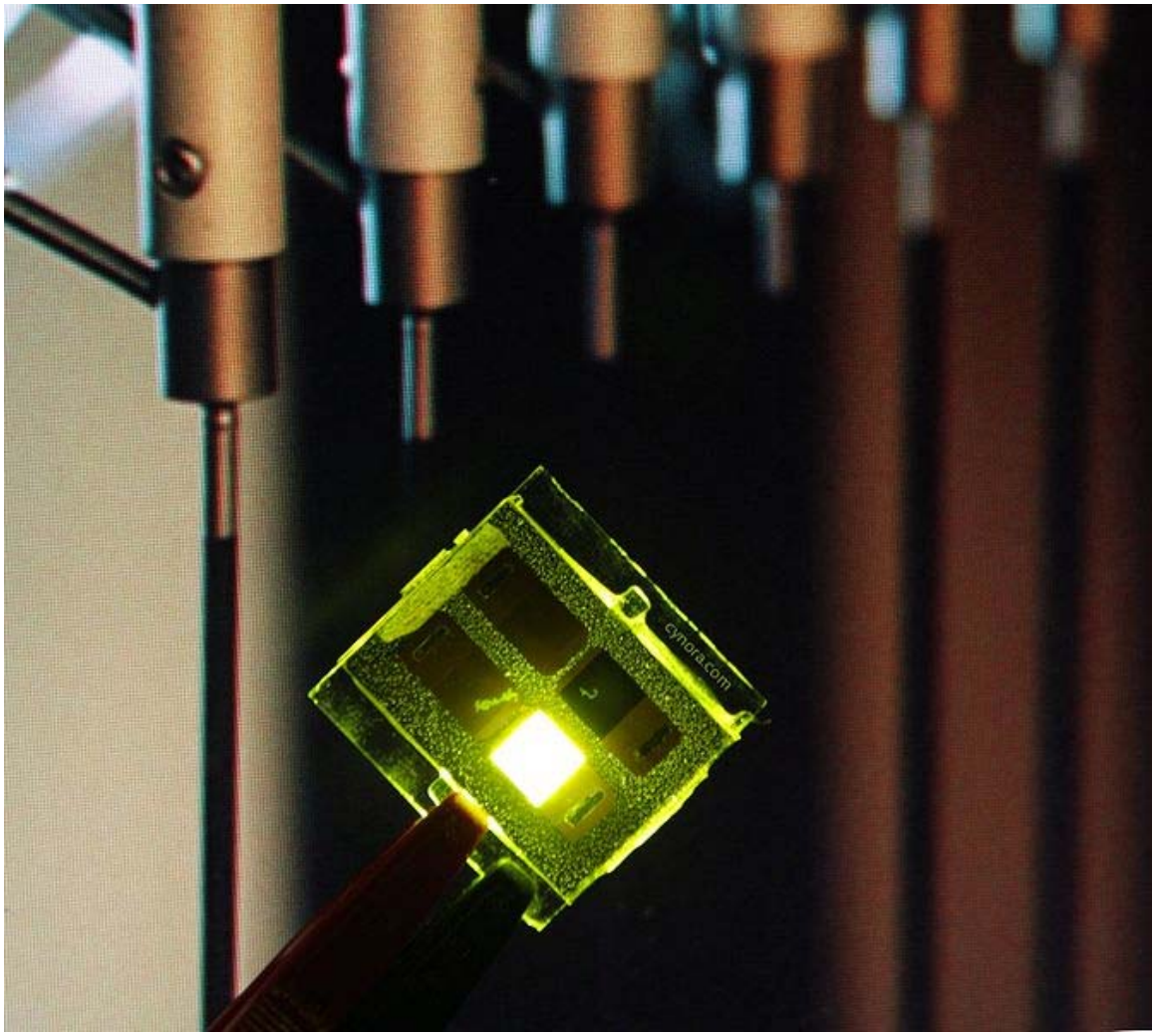

A green emitting OLED device

Sony XEL-1, the world's first OLED TV.

An **organic light emitting diode** (**OLED**) is a light-emitting diode (LED) in which the emissive electroluminescent layer is a film of organic compounds which emit light in response to an electric current. This layer of organic semiconductor material is situated between two electrodes. Generally, at least one of these electrodes is transparent.

OLEDs are used in television screens, computer monitors, small, portable system screens such as mobile phones and PDAs, watches, advertising, information and indication. OLEDs are also used in light sources for general space illumination and in large-area light-emitting elements. Due to their comparatively early stage of development, they typically emit less light per unit area than inorganic solid-state based LED point-light sources.

An OLED display functions without a backlight. Thus, it can display deep black levels and can also be thinner and lighter than established liquid crystal displays. Similarly, in low ambient light conditions such as dark rooms, an OLED screen can achieve a higher contrast ratio than an LCD screen using either cold cathode fluorescent lamps or the more recently developed LED backlight.

There are two main families of OLEDs: those based upon small molecules and those employing polymers. Adding mobile ions to an OLED creates a Light-emitting Electrochemical Cell or LEC, which has a slightly different mode of operation.

OLED displays can use either passive-matrix (PMOLED) or active-matrix addressing schemes. Active-matrix OLEDs (AMOLED) require a thin-film transistor backplane to switch each individual pixel on or off, and can make higher resolution and larger size displays possible.

History

The first observations of electroluminescence in organic materials were in the early 1950s by A. Bernanose and co-workers at the Nancy-Université, France. They applied high-voltage alternating current (AC) fields in air to materials such as acridine orange, either deposited on or dissolved in cellulose or cellophane thin films. The proposed mechanism was either direct excitation of the dye molecules or excitation of electrons.

In 1960, Martin Pope and co-workers at New York University developed ohmic dark-injecting electrode contacts to organic crystals. They further described the necessary energetic requirements (work functions) for hole and electron injecting electrode contacts. These contacts are the basis of charge injection in all modern OLED devices. Pope's group also first observed direct current (DC) electroluminescence under vacuum on a pure single crystal of anthracene and on anthracene crystals doped with tetracene in 1963 using a small area silver electrode at 400V. The proposed mechanism was field-accelerated electron excitation of molecular fluorescence.

Pope's group reported in 1965 that in the absence of an external electric field, the electroluminescence in anthracene crystals is caused by the recombination of a thermalized electron and hole, and that the conducting level of anthracene is higher in energy than the exciton energy level. Also in 1965, W. Helfrich and W. G. Schneider of the National Research Council in Canada produced double injection recombination electroluminescence for the first time in an anthracene single crystal using hole and electron injecting electrodes, the forerunner of modern double injection devices. In the same year, Dow Chemical researchers patented a method of preparing electroluminescent cells using high voltage (500–1500 V) AC-driven (100–3000 Hz) electrically-insulated one millimetre thin layers of a melted phosphor consisting of ground anthracene powder, tetracene, and graphite powder. Their proposed mechanism involved electronic excitation at the contacts between the graphite particles and the anthracene molecules.

Device performance was limited by the poor electrical conductivity of contemporary organic materials. However this was overcome by the discovery and development of highly conductive polymers.

Electroluminescence from polymer films was first observed by Roger Partridge at the National Physical Laboratory in the United Kingdom. The device consisted of a film of

poly(n-vinylcarbazole) up to 2.2 micrometres thick located between two charge injecting electrodes. The results of the project were patented in 1975 and published in 1983.

The first diode device was reported at Eastman Kodak by Ching W. Tang and Steven Van Slyke in 1987. This device used a novel two-layer structure with separate hole transporting and electron transporting layers such that recombination and light emission occurred in the middle of the organic layer. This resulted in a reduction in operating voltage and improvements in efficiency and led to the current era of OLED research and device production.

Research into polymer electroluminescence culminated in 1990 with J. H. Burroughes *et al.* at the Cavendish Laboratory in Cambridge reporting a high efficiency green light-emitting polymer based device using 100 nm thick films of poly(p-phenylene vinylene).

Working principle

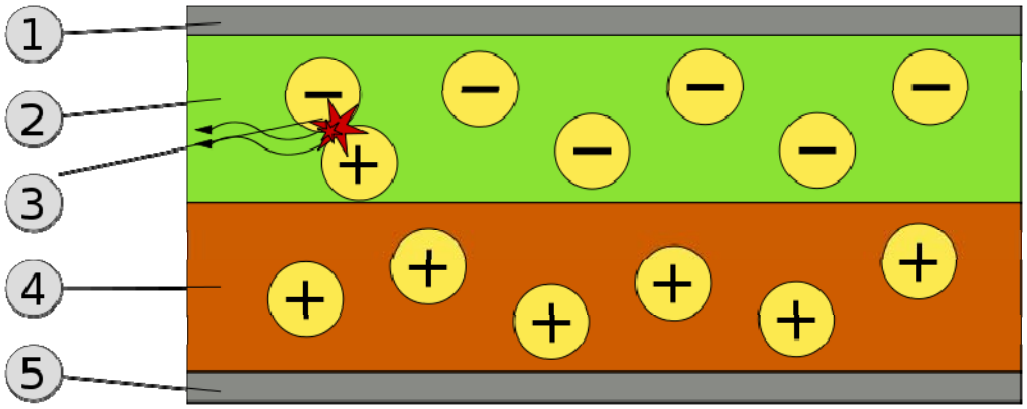

Schematic of a bilayer OLED: 1. Cathode (−), 2. Emissive Layer, 3. Emission of radiation, 4. Conductive Layer, 5. Anode (+)

A typical OLED is composed of a layer of organic materials situated between two electrodes, the anode and cathode, all deposited on a substrate. The organic molecules are electrically conductive as a result of delocalization of pi electrons caused by conjugation over all or part of the molecule. These materials have conductivity levels ranging from insulators to conductors, and therefore are considered organic semiconductors. The highest occupied and lowest unoccupied molecular orbitals (HOMO and LUMO) of organic semiconductors are analogous to the valence and conduction bands of inorganic semiconductors.

Originally, the most basic polymer OLEDs consisted of a single organic layer. One example was the first light-emitting device synthesised by J. H. Burroughes *et al.*, which involved a single layer of poly(p-phenylene vinylene). However multilayer OLEDs can be fabricated with two or more layers in order to improve device efficiency. As well as conductive properties, different materials may be chosen to aid charge injection at

electrodes by providing a more gradual electronic profile, or block a charge from reaching the opposite electrode and being wasted. Many modern OLEDs incorporate a simple bilayer structure, consisting of a conductive layer and an emissive layer.

During operation, a voltage is applied across the OLED such that the anode is positive with respect to the cathode. A current of electrons flows through the device from cathode to anode, as electrons are injected into the LUMO of the organic layer at the cathode and withdrawn from the HOMO at the anode. This latter process may also be described as the injection of electron holes into the HOMO. Electrostatic forces bring the electrons and the holes towards each other and they recombine forming an exciton, a bound state of the electron and hole. This happens closer to the emissive layer, because in organic semiconductors holes are generally more mobile than electrons. The decay of this excited state results in a relaxation of the energy levels of the electron, accompanied by emission of radiation whose frequency is in the visible region. The frequency of this radiation depends on the band gap of the material, in this case the difference in energy between the HOMO and LUMO.

As electrons and holes are fermions with half integer spin, an exciton may either be in a singlet state or a triplet state depending on how the spins of the electron and hole have been combined. Statistically three triplet excitons will be formed for each singlet exciton. Decay from triplet states (phosphorescence) is spin forbidden, increasing the timescale of the transition and limiting the internal efficiency of fluorescent devices. Phosphorescent organic light-emitting diodes make use of spin–orbit interactions to facilitate intersystem crossing between singlet and triplet states, thus obtaining emission from both singlet and triplet states and improving the internal efficiency.

Indium tin oxide (ITO) is commonly used as the anode material. It is transparent to visible light and has a high work function which promotes injection of holes into the HOMO level of the organic layer. A typical conductive layer may consist of PEDOT:PSS as the HOMO level of this material generally lies between the workfunction of ITO and the HOMO of other commonly used polymers, reducing the energy barriers for hole injection. Metals such as barium and calcium are often used for the cathode as they have low work functions which promote injection of electrons into the LUMO of the organic layer. Such metals are reactive, so require a capping layer of aluminium to avoid degradation.

Single carrier devices are typically used to study the kinetics and charge transport mechanisms of an organic material and can be useful when trying to study energy transfer processes. As current through the device is composed of only one type of charge carrier, either electrons or holes, recombination does not occur and no light is emitted. For example, electron only devices can be obtained by replacing ITO with a lower work function metal which increases the energy barrier of hole injection. Similarly, hole only devices can be made by using a cathode comprised solely of aluminium, resulting in an energy barrier too large for efficient electron injection.

Material technologies

Small molecules

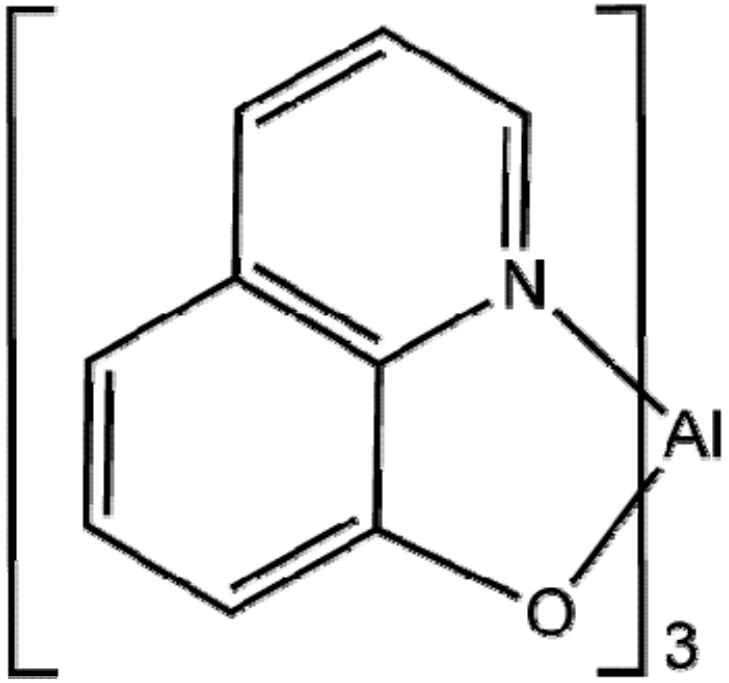

Alq_3, commonly used in small molecule OLEDs.

Efficient OLEDs using small molecules were first developed by Dr. Ching W. Tang *et al.* at Eastman Kodak. The term OLED traditionally refers specifically to this type of device, though the term SM-OLED is also in use.

Molecules commonly used in OLEDs include organometallic chelates (for example Alq_3, used in the organic light-emitting device reported by Tang *et al.*), fluorescent and phosphorescent dyes and conjugated dendrimers. A number of materials are used for their charge transport properties, for example triphenylamine and derivatives are commonly used as materials for hole transport layers. Fluorescent dyes can be chosen to obtain light emission at different wavelengths, and compounds such as perylene, rubrene and quinacridone derivatives are often used. Alq_3 has been used as a green emitter, electron transport material and as a host for yellow and red emitting dyes.

The production of small molecule devices and displays usually involves thermal evaporation in a vacuum. This makes the production process more expensive and of limited use for large-area devices than other processing techniques. However, contrary to polymer-based devices, the vacuum deposition process enables the formation of well controlled, homogeneous films, and the construction of very complex multi-layer structures. This high flexibility in layer design, enabling distinct charge transport and charge blocking layers to be formed, is the main reason for the high efficiencies of the small molecule OLEDs.

Coherent emission from a laser dye-doped tandem SM-OLED device, excited in the pulsed regime, has been demonstrated. The emission is nearly diffraction limited with a spectral width similar to that of broadband dye lasers.

Polymer light-emitting diodes

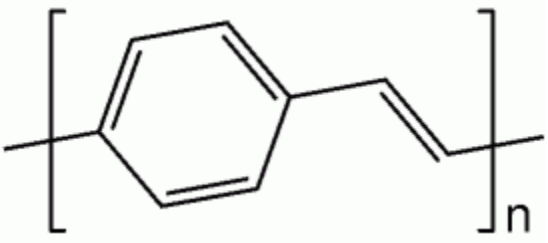

poly(*p*-phenylene vinylene), used in the first PLED.

Polymer light-emitting diodes (PLED), also light-emitting polymers (LEP), involve an electroluminescent conductive polymer that emits light when connected to an external voltage. They are used as a thin film for full-spectrum colour displays. Polymer OLEDs are quite efficient and require a relatively small amount of power for the amount of light produced.

Vacuum deposition is not a suitable method for forming thin films of polymers. However, polymers can be processed in solution, and spin coating is a common method of depositing thin polymer films. This method is more suited to forming large-area films than thermal evaporation. No vacuum is required, and the emissive materials can also be applied on the substrate by a technique derived from commercial inkjet printing. However, as the application of subsequent layers tends to dissolve those already present, formation of multilayer structures is difficult with these methods. The metal cathode may still need to be deposited by thermal evaporation in vacuum.

Typical polymers used in PLED displays include derivatives of poly(*p*-phenylene vinylene) and polyfluorene. Substitution of side chains onto the polymer backbone may determine the colour of emitted light or the stability and solubility of the polymer for performance and ease of processing.

While unsubstituted poly(p-phenylene vinylene) (PPV) is typically insoluble, a number of PPVs and related poly(naphthalene vinylene)s (PNVs) that are soluble in organic solvents or water have been prepared via ring opening metathesis polymerization.

Phosphorescent materials

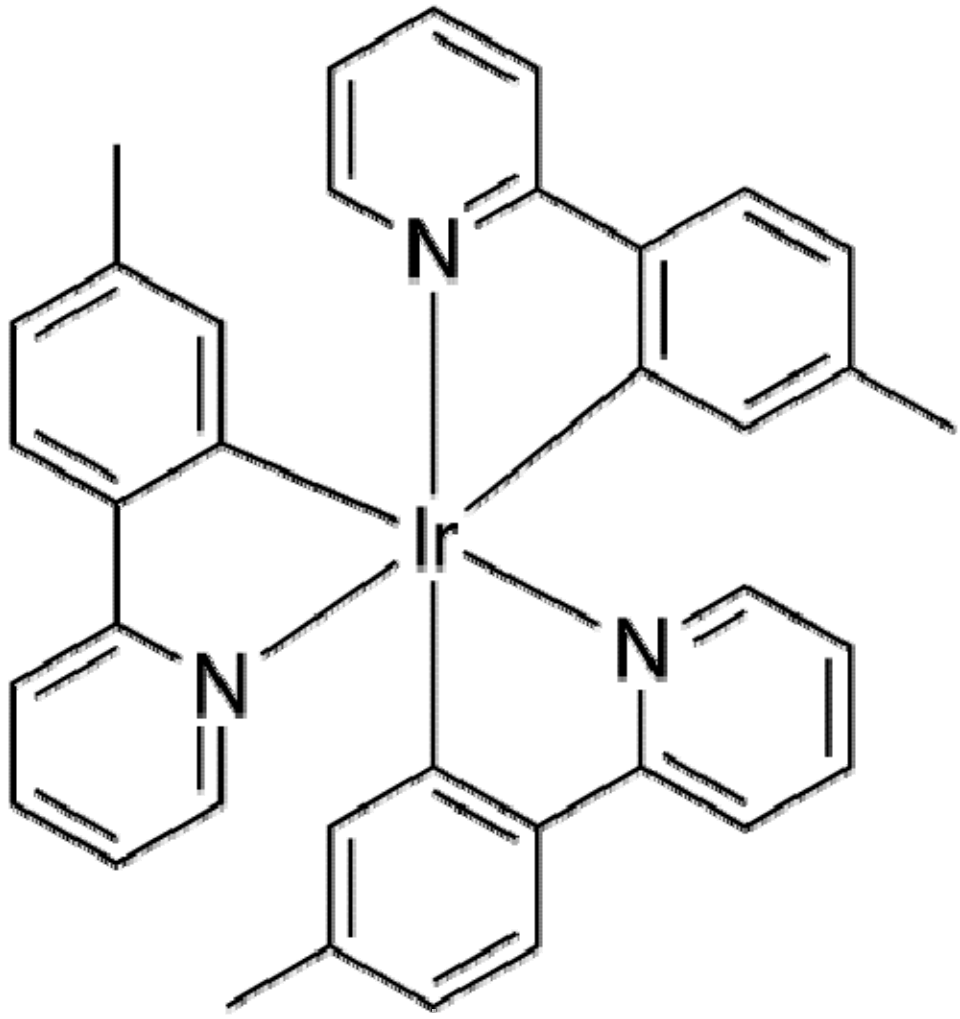

$Ir(mppy)_3$, a phosphorescent dopant which emits green light.

Phosphorescent organic light emitting diodes use the principle of electrophosphorescence to convert electrical energy in an OLED into light in a highly efficient manner, with the internal quantum efficiencies of such devices approaching 100%.

Typically, a polymer such as poly(n-vinylcarbazole) is used as a host material to which an organometallic complex is added as a dopant. Iridium complexes such as $Ir(mppy)_3$ are currently the focus of research, although complexes based on other heavy metals such as platinum have also been used.

The heavy metal atom at the centre of these complexes exhibits strong spin-orbit coupling, facilitating intersystem crossing between singlet and triplet states. By using these phosphorescent materials, both singlet and triplet excitons will be able to decay radiatively, hence improving the internal quantum efficiency of the device compared to a standard PLED where only the singlet states will contribute to emission of light.

Applications of OLEDs in solid state lighting require the achievement of high brightness with good CIE coordinates (for white emission). The use of macromolecular species like polyhedral oligomeric silsesquioxanes (POSS) in conjunction with the use of phosphorescent species such as Ir for printed OLEDs have exhibited brightnesses as high as 10,000 cd/m^2.

Device Architectures

Structure

- **Bottom or top emission:** Bottom emission devices use a transparent or semi-transparent bottom electrode to get the light through a transparent substrate. Top emission devices use a transparent or semi-transparent top electrode emitting light directly. Top-emitting OLEDs are better suited for active-matrix applications as they can be more easily integrated with a non-transparent transistor backplane.

- **Transparent OLEDs** use transparent or semi-transparent contacts on both sides of the device to create displays that can be made to be both top and bottom emitting (transparent). TOLEDs can greatly improve contrast, making it much easier to view displays in bright sunlight. This technology can be used in Head-up displays, smart windows or augmented reality applications. Novaled's OLED panel presented in Finetech Japan 2010, boasts a transparency of 60-70%.

- **Stacked OLEDs** use a pixel architecture that stacks the red, green, and blue subpixels on top of one another instead of next to one another, leading to substantial increase in gamut and color depth, and greatly reducing pixel gap. Currently, other display technologies have the RGB (and RGBW) pixels mapped next to each other decreasing potential resolution.

- **Inverted OLED:** In contrast to a conventional OLED, in which the anode is placed on the substrate, an Inverted OLED uses a bottom cathode that can be connected to the drain end of an n-channel TFT especially for the low cost amorphous silicon TFT backplane useful in the manufacturing of AMOLED displays.

Patterning technologies

Patternable organic light-emitting devices use a light or heat activated electroactive layer. A latent material (PEDOT-TMA) is included in this layer that, upon activation, becomes highly efficient as a hole injection layer. Using this process, light-emitting devices with arbitrary patterns can be prepared.

Colour patterning can be accomplished by means of laser, such as radiation-induced sublimation transfer (RIST).

Organic vapour jet printing (OVJP) uses an inert carrier gas, such as argon or nitrogen, to transport evaporated organic molecules (as in Organic Vapor Phase Deposition). The gas is expelled through a micron sized nozzle or nozzle array close to the substrate as it is being translated. This allows printing arbitrary multilayer patterns without the use of solvents.

Conventional OLED displays are formed by vapor thermal evaporation (VTE) and are patterned by shadow-mask. A mechanical mask has openings allowing the vapor to pass only on the desired location.

Backplane technologies

For a high resolution display like a TV, a TFT backplane is necessary to drive the pixels correctly. Currently, Low Temperature Polycrystalline silicon LTPS-TFT is used for commercial AMOLED displays. LTPS-TFT has variation of the performance in a display, so various compensation circuits have been reported. Due to the size limitation of the excimer laser used for LTPS, the AMOLED size was limited. To cope with the hurdle related to the panel size, amorphous-silicon/microcrystalline-silicon backplanes have been reported with large display prototype demonstrations.

Advantages

Demonstration of a 4.1" prototype flexible display from Sony

The different manufacturing process of OLEDs lends itself to several advantages over flat-panel displays made with LCD technology.

- **Lower cost in the future:** OLEDs can be printed onto any suitable substrate by an inkjet printer or even by screen printing,theoretically making them cheaper to produce than LCD or plasma displays. However, fabrication of the OLED substrate is more costly than that of a TFT LCD, until mass production methods lower cost through scaleability.

- **Light weight & flexible plastic substrates:** OLED displays can be fabricated on flexible plastic substrates leading to the possibility of Organic light-emitting diode roll-up display being fabricated or other new applications such as roll-up displays

embedded in fabrics or clothing. As the substrate used can be flexible such as PET., the displays may be produced inexpensively.

- **Wider viewing angles & improved brightness:** OLEDs can enable a greater artificial contrast ratio (both dynamic range and static, measured in purely dark conditions) and viewing angle compared to LCDs because OLED pixels directly emit light. OLED pixel colours appear correct and unshifted, even as the viewing angle approaches 90 degrees from normal.

- **Better power efficiency:** LCDs filter the light emitted from a backlight, allowing a small fraction of light through so they cannot show true black, while an inactive OLED element does not produce light or consume power.

- **Response time:** OLEDs can also have a faster response time than standard LCD screens. Whereas LCD displays are capable of a 1 ms response time or less offering a frame rate of 1,000 Hz or higher, an OLED can theoretically have less than 0.01 ms response time enabling 100,000 Hz refresh rates.

Disadvantages

LEP display showing partial failure

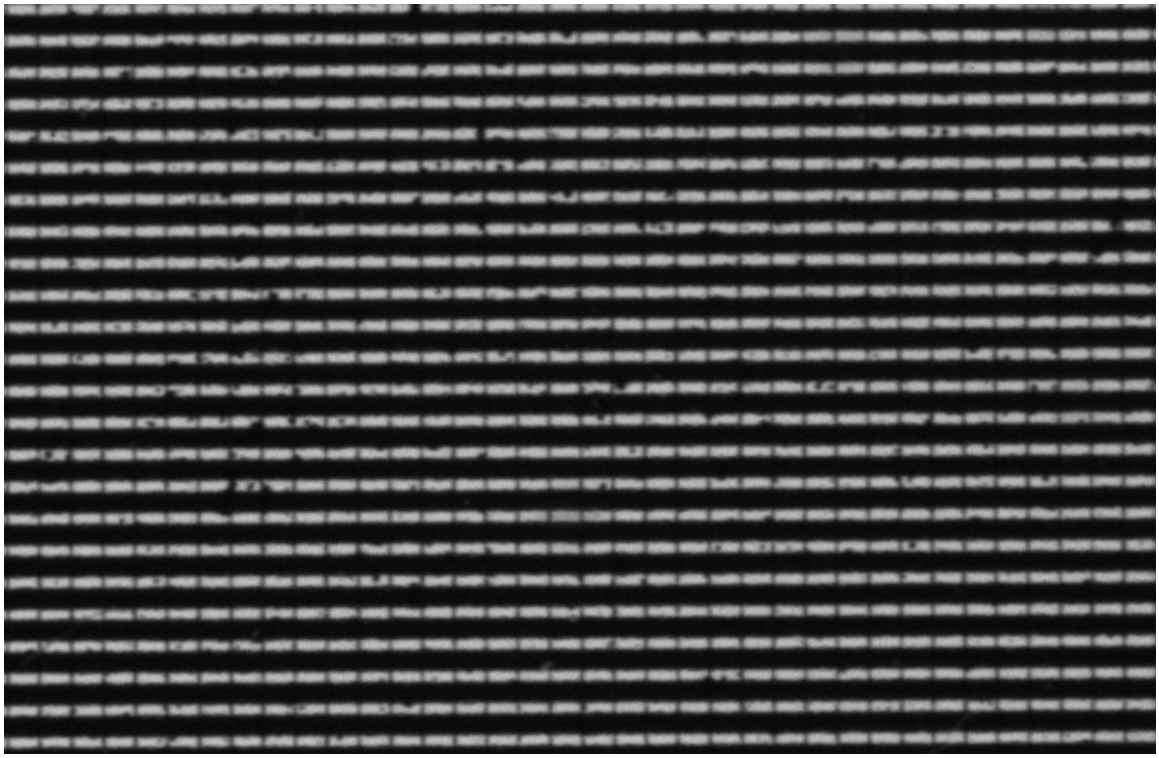

An old OLED display showing wear

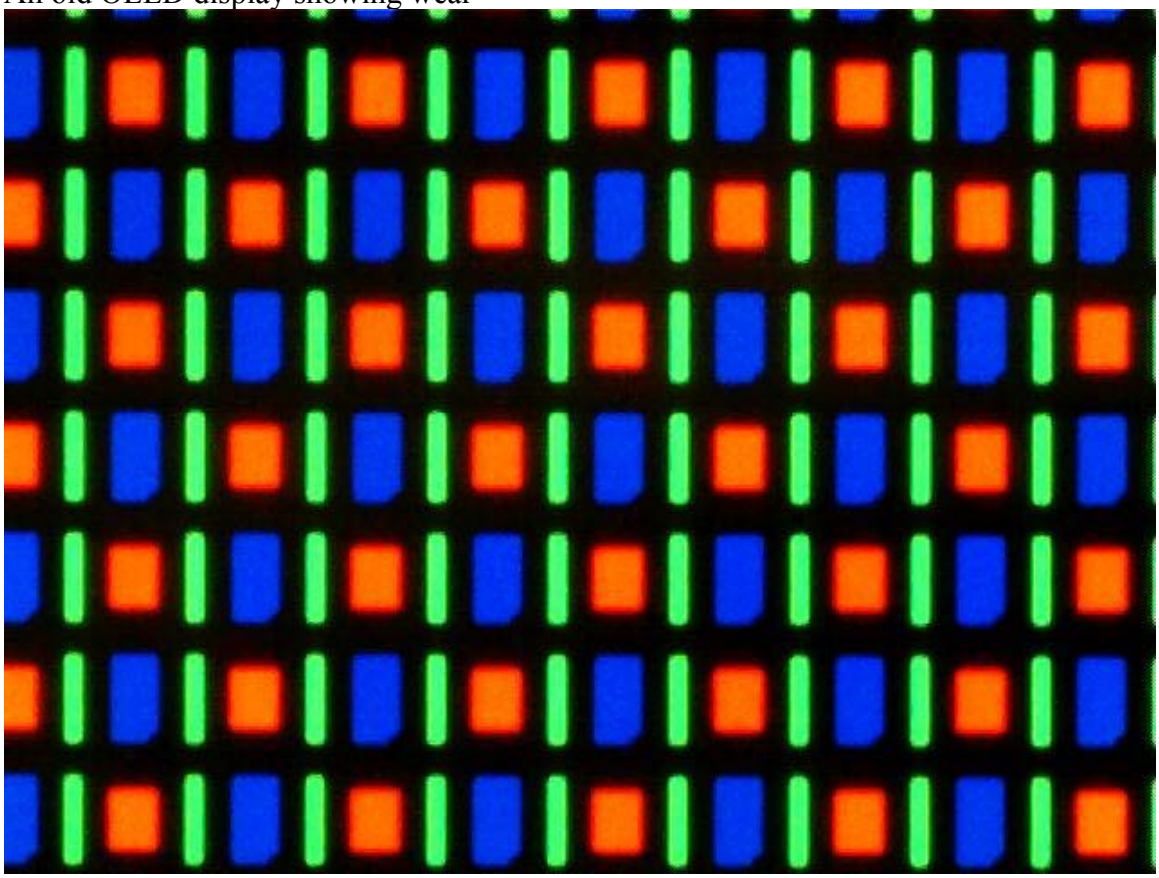

Magnified image of the AMOLED screen on the Google Nexus One smartphone using the RGBG system of the PenTile Matrix Family.

- **Lifespan:** The biggest technical problem for OLEDs was the limited lifetime of the organic materials. In particular, blue OLEDs historically have had a lifetime of around 14,000 hours to half original brightness (five years at 8 hours a day) when used for flat-panel displays. This is lower than the typical lifetime of LCD, LED or PDP technology—each currently rated for about 60,000 hours to half brightness, depending on manufacturer and model. However, some manufacturers' displays aim to increase the lifespan of OLED displays, pushing their expected life past that of LCD displays by improving light outcoupling, thus achieving the same brightness at a lower drive current. In 2007, experimental OLEDs were created which can sustain 400 cd/m^2 of luminance for over 198,000 hours for green OLEDs and 62,000 hours for blue OLEDs.

- **Color balance issues:** Additionally, as the OLED material used to produce blue light degrades significantly more rapidly than the materials that produce other colors, blue light output will decrease relative to the other colors of light. This differential color output change will change the color balance of the display and is much more noticeable than a decrease in overall luminance. This can be partially avoided by adjusting colour balance but this may require advanced control circuits and interaction with the user, which is unacceptable for some users. In order to delay the problem, manufacturers bias the colour balance towards blue so that the display initially has an artificially blue tint, leading to complaints of artificial-looking, over-saturated colors. More commonly, though, manufacturers optimize the size of the R, G and B subpixels to reduce the current density through the subpixel in order to equalize lifetime at full luminance. For example, a blue subpixel may be 100% larger than the green subpixel. The red subpixel may be 10% smaller than the green.

- **Efficiency of blue OLEDs:** Improvements to the efficiency and lifetime of blue OLED's is vital to the success of OLED's as replacements for LCD technology. Considerable research has been invested in developing blue OLEDs with high external quantum efficiency as well as a deeper blue color. External quantum efficiency values of 20% and 19% have been reported for red (625 nm) and green (530 nm) diodes, respectively. However, blue diodes (430 nm) have only been able to achieve maximum external quantum efficiencies in the range between 4% to 6%. By calculating the band gap ($E_g = hc/\lambda$), it is clear that the shorter wavelength of the blue OLED results in a larger band gap at 2.9 eV. This leads to higher barriers, causing lower efficiency.

- **Water damage:** Water can damage the organic materials of the displays. Therefore, improved sealing processes are important for practical manufacturing. Water damage may especially limit the longevity of more flexible displays.

- **Outdoor performance:** As an emissive display technology, OLEDs rely completely upon converting electricity to light, unlike most LCDs which are to some extent reflective; e-ink leads the way in efficiency with ~ 33% ambient light reflectivity, enabling the display to be used without any internal light source. The

metallic cathode in an OLED acts as a mirror, with reflectance approaching 80%, leading to poor readability in bright ambient light such as outdoors. However, with the proper application of a circular polarizer and anti-reflective coatings, the diffuse reflectance can be reduced to less than 0.1%. With 10,000 fc incident illumination (typical test condition for simulating outdoor illumination), that yields an approximate photopic contrast of 5:1.

- **Power consumption:** While an OLED will consume around 40% of the power of an LCD displaying an image which is primarily black, for the majority of images it will consume 60–80% of the power of an LCD - however it can use over three times as much power to display an image with a white background such as a document or website. This can lead to disappointing real-world battery life in mobile devices. Websites and tools exist to help disappointed mobile phone users display a black background in places where it would normally be white. For example, the mobile Google search engine can now be used in black to save battery power by using a custom version called Black Google Mobile.

- **Screen burn-in:** Unlike displays with a common light source, the brightness of each OLED pixel fades depending on the content displayed. The varied lifespan of the organic dyes can cause a discrepancy between red, green, and blue intensity. This leads to image persistence, also known as burn-in.

Manufacturers and Commercial Uses

A 3.8 cm (1.5 in) OLED display from a Creative ZEN V media player

OLED technology is used in commercial applications such as displays for mobile phones and portable digital media players, car radios and digital cameras among others. Such portable applications favor the high light output of OLEDs for readability in sunlight and their low power drain. Portable displays are also used intermittently, so the lower lifespan of organic displays is less of an issue. Prototypes have been made of flexible and rollable displays which use OLEDs' unique characteristics. Applications in flexible signs and lighting are also being developed. Philips Lighting have made OLED lighting samples under the brand name 'Lumiblade' available online.

OLEDs have been used in most Motorola and Samsung colour cell phones, as well as some HTC, LG and Sony Ericsson models. Nokia has also recently introduced some OLED products including the N85 and the N86 8MP, both of which feature an AMOLED display. OLED technology can also be found in digital media players such as the Creative ZEN V, the iriver clix, the Zune HD and the Sony Walkman X Series.

The Google and HTC Nexus One smartphone includes an AMOLED screen, as does HTC's own Desire and Legend phones. However due to supply shortages of the Samsung-produced displays, certain HTC models will use Sony's SLCD displays in the future.

The Google and Samsung Nexus S smartphone includes a Super AMOLED screen, as does Samsung's own Galaxy S phone. However due to supply shortages of the Samsung-produced displays certain countries, such as Russia, will have Nexus S models that use "Super Clear LCD" instead; the same display used by Samsung for its new Wave II S8530.

Other manufacturers of OLED panels include Anwell Technologies Limited, Chi Mei Corporation, LG, and others.

DuPont stated in a press release in May 2010 that they can produce a 50-inch OLED TV in two minutes with a new printing technology. If this can be scaled up in terms of manufacturing, then the total cost of OLED TVs would be greatly reduced. Dupont also states that OLED TVs made with this less expensive technology can last up to 15 years if left on for a normal eight hour day.

Handheld computer manufacturer OQO introduced the smallest Windows netbook computer, including an OLED display, in 2009.

The use of OLEDs may be subject to patents held by Eastman Kodak, DuPont, General Electric, Royal Philips Electronics, numerous universities and others. There are by now literally thousands of patents associated with OLEDs, both from larger corporations and smaller technology companies.

Samsung applications

By 2004 Samsung, South Korea's largest conglomerate, was the world's largest OLED manufacturer, producing 40% of the OLED displays made in the world, and as of 2010 has a 98% share of the global AMOLED market. The company is leading the world OLED industry, generating $100.2 million out of the total $475 million revenues in the global OLED market in 2006. As of 2006, it held more than 600 American patents and more than 2800 international patents, making it the largest owner of AMOLED technology patents.

Samsung SDI announced in 2005 the world's largest OLED TV at the time, at 21 inches (53 cm). This OLED featured the highest resolution at the time, of 6.22 million pixels. In addition, the company adopted active matrix based technology for its low power consumption and high-resolution qualities. This was exceeded in January 2008, when Samsung showcased the world's largest and thinnest OLED TV at the time, at 31 inches and 4.3 mm.

In May 2008, Samsung unveiled an ultra-thin 12.1 inch laptop OLED display concept, with a 1,280×768 resolution with infinite contrast ratio. According to Woo Jong Lee, Vice President of the Mobile Display Marketing Team at Samsung SDI, the company expected OLED displays to be used in notebook PCs as soon as 2010.

In October 2008, Samsung showcased the world's thinnest OLED display, also the first to be 'flappable' and bendable. It measures just 0.05 mm (thinner than paper), yet a Samsung staff member said that it is "technically possible to make the panel thinner". To achieve this thickness, Samsung etched an OLED panel that uses a normal glass substrate. The drive circuit was formed by low-temperature polysilicon TFTs. Also, low-molecular organic EL materials were employed. The pixel count of the display is 480 × 272. The contrast ratio is 100,000:1, and the luminance is 200 cd/m². The colour reproduction range is 100% of the NTSC standard.

In the same month, Samsung unveiled what was then the world's largest OLED Television at 40-inch with a Full HD resolution of 1920×1080 pixel. In the FPD International, Samsung stated that its 40-inch OLED Panel is the largest size currently possible. The panel has a contrast ratio of 1,000,000:1, a colour gamut of 107% NTSC, and a luminance of 200 cd/m² (peak luminance of 600 cd/m²).

At the Consumer Electronics Show (CES) in January 2010, Samsung demonstrated a laptop computer with a large, transparent OLED display featuring up to 40% transparency and an animated OLED display in a photo ID card.

Samsung's latest AMOLED smartphones use their Super AMOLED trademark, with the Samsung Wave S8500 and Samsung i9000 Galaxy S being launched in June 2010.

Sony applications

Sony XEL-1, the world's first OLED TV. (front)

Sony XEL-1 (side)

The Sony CLIÉ PEG-VZ90 was released in 2004, being the first PDA to feature an OLED screen. Other Sony products to feature OLED screens include the MZ-RH1 portable minidisc recorder, released in 2006 and the Walkman X Series.

At the Las Vegas CES 2007, Sony showcased 11-inch (28 cm, resolution 960×540) and 27-inch (68.5 cm, full HD resolution at 1920×1080) OLED TV models. Both claimed 1,000,000:1 contrast ratios and total thicknesses (including bezels) of 5 mm. In April 2007, Sony announced it would manufacture 1000 11-inch OLED TVs per month for market testing purposes. On October 1, 2007, Sony announced that the 11-inch model, now called the XEL-1, would be released commercially; the XEL-1 was first released in Japan in December 2007.

In May 2007, Sony publicly unveiled a video of a 2.5-inch flexible OLED screen which is only 0.3 millimeters thick. At the Display 2008 exhibition, Sony demonstrated a 0.2 mm thick 3.5 inch display with a resolution of 320×200 pixels and a 0.3 mm thick 11 inch display with 960×540 pixels resolution, one-tenth the thickness of the XEL-1.

In July 2008, a Japanese government body said it would fund a joint project of leading firms, which is to develop a key technology to produce large, energy-saving organic displays. The project involves one laboratory and 10 companies including Sony Corp.

NEDO said the project was aimed at developing a core technology to mass-produce 40 inch or larger OLED displays in the late 2010s.

In October 2008, Sony published results of research it carried out with the Max Planck Institute over the possibility of mass-market bending displays, which could replace rigid LCDs and plasma screens. Eventually, bendable, transparent OLED screens could be stacked to produce 3D images with much greater contrast ratios and viewing angles than existing products.

Sony exhibited a 24.5" prototype OLED 3D television during the Consumer Electronics Show in January 2010.

LG applications

Since 2010 LG sells one 15" OLED TV, the 15EL9500 and has announced a 31" OLED 3D TV for March 2011.

Range of OLED screens sizes in production products

- Media Player - 2.2" to 3.3" - various
- Mobile Phone - 2.6" to 4.1" - various
- Tablet - none
- Laptop - none
- PC monitor - none
- TV - 11" to 15" - Sony XEL-1 and LG 15EL9500

Chapter- 7

Organic Field-Effect Transistor

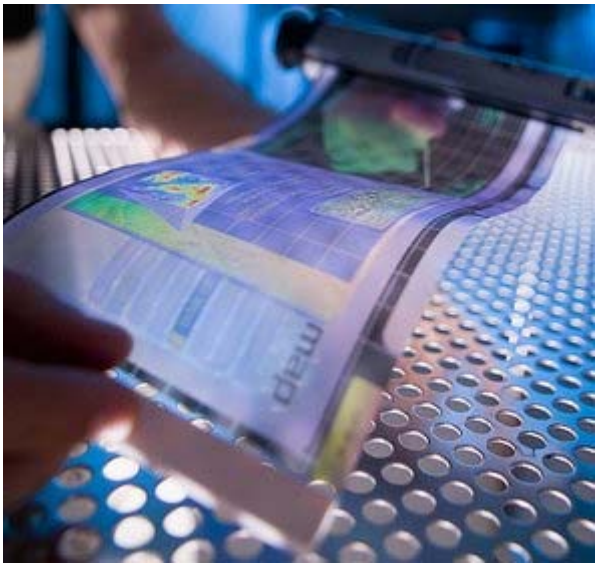

OFET-based flexible display

An **organic field-effect transistor (OFET)** is a field effect transistor using an organic semiconductor in its channel. OFETs can be prepared either by vacuum evaporation of small molecules, by solution-casting of polymers or small molecules, or by mechanical transfer of a peeled single-crystalline organic layer onto a substrate. These devices have been developed to realize low-cost, large-area electronic products. OFETs have been fabricated with various device geometries. The most commonly used device geometry is bottom gate with top drain- and source electrodes, because this geometry is similar to the thin-film silicon transistor (TFT) using thermally grown Si/SiO_2 oxide as gate dielectric. Organic polymers, such as poly(methyl-methacrylate) (PMMA), can be used as dielectric, too.

In May 2007, Sony reported the first full-color, video-rate, flexible, all plastic display, in which both the thin film transistors and the light emitting pixels were made of organic materials.

History of OFETs

The field-effect transistor (FET) was first proposed by J.E. Lilienfeld, who received a patent for his idea in 1930. He proposed that a field-effect transistor behaves as a capacitor with a conducting channel between a source and a drain electrode. Applied voltage on the gate electrode controls the amount of charge carriers flowing through the system.

The first field-effect transistor was designed and prepared in 1960 by Kahng and Atalla using a metal-oxide-semiconductor. However, rising costs of materials and manufacturing, as well as public interest in more environmentally friendly electronics materials have supported development of organic based electronics in more recent years. In 1987, Koezuka and co-workers reported the first organic field-effect transistor based on a polymer of thiophene molecules. The thiophene polymer is a type of conjugated polymer that is able to conduct charge, eliminating the need to use expensive metal oxide semiconductors. Additionally, other conjugated polymers have been shown to have semi-conducting properties. OFET design has also improved in the past few decades. Many OFETs are now designed based on the thin-film transistor (TFT) model, which allows the devices to use less conductive materials in their design. Improvement on these models in the past few years have been made to field-effect mobility and on-off current ratios.

Materials

One common feature of OFET materials is the inclusion of an aromatic or otherwise conjugated π-electron system, facilitating the delocalization of orbital wavefunctions. Electron withdrawing groups or donating groups can be attached that facilitate hole or electron transport.

OFETs employing many aromatic and conjugated materials as the active semiconducting layer have been reported, including small molecules such as rubrene, tetracene, pentacene, diindenoperylene, perylenediimides, tetracyanoquinodimethane (TCNQ), and polymers such as polythiophenes (especially poly 3-hexylthiophene (P3HT)), polyfluorene, polydiacetylene, poly 2,5-thienylene vinylene, poly p-phenylene vinylene (PPV).

The field is very active, with newly synthesized and tested compounds reported weekly in prominent research journals. Many review articles exist documenting the development of these materials.

Rubrene-based OFETs show the highest carrier mobility 20–40 $cm^2/(V \cdot s)$. Another popular OFET material is pentacene, which has been used since 1980s, but resulted in about 10 times lower mobilities than rubrene. The major problem with pentacene, as well as many other organic conductors, is its rapid oxidation in air to form pentacene-quinone. However if the pentacene is preoxidized, and the thus formed pentacene-quinone is used

as the gate insulator, then the mobility can approach the rubrene values. This pentacene oxidation technique is akin to the silicon oxidation used in the silicon electronics.

Polycrystalline tetrathiafulvalene and its analogues result in mobilities in the range 0.1–1.4 $cm^2/(V \cdot s)$. However, the mobility exceeds 10 $cm^2/(V \cdot s)$ in solution-grown or vapor-transport-grown single crystalline hexamethylene-tetrathiafulvalene (HMTTF). The ON/OFF voltage is different for devices grown by those two techniques, presumably due to the higher processing temperatures using in the vapor transport grows.

All the above-mentioned devices are based on p-type conductivity. N-type organic OFETs are yet poorly developed. They are usually based on perylenediimides or fullerenes or their derivatives, and show electron mobilities below 2 $cm^2/(V \cdot s)$.

Device design of organic field-effect transistors

Three essential components of field-effect transistors are the source, the drain and the gate. Field-effect transistors usually operate as a capacitor. They are composed of two plates. One plate works as a conducting channel between two ohmic contacts, which are called the source and the drain contacts. The other plate works to control the charge induced into the channel, and it is called the gate. The direction of the movement of the carriers in the channel is from the source to the drain. Hence the relationship between these three components is that the gate controls the carrier movement from the source to the drain.

When this capacitor concept is applied to the device design, various devices can be built up based on the difference in the controller-the gate. This can be the gate material, the location of the gate with respect to the channel, how the gate is isolated from the channel, and what type of carrier is induced by the gate voltage into channel (such as electrons in an n-channel device, holes in a p-channel device, and both electrons and holes in a double injection device).

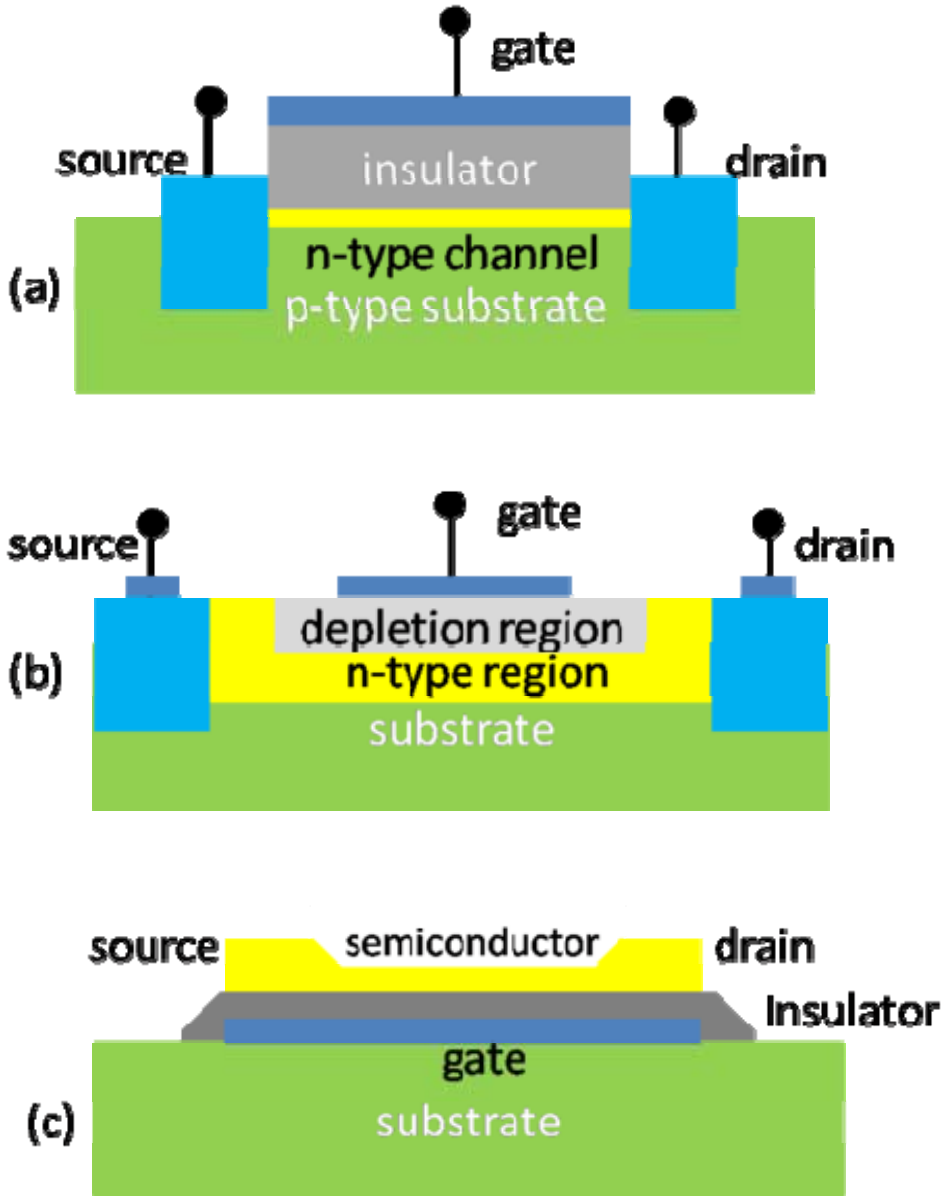

Figure 1 Schematic graphs of three different kinds of Field-Effect Transistor (FET): (a) the metal- insulator -semiconductor FET(MISFET); (b) the metal-semiconductor FET (MESFET); (c) the thin-film transistor (TFT).

Classified by the properties of the carrier, three types of FETs are shown schematically in Figure 1. They are MOSFET (Metal Oxide Semiconductor Field-Effect Transistor), MESFET (MEtal Semiconductor Field-Effect Transistor) and TFT (Thin Film Transistor).

MISFET

The most prominent and widely used FET in modern microelectronics is the MOSFET. There are different kinds in this category, such as MISFET (Metal Insulator

Semiconductor Field-Effect Transistor), and IGFET (Insulator Gate Field-Effect Transistor). The scheme of a MISFET is shown in Figure 1a. The source and the drain are connected by a semiconductor and the gate is separated from the channel by a layer of insulator. If there is no bias (potential difference) applied on the gate, the band bending is induced due to the energy difference of metal conducting band and the semiconductor Fermi-level. Therefore a higher concentration of holes is formed on the interface of the semiconductor and the insulator. When an enough positive bias is applied on the gate contact, the bended band becomes flat. If a larger positive bias is applied, the band bending in the opposite direction occurs and the region close to the insulator-semiconductor interface becomes depleted of holes. Then the depleted region is formed. At an even larger positive bias, the band bending becomes so large that the Fermi-level at the interface of the semiconductor and the insulator becomes closer to the bottom of the conduction band than to the top of the valence band, therefore, it forms an inversion layer of electrons, providing the conducting channel. Finally, it turns the device on.

MESFET

The second type of device is described in Fig.1b. The only difference of this one from the MISFET is that the n-type source and drain are connected by an n-type region. In this case, the depletion region extends all over the n-type channel at zero gate voltage in a normally “off” device (it is similar to the larger positive bias in MISFET case). In the normally “on” device, a portion of the channel is not depleted, and thus leads to passage of a current at zero gate voltage.

TFT

The concept of TFT was first proposed by Paul Weimer in 1962. This is illustrated in Fig. 1c. Here the source and drain electrodes are directly deposited onto the conducting channel (a thin layer of semiconductor) then a thin film of insulator is deposited between the semiconductor and the metal gate contact. This structure suggests that there is no depletion region to separate the device from the substrate. If there is zero bias, the electrons are expelled from the surface due to the Fermi-level energy difference of the semiconductor and the metal. This leads to band bending of semiconductor. In this case, there is no carrier movement between the source and drain. When the positive charge is applied, the accumulation of electrons on the interface leads to the bending of the semiconductor in an opposite way and leads to the lowering of the conduction band with regards to the Fermi-level of the semiconductor. Then a highly conductive channel forms at the interface (shown in Figure 2).

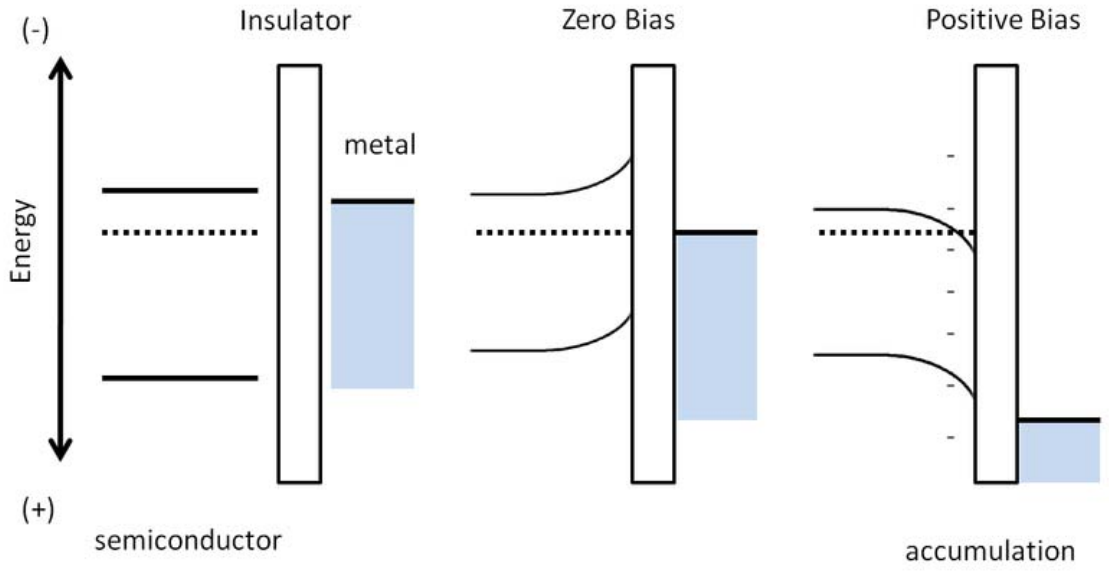

Figure 2: Schematic graphs of band-bending in the TFT device model.

OFET

OFETs adopt the architecture of TFT. With the development of the conducting polymer, the semiconducting properties of small conjugated molecules have been recognized. The interest in OFETs has grown enormously in the past ten years. The reasons for this surge of interest are manifold. The performance of OFETs, which can compete with that of amorphous silicon (a-Si) TFTs with field-effect mobilities of 0.5^{-1} cm^2 V^{-1} s^{-1} and ON/OFF current ratios (which indicate the ability of the device to shut down) of 106–108, has improved significantly. Currently, thin-film OFET mobility values of 5 $cm^2V^{-1}s^{-1}$ in the case of vacuum-deposited small molecules and 0.6 cm^2 V^{-1} s^{-1} for solution-processed polymers have been reported. As a result, there is now a greater industrial interest in using OFETs for applications that are currently incompatible with the use of a-Si or other inorganic transistor technologies. One of their main technological attractions is that all the layers of an OFET can be deposited and patterned at room temperature by a combination of low-cost solution-processing and direct-write printing, which makes them ideally suited for realization of low-cost, large-area electronic functions on flexible substrates.

Device preparation

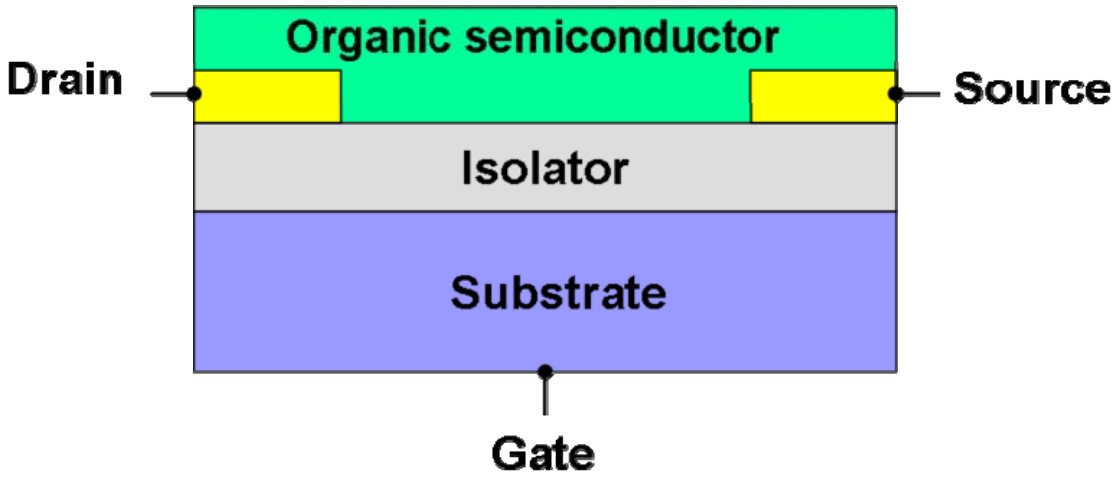

OFET schematic

Thermally oxidized silicon is a traditional substrate for OFETs where the silicon dioxide serves as the gate insulator. The active FET layer is usually deposited onto this substrate using either (i) thermal evaporation, (ii) coating from organic solution, or (iii) electrostatic lamination. The first two techniques result in polycrystalline active layers; they are much easier to produce, but result in relatively poor transistor performance. Numerous variations of the solution coating technique (ii) are known, including dip-coating, spin-coating, inkjet printing and screen printing. The electrostatic lamination technique is based on manual peeling of a thin layer off a single organic crystal; it results in a superior single-crystalline active layer, yet it is more tedious. The thickness of the gate oxide and the active layer is below one micrometer.

Carrier transport

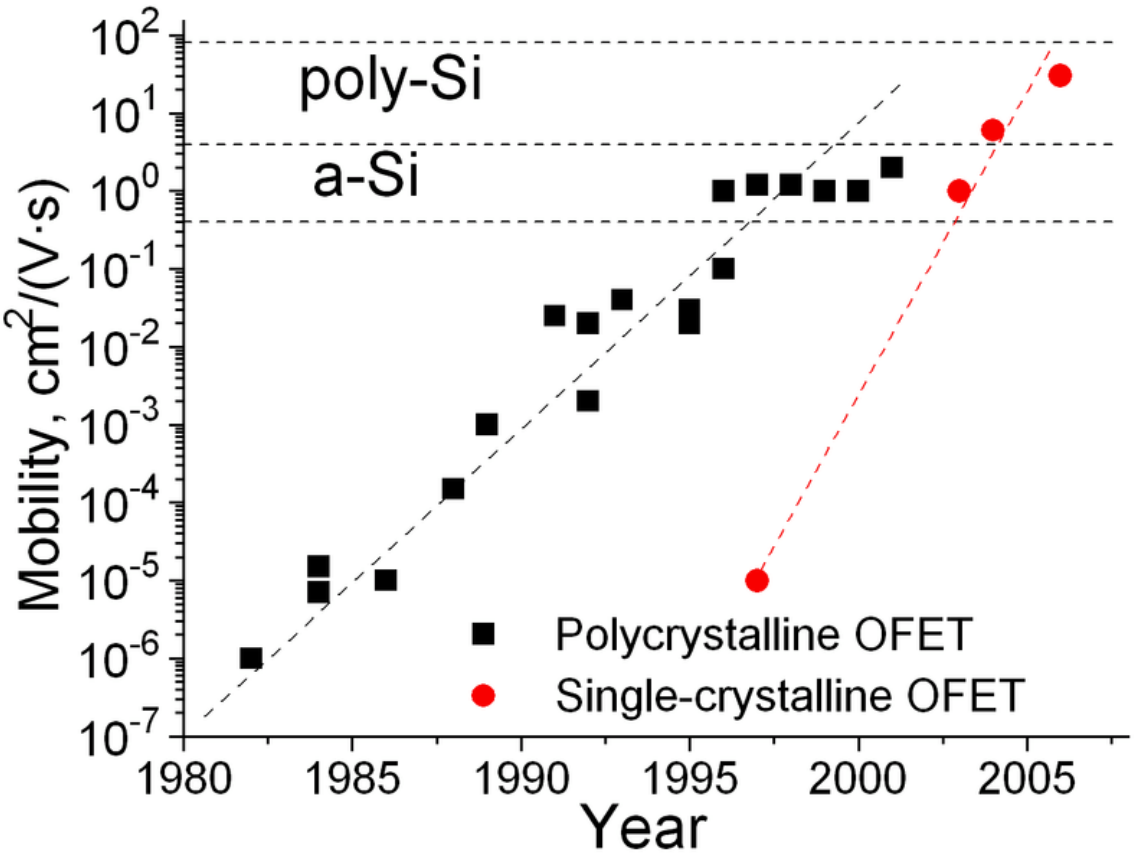

Evolution of carrier mobility in organic field-effect transistor.

The carrier transport in OFET is specific for two-dimensional (2D) carrier propagation through the device. Various experimental techniques were used for this study, such as Haynes - Shockley experiment on the transit times of injected carriers, time-of-flight (TOF) experiment for the determination of carrier mobility, pressure-wave propagation experiment for probing electric-field distribution in insulators, organic monolayer experiment for probing orientational dipolar changes, optical time-resolved second harmonic generation (TRM-SHG), etc. Whereas carriers propagate through polycrystalline OFETs in a diffusion-like (trap-limited) manner, they move through the conduction band in the best single-crystalline OFETs.

The most important parameter of OFET carrier transport is carrier mobility. Its evolution over the years of OFET research is shown in the graph for polycrystalline and single crystalline OFETs. The horizontal lines indicate the comparison guides to the main OFET competitors – amorphous (a-Si) and polycrystalline silicon. The graph reveals that the mobility in polycrystalline OFETs is comparable to that of a-Si whereas mobility in rubrene-based OFETs (20–40 $cm^2/(V \cdot s)$) approaches that of best poly-silicon devices.

Light-emitting OFETs

Because an electric current flows through such a transistor, it can be used as a light-emitting device, thus integrating current modulation and light emission. In 2003, a German group reported the first organic light-emitting field-effect transistor (OLET). The device structure comprises interdigitated gold source- and drain electrodes and a polycrystalline tetracene thin film. Both, positive charges (holes) as well as negative charges (electrons) are injected from the gold contacts into this layer leading to electroluminescence from the tetracene.

Chapter- 8

Polythiophene

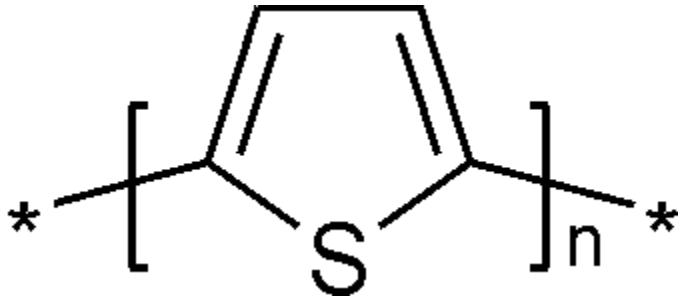

The monomer repeat unit of unsubstituted polythiophene.

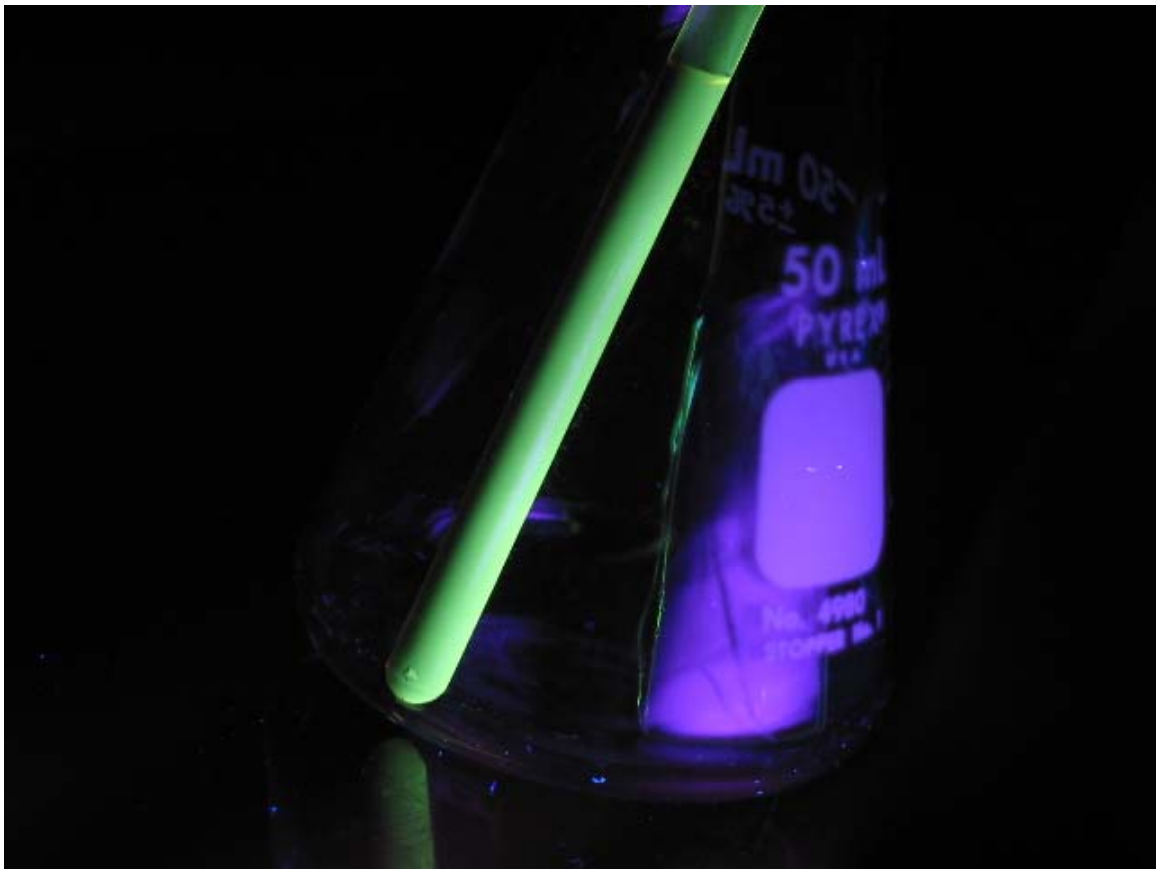

Polythiophenes demonstrate interesting optical properties resulting from their conjugated backbone, as demonstrated by the fluorescence of a substituted polythiophene solution under UV irradiation.

Polythiophenes (PTs) result from the polymerization of thiophenes, a sulfur heterocycle, that can become conducting when electrons are added or removed from the conjugated π-orbitals via doping.

The study of polythiophenes has intensified over the last three decades. The maturation of the field of conducting polymers was confirmed by the awarding of the 2000 Nobel Prize in Chemistry to Alan Heeger, Alan MacDiarmid, and Hideki Shirakawa “for the discovery and development of conductive polymers." The most notable property of these materials, electrical conductivity, results from the delocalization of electrons along the polymer backbone – hence the term “synthetic metals”. However, conductivity is not the only interesting property resulting from electron delocalization. The optical properties of these materials respond to environmental stimuli, with dramatic color shifts in response to changes in solvent, temperature, applied potential, and binding to other molecules. Both color changes and conductivity changes are induced by the same mechanism—twisting of the polymer backbone, disrupting conjugation—making conjugated polymers attractive as sensors that can provide a range of optical and electronic responses.

A number of comprehensive reviews have been published on PTs, the earliest dating from 1981. Schopf and Koßmehl published a comprehensive review of the literature published between 1990 and 1994. Roncali surveyed electrochemical synthesis in 1992, and the electronic properties of substituted PTs in 1997. McCullough's 1998 review focussed on chemical synthesis of conducting PTs. A general review of conjugated polymers from the 1990s was conducted by Reddinger and Reynolds in 1999. Finally, Swager *et al.* examined conjugated-polymer-based chemical sensors in 2000. These reviews are an excellent guide to the highlights of the primary PT literature from the last two decades.

Mechanism of conductivity and doping

Electrons are delocalized along the conjugated backbones of conducting polymers, usually through overlap of π-orbitals, resulting in an extended π-system with a filled valence band. By removing electrons from the π-system ("p-doping"), or adding electrons into the π-system ("n-doping"), a charged unit called a bipolaron is formed (see Figure 1).

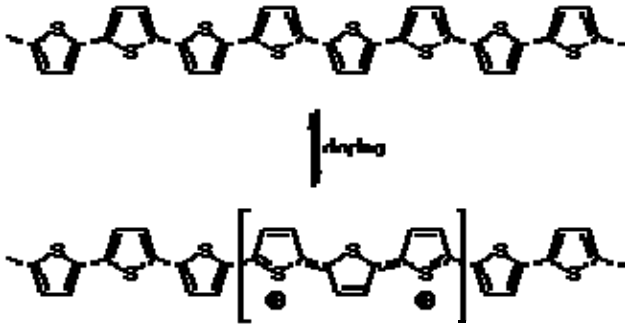

Figure 1. Removal of two electrons (p-doping) from a PT chain produces a bipolaron.

Doping is performed at much higher levels (20–40%) in conducting polymers than in semiconductors (<1%). The bipolaron moves as a unit up and down the polymer chain, and is responsible for the macroscopically observed conductivity of the polymer. For some samples of poly(3-dodecylthiophene) doped with iodine, the conductivity can approach 1000 S/cm. (In comparison, the conductivity of copper is approximately 5×10^5 S/cm.) Generally, the conductivity of PTs is lower than 1000 S/cm, but high conductivity is not necessary for many applications of conducting polymers (see below for examples).

Simultaneous oxidation of the conducting polymer and introduction of counterions, p-doping, can be accomplished electrochemically or chemically. During the electrochemical synthesis of a PT, counterions dissolved in the solvent can associate with the polymer as it is deposited onto the electrode in its oxidized form. By doping the polymer as it is synthesized, a thick film can build up on an electrode—the polymer conducts electrons from the substrate to the surface of the film. Alternatively, a neutral conducting polymer film or solution can be doped post-synthesis.

Reduction of the conducting polymer, n-doping, is much less common than p-doping. An early study of electrochemical n-doping of poly(bithiophene) found that the n-doping

levels are less than those of p-doping, the n-doping cycles were less efficient, the number of cycles required to reach maximum doping was higher, and the n-doping process appeared to be kinetically limited, possibly due to counterion diffusion in the polymer.

A variety of reagents have been used to dope PTs. Iodine and bromine produce high conductivities but are unstable and slowly evaporate from the material. Organic acids, including trifluoroacetic acid, propionic acid, and sulfonic acids produce PTs with lower conductivities than iodine, but with higher environmental stabilities. Oxidative polymerization with ferric chloride can result in doping by residual catalyst, although matrix-assisted laser desorption/ionization mass spectrometry (MALDI-MS) studies have shown that poly(3-hexylthiophene)s are also partially halogenated by the residual oxidizing agent. Poly(3-octylthiophene) dissolved in toluene can be doped by solutions of ferric chloride hexahydrate dissolved in acetonitrile, and can be cast into films with conductivities reaching 1 S/cm. Other, less common p-dopants include gold trichloride and trifluoromethanesulfonic acid.

Structure and optical properties

Conjugation length and chromisms

The extended π-systems of conjugated PTs produce some of the most interesting properties of these materials—their optical properties. As an approximation, the conjugated backbone can be considered as a real-world example of the "electron-in-a-box" solution to the Schrödinger equation; however, the development of refined models to accurately predict absorption and fluorescence spectra of well-defined oligo(thiophene) systems is ongoing. Conjugation relies upon overlap of the π-orbitals of the aromatic rings, which, in turn, requires the thiophene rings to be coplanar (see Figure 2, top).

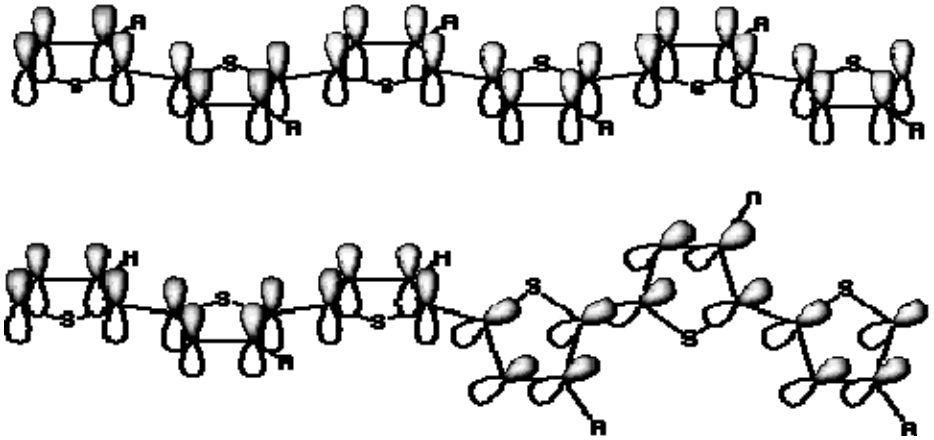

Figure 2. Conjugated π-orbitals of a coplanar and a twisted substituted PT.

The number of coplanar rings determines the conjugation length—the longer the conjugation length, the lower the separation between adjacent energy levels, and the longer the absorption wavelength. Deviation from coplanarity may be permanent,

resulting from mislinkages during synthesis or especially bulky side chains; or temporary, resulting from changes in the environment or binding. This twist in the backbone reduces the conjugation length (see Figure 2, bottom), and the separation between energy levels is increased. This results in a shorter absorption wavelength.

Determining the maximum effective conjugation length requires the synthesis of regioregular PTs of defined length. The absorption band in the visible region is increasingly red-shifted as the conjugation length increases, and the maximum effective conjugation length is calculated as the saturation point of the red-shift. Early studies by ten Hoeve *et al.* estimated that the effective conjugation extended over 11 repeat units, while later studies increased this estimate to 20 units. More recently, Otsubo *et al.* synthesized 48- and 96-mer oligothiophenes, and found that the red-shift, while small (a difference of 0.1 nm between the 72- and the 96-mer), does not saturate, meaning that the effective conjugation length may be even longer than 96 units.

A variety of environmental factors can cause the conjugated backbone to twist, reducing the conjugation length and causing an absorption band shift, including solvent, temperature, application of an electric field, and dissolved ions. The absorption band of poly (3-thiophene acetic acid) in aqueous solutions of poly(vinyl alcohol) (PVA) shifts from 480 nm at pH 7 to 415 nm at pH 4. This is attributed to formation of a compact coil structure which can form hydrogen bonds with PVA upon partial deprotonation of the acetic acid group. Chiral PTs showed no induced circular dichroism (ICD) in chloroform, but displayed intense, but opposite, ICDs in chloroform–acetonitrile mixtures versus chloroform–acetone mixtures. Also, a PT with a chiral amino acid side chain displayed moderate absorption band shifts and ICDs, depending upon the pH and the concentration of buffer.

Shifts in PT absorption bands due to changes in temperature result from a conformational transition from a coplanar, rodlike structure at lower temperatures to a nonplanar, coiled structure at elevated temperatures. For example, poly(3-(octyloxy)-4-methylthiophene) undergoes a color change from red–violet at 25 °C to pale yellow at 150 °C. An isosbestic point (a point where the absorbance curves at all temperatures overlap) indicates coexistence between two phases, which may exist on the same chain or on different chains. Not all thermochromic PTs exhibit an isosbestic point: highly regioregular poly(3-alkylthiophene)s (PATs) show a continuous blue-shift with increasing temperature if the side chains are short enough so that they do not melt and interconvert between crystalline and disordered phases at low temperatures.

Finally, PTs can exhibit absorption shifts due to application of electric potentials (electrochromism), or to introduction of alkali ions (ionochromism). These effects will be discussed in the context of applications of PTs below.

Regioregularity

The asymmetry of 3-substituted thiophenes results in three possible couplings when two monomers are linked between the 2- and the 5-positions. These couplings are:

- 2,5', or head–tail (HT), coupling
- 2,2', or head–head (HH), coupling
- 5,5', or tail–tail (TT), coupling

These three diads can be combined into four distinct triads, shown in Figure 3.

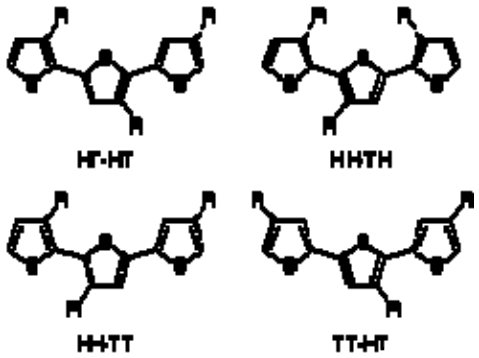

Figure 3. The four possible triads resulting from coupling of 3-substituted thiophenes.

The triads are distinguishable by NMR spectroscopy, and the degree of regioregularity can be estimated by integration.

Elsenbaumer *et al.* first noticed the effect of regioregularity on the properties of PTs. A regiorandom copolymer of 3-methylthiophene and 3-butylthiophene possessed a conductivity of 50 S/cm, while a more regioregular copolymer with a 2:1 ratio of HT to HH couplings had a higher conductivity of 140 S/cm. Films of regioregular poly(3-(4-octylphenyl)thiophene) (POPT) with greater than 94% HT content possessed conductivities of 4 S/cm, compared with 0.4 S/cm for regioirregular POPT. PATs prepared using Rieke zinc formed "crystalline, flexible, and bronze-colored films with a metallic luster." On the other hand, the corresponding regiorandom polymers produced "amorphous and orange-colored films." Comparison of the thermochromic properties of the Rieke PATs showed that, while the regioregular polymers showed strong thermochromic effects, the absorbance spectra of the regioirregular polymers did not change significantly at elevated temperatures. This was likely due to the formation of only weak and localized conformational defects. Finally, Xu and Holdcroft demonstrated that the fluorescence absorption and emission maxima of poly(3-hexylthiophene)s occur at increasingly lower wavelengths (higher energy) with increasing HH dyad content. The difference between absorption and emission maxima, the Stokes shift, also increases with HH dyad content, which they attributed to greater relief from conformational strain in the first excited state.

Solubility

Unsubstituted PTs are conductive after doping, and have excellent environmental stability compared with some other conducting polymers such as polyacetylene, but are intractable and soluble only in solutions like mixtures of arsenic trifluoride and arsenic pentafluoride. However, in 1987 examples of organic-soluble PTs were reported. Elsenbaumer *et al.*, using a nickel-catalyzed Grignard cross-coupling, synthesized two

soluble PTs, poly(3-butylthiophene) and poly(3-methylthiophene-'co'-3'-octylthiophene), which could be cast into films and doped with iodine to reach conductivities of 4 to 6 S/cm. Hotta *et al.* synthesized poly(3-butylthiophene) and poly(3-hexylthiophene) electrochemically (and later chemically), and characterized the polymers in solution and cast into films. The soluble PATs demonstrated both thermochromism and solvatochromism (see above) in chloroform and 2,5-dimethyltetrahydrofuran.

Also in 1987, Wudl *et al.* reported the syntheses of water-soluble sodium poly(3-thiophenealkanesulfonate)s. In addition to conferring water solubility, the pendant sulfonate groups act as counterions, producing self-doped conducting polymers. Substituted PTs with tethered carboxylic acids, acetic acids, amino acids, and urethanes are also water-soluble.

More recently, poly(3-(perfluorooctyl)thiophene)s soluble in supercritical carbon dioxide were electrochemically and chemically synthesized by Collard *et al.* Finally, unsubstituted oligothiophenes capped at both ends with thermally-labile alkyl esters were cast as films from solution, and then heated to remove the solublizing end groups. Atomic force microscopy (AFM) images showed a significant increase in long-range order after heating.

Synthesis

PTs can be synthesized electrochemically, by applying a potential across a solution of the monomer to be polymerized, or chemically, using oxidants or cross-coupling catalysts. Both methods have their advantages and disadvantages.

Electrochemical synthesis

In an electrochemical polymerization, a potential is applied across a solution containing thiophene and an electrolyte, producing a conductive PT film on the anode. Electrochemical polymerization is convenient, since the polymer does not need to be isolated and purified, but it produces structures with varying degrees of structural irregularities, such as crosslinking.

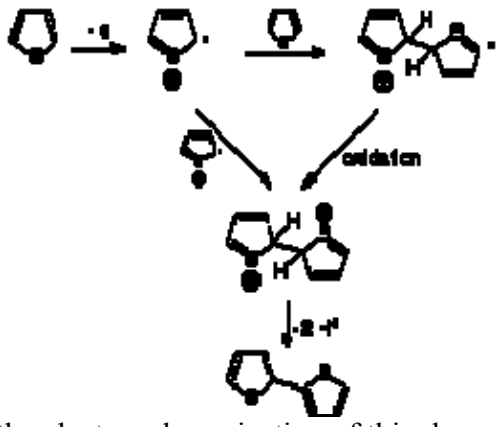

Figure 4. Initial steps in the electropolymerization of thiophenes.

As shown in Figure 4, oxidation of a monomer produces a radical cation, which can then couple with a second radical cation to form a dication dimer, or with another monomer to produce a radical cation dimer. A number of techniques including in situ video microscopy, cyclic spectrovoltammetry, photocurrent spectroscopy, and electrochemical quartz crystal microbalance measurements, have been used to elucidate the nucleation and growth mechanism leading to deposition of polymer onto the anode. Deposition of long, well-ordered chains onto the electrode surface is followed by growth of either long, flexible chains, or shorter, more crosslinked chains, depending upon the polymerization conditions.

The quality of an electrochemically prepared PT film is affected by a number of factors. These include the electrode material, current density, temperature, solvent, electrolyte, presence of water, and monomer concentration. Two other important but interrelated factors are the structure of the monomer and the applied potential. The potential required to oxidize the monomer depends upon the electron density in the thiophene ring π-system. Electron-donating groups lower the oxidation potential, while electron-withdrawing groups increase the oxidation potential. Thus, 3-methylthiophene polymerizes in acetonitrile and tetrabutylammonium tetrafluoroborate at a potential of about 1.5 V vs. SCE (saturated calomel electrode), while unsubstituted thiophene polymerizes at about 1.7 V vs. SCE. Steric hindrance resulting from branching at the α-carbon of a 3-substituted thiophene inhibits polymerization. This observation leads to the so-called "polythiophene paradox": the oxidation potential of many thiophene monomers is higher than the oxidation potential of the resulting polymer. In other words, the polymer can be irreversibly oxidized and decompose at a rate comparable to the polymerization of the corresponding monomer. This remains one of the major disadvantages of electrochemical polymerization, and limits its application for many thiophene monomers with complex side groups.

Chemical synthesis

Chemical synthesis offers two advantages compared with electrochemical synthesis of PTs: a greater selection of monomers, and, using the proper catalysts, the ability to synthesize perfectly regioregular substituted PTs. While PTs may have been chemically synthesized by accident more than a century ago, the first planned chemical syntheses using metal-catalyzed polymerization of 2,5-dibromothiophene were reported by two groups independently in 1980. Yamamoto *et al.* used magnesium in tetrahydrofuran (THF) and nickel(bipyridine) dichloride, analogous to the Kumada coupling of Grignard reagents to aryl halides. Lin and Dudek also used magnesium in THF, but with a series of acetylacetonate catalysts ($Pd(acac)_2$, $Ni(acac)_2$, $Co(acac)_2$, and $Fe(acac)_3$).

Later developments produced higher molecular weight PTs than those initial efforts, and can be grouped into two categories based on their structure. Regioregular PTs can be synthesized by catalytic cross-coupling reactions of bromothiophenes, while polymers with varying degrees of regioregularity can be simply synthesized by oxidative polymerization.

The first synthesis of perfectly regioregular PATs was described by McCullough *et al.* in 1992. As shown in Figure 5 (top),

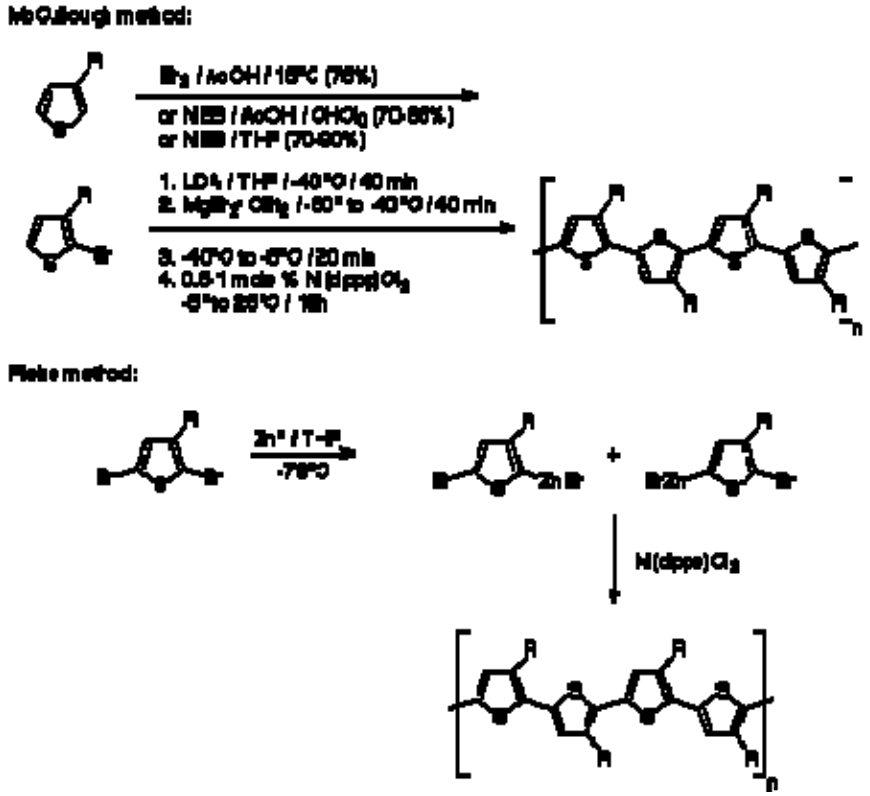

Figure 5. Cross-coupling methods for preparing regioregular PATs.

selective bromination produces 2-bromo-3-alkylthiophene, which is followed by transmetallation and then Kumada cross-coupling in the presence of a nickel catalyst. This method produces approximately 100% HT–HT couplings, according to NMR spectroscopy analysis of the diads. In the method subsequently described by Rieke *et al.* in 1993, 2,5-dibromo-3-alkylthiophene is treated with highly reactive “Rieke zinc" to form a mixture of organometallic isomers (Figure 5, bottom). Addition of a catalytic amount of $Pd(PPh_3)_4$ produces a regiorandom polymer, but treatment with $Ni(dppe)Cl_2$ yields regioregular PAT in quantitative yield.

While the McCullough and Rieke methods produce structurally homogenous PATs, they require low temperatures, the careful exclusion of water and oxygen, and brominated monomers. In contrast, the oxidative polymerization of thiophenes using ferric chloride described by Sugimoto in 1986 can be performed at room temperature under less demanding conditions. This method has proven to be extremely popular; H.C. Stark's antistatic coating Clevios P is prepared on a commercial scale using ferric chloride (see below).

A number of studies have been conducted in attempts to improve the yield and quality of the product obtained using the oxidative polymerization technique. In addition to ferric chloride, other oxidizing agents, including ferric chloride hydrate, copper perchlorate,

and iron perchlorate have also been used successfully to polymerize 2,2'-bithiophene. Slow addition of ferric chloride to the monomer solution produced poly(3-(4-octylphenyl)thiophene)s with approximately 94% H–T content. Precipitation of ferric chloride in situ (in order to maximize the surface area of the catalyst) produced significantly higher yields and monomer conversions than adding monomer directly to crystalline catalyst. Higher molecular weights were reported when dry air was bubbled through the reaction mixture during polymerization. Exhaustive Soxhlet extraction after polymerization with polar solvents was found to effectively fractionate the polymer and remove residual catalyst before NMR spectroscopy. Using a lower ratio of catalyst to monomer (2:1, rather than 4:1) may increase the regioregularity of poly(3-dodecylthiophene)s. Andreani *et al.* reported higher yields of soluble poly(dialkylterthiophene)s in carbon tetrachloride rather than chloroform, which they attributed to the stability of the radical species in carbon tetrachloride. Higher-quality catalyst, added at a slower rate and at reduced temperature, was shown to produce high molecular weight PATs with no insoluble polymer residue. Laakso *et al.* used a factorial design to determine that increasing the ratio of catalyst to monomer increased the yield of poly(3-octylthiophene), and claimed that a longer polymerization time also increased the yield.

The mechanism of the oxidative polymerization using ferric chloride has been controversial. Sugimoto *et al.* did not speculate on a mechanism in their 1986 report. In 1992, Niemi *et al.* proposed a radical mechanism, shown in Figure 6(top).

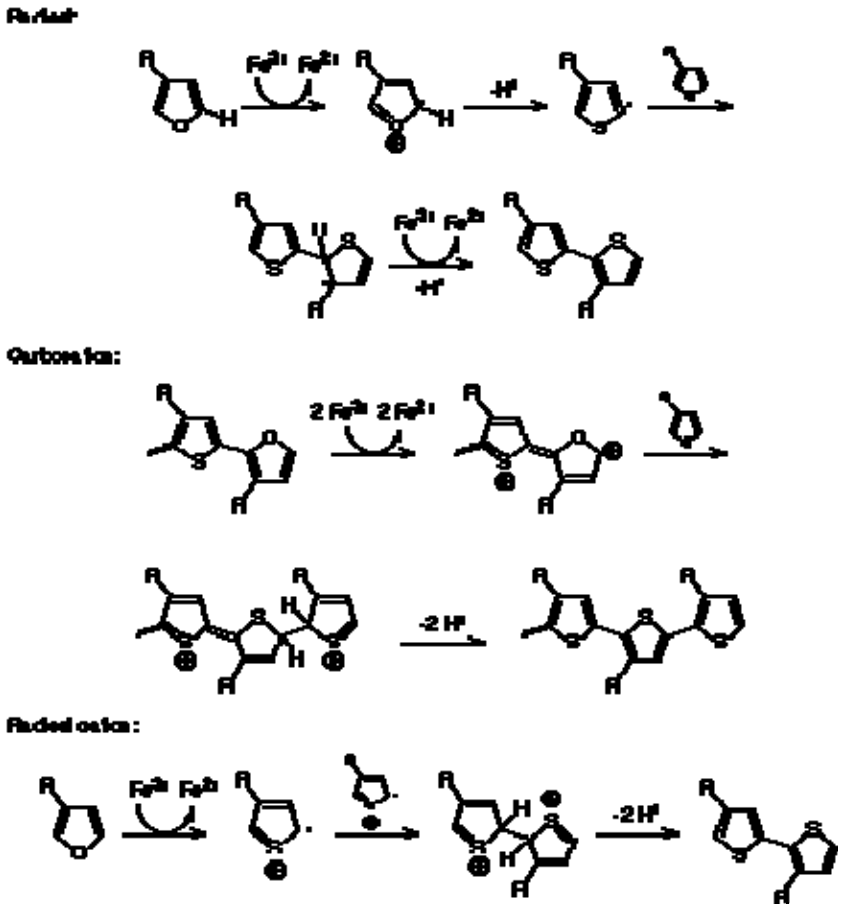

Figure 6. Proposed mechanisms for ferric chloride oxidative polymerizations of thiophenes.

They based their mechanism on two assumptions. First, since they observed polymerization only in solvents where the catalyst was either partially or completely insoluble (chloroform, toluene, carbon tetrachloride, pentane, and hexane, and not diethyl ether, xylene, acetone, or formic acid), they concluded that the active sites of the polymerization must be at the surface of solid ferric chloride. Therefore, they discounted the possibilities of either two radical cations reacting with each other, or two radicals reacting with each other, "because the chloride ions at the surface of the crystal would prevent the radical cations or radicals from assuming positions suitable for dimerization." Second, using 3-methylthiophene as a prototypical monomer, they performed quantum mechanical calculations to determine the energies and the total atomic charges on the carbon atoms of the four possible polymerization species (neutral 3-methylthiophene, the radical cation, the radical on carbon 2, and the radical on carbon 5).

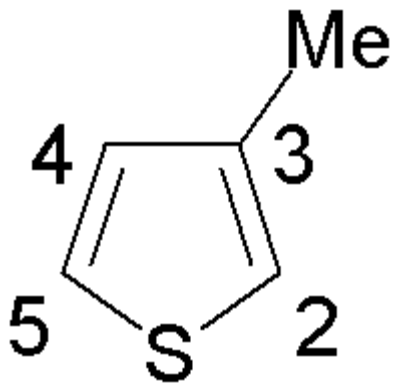

Since the most negative carbon of the neutral 3-methylthiophene is also carbon 2, and the carbon with the highest odd electron population of the radical cation is carbon 2, they concluded that a radical cation mechanism would lead to mostly 2–2, H–H links. They then calculated the total energies of the species with the radicals at the 2 and the 5 carbons, and found that the latter was more stable by 1.5 kJ/mol. Therefore, the more stable radical could react with the neutral species, forming head-to-tail couplings as shown in Figure 6 (top).

Andersson *et al.* offered an alternative mechanism in the course of their studies of the polymerization of 3-(4-octylphenyl)thiophene with ferric chloride, where they found a high degree of regioregularity when the catalyst was added to the monomer mixture slowly. They concluded that, given the selectivity of the couplings, and the strong oxidizing conditions, the reaction could proceed via a carbocation mechanism (Figure 6, middle).

The radical mechanism was directly challenged in a short communication in 1995, when Olinga and François noted that thiophene could be polymerized by ferric chloride in acetonitrile, a solvent in which the catalyst is completely soluble. Their analysis of the kinetics of thiophene polymerization also seemed to contradict the predictions of the radical polymerization mechanism. Barbarella *et al.* studied the oligomerization of 3-(alkylsulfanyl)thiophenes, and concluded from their quantum mechanical calculations, and considerations of the enhanced stability of the radical cation when delocalized over a planar conjugated oligomer, that a radical cation mechanism analogous to that generally accepted for electrochemical polymerization was more likely (Figure 6, bottom). Given the difficulties of studying a system with a heterogeneous, strongly oxidizing catalyst that produces difficult to characterize rigid-rod polymers, the mechanism of oxidative polymerization is by no means decided. However, the radical cation mechanism shown in Figure 6 is generally accepted as the most likely route for PT synthesis.

Applications

A number of applications have been proposed for conducting PTs, but none has been commercialized. Potential applications include field-effect transistors, electroluminescent devices, solar cells, photochemical resists, nonlinear optic devices, batteries, diodes, and

chemical sensors. In general, there are two categories of applications for conducting polymers. Static applications rely upon the intrinsic conductivity of the materials, combined with their ease of processing and material properties common to polymeric materials. Dynamic applications utilize changes in the conductive and optical properties, resulting either from application of electric potentials or from environmental stimuli.

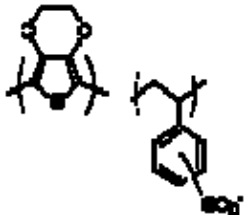

Figure 7. PEDOT-PSS (Clevios P).

As an example of a static application, H.C. Starck's poly(3,4-ethylenedioxythiophene)-poly(styrene sulfonate) (PEDOT-PSS) product Clevios P (Figure 7) has been extensively used as an antistatic coating (as packaging materials for electronic components, for example). AGFA coats 200 m × 10 m of photographic film per year with Clevios because of its antistatic properties. The thin layer of Clevios is virtually transparent and colorless, prevents electrostatic discharges during film rewinding, and reduces dust buildup on the negatives after processing.

PEDOT can also be used in dynamic applications where a potential is applied to a polymer film. The electrochromic properties of PEDOT are used to manufacture windows and mirrors which can become opaque or reflective upon the application of an electric potential. Widespread adoption of electrochromic windows could save billions of dollars per year in air conditioning costs. Finally, Phillips has commercialized a mobile phone with an electrically switchable PEDOT mirror.

Figure 8. Ionoselective PTs reported by Bäuerle (left) and Swager (right).

The use of PTs as sensors responding to an analyte has also been the subject of intense research. In addition to biosensor applications, PTs can also be functionalized with synthetic receptors for detecting metal ions or chiral molecules as well. PTs with pendant and main-chain crown ether functionalities were reported in 1993 by the research groups of Bäuerle and Swager, respectively (Figure 8). Electrochemically polymerized thin films of the Bäuerle pendant crown ether PT were exposed to millimolar concentrations of alkali cations (Li, Na, and K). The current which passed through the film at a fixed potential dropped dramatically in lithium ion solutions, less so for sodium ion solutions, and only slightly for potassium ion solutions. The Swager main chain crown ether PTs

were prepared by chemical coupling and characterized by absorbance spectroscopy. Addition of the same alkali cations resulted in absorbance shifts of 46 nm (Li), 91 nm (Na), and 22 nm (K). The size of the shifts corresponds to the ion-binding preferences of the corresponding crown ether, resulting from a twist in the conjugated polymer backbone induced by ion binding.

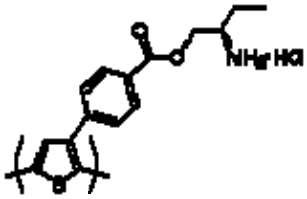

Figure 9. Chiral PT synthesized by Yashima and Goto.

In the course of their studies of the optical properties of chiral PTs, Yashima and Goto found that a PT with a chiral primary amine (Figure 9) was sensitive to chiral amino alcohols, producing mirror-image-split ICD responses in the π–transition region. This was the first example of chiral recognition by PTs using a chiral detection method (CD spectroscopy). This distinguished it from earlier work by Lemaire *et al.* who used an achiral detection method (cyclic voltammetry) to detect incorporation of chiral dopant anions into an electrochemically polymerized chiral PT.

Chapter- 9

Molecular Electronics Applications

Active-Matrix OLED

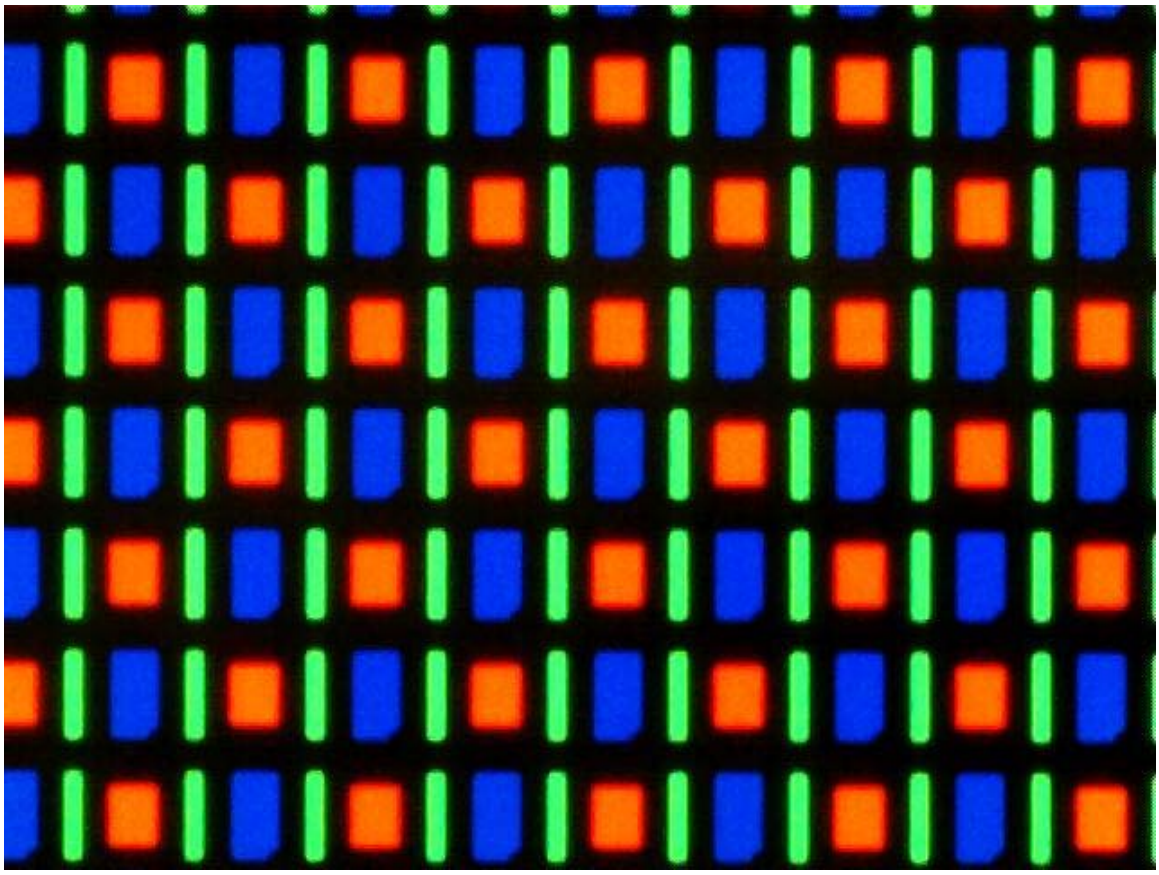

Magnified image of the AMOLED screen on the Google Nexus One smartphone using the RGBG system of the PenTile Matrix Family.

Active-matrix OLED (**Active-matrix organic light-emitting diode** or **AMOLED**) is a display technology for use in mobile devices and televisions. OLED describes a specific type of thin film display technology in which organic compounds form the electroluminescent material, and active matrix refers to the technology behind the addressing of pixels. AMOLED technology is currently used in mobile phone and media players and continues to make progress towards low power, low cost and large size (for example 40 inch) for applications such as televisions.

Technical

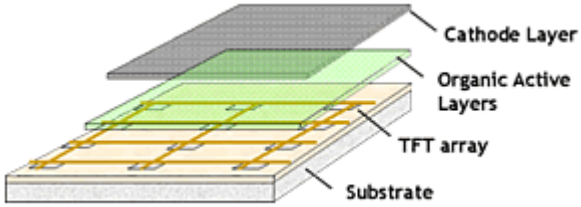

Schematic of an active matrix OLED display

An active matrix OLED display consists of a matrix of OLED pixels that generate light upon electrical activation that have been deposited or integrated onto a thin film transistor (TFT) array, which functions as a series of switches to control the current flowing to each individual pixel.

Typically, this continuous current flow is controlled by at least two TFTs at each pixel, one to start and stop the charging of a storage capacitor and the second to provide a voltage source at the level needed to create a constant current to the pixel and eliminating need for the very high currents required for passive matrix OLED operation.

TFT backplane technology is crucial in the fabrication of AMOLED displays. Two primary TFT backplane technologies, namely polycrystalline silicon (poly-Si) and amorphous silicon (a-Si), are used today in AMOLEDs. These technologies offer the potential for fabricating the active matrix backplanes at low temperatures (below 150°C) directly onto flexible plastic substrates for producing flexible AMOLED displays.

AMOLED In-Cell Touch Panels

Manufacturers have developed in-cell touch panels, integrating the production of capacitive sensor arrays in the AMOLED module fabrication process. In-cell sensor AMOLED fabricators include AU Optronics and Samsung. Samsung has marketed their version of this technology as Super AMOLED.

Advantages

Active-matrix OLED displays provide higher refresh rates than their passive-matrix OLED counterparts, and they consume significantly less power. This advantage makes active-matrix OLEDs well suited for portable electronics, where power consumption is critical to battery life.

The amount of power the display consumes varies significantly depending on the color and brightness shown. As an example, one commercial QVGA OLED display consumes 3 watts while showing black text on a white background, but only 0.7 watts showing white text on a black background.

Disadvantages

AMOLED displays may be difficult to view in direct sunlight compared to LCD displays. Samsung's Super AMOLED technology addresses this issue by reducing the size of gaps between layers of the screen.

The organic materials used in AMOLED displays are prone to degradation over a period of time. However, technology has been developed to compensate for material degradation.

The current demand for AMOLED screens is high but production rate is slow until new factories are established and begin more production in 2011. Thus many smartphone models such as those from HTC and even some of Samsung's own cannot keep up with the high demand in AMOLED screens for long and turns to Sony's Super LCD technology.

Commercial devices

Phones:

- Dell Venue Pro
- Google Nexus one
- Google Nexus S
- HTC Desire
- HTC Droid Incredible
- HTC Legend
- Nokia C7-00
- Nokia C6-01
- Nokia E7-00
- Nokia N8
- Nokia N85
- Nokia N86 8MP
- Orange San Francisco
- Samsung i7500 Galaxy
- Samsung i8910

- Samsung Jet
- Samsung Omnia 2
- Samsung Impression A-887
- Samsung Rogue
- Samsung Galaxy S series (Super AMOLED)
- Samsung Wave S8500 (Super AMOLED)
- Samsung Focus (Super AMOLED)
- Samsung Omnia 7 (Super AMOLED)

Music Players:

- Cowon S9
- Cowon J3
- Iriver Clix
- Zune HD

Break junction

A **break junction** is an electrical junction between two wires formed by pulling the wires apart to produce electrodes separated by a few atomic distances. In this technique a metal wire is bent or pulled, often using a piezoelectric crystal to apply the necessary force. The bending or pulling causes the metal wire to break in a controlled manner since piezoelectric elongation can be controlled to a precision of angstroms or less (such crystals are used for motion control in scanning tunneling microscopy). As the wire breaks, the separation between the electrodes can be indirectly controlled by monitoring the electrical current through the junction.

A typical conductance versus time trace during the breaking process (conductance is simply current divided by applied voltage bias) shows two regimes. First is a regime where the break junction comprises a quantum point contact. In this regime conductance decreases in steps equal to the conductance quantum $G_Q = 2e^2 / h$ which is expressed through the electron charge ($-e$) and Planck's constant h. The conductance quantum has a value of 7.74×10^{-5} siemens, corresponding to a resistance increase of roughly 12.9 kΩ. These step decreases are interpreted as the result of a decrease, as the electrodes are pulled apart, in the number of single-atom-wide metal strands bridging between the two electrodes, each strand having a conductance equal to the quantum of conductance. As the wire is pulled, the neck becomes thinner with fewer atomic strands in it. Each time the neck reconfigures, which happens abruptly, a step-like decrease of the conductance can be observed. This picture inferred from the current measurement has been confirmed by "in-situ" TEM imaging of the breaking process combined with current measurement.

In a second regime, when the wire is pulled further apart, the conductance collapses to values less than the quantum of conductance. This is the tunneling regime where electrons tunnel through vacuum between the electrodes.

Although the above conceptual description is somewhat oversimplified, it is a good first approach to understanding the topic of break junctions and quantum point contacts.

Capillary Action through Synthetical Mesh

Capillary Action through Synthetical Mesh is the result of the intermolecular attraction between moisture and semi-synthetic polymers causing a current of thermionic-energy flowing through a specific pathway within a mesh material. The combination of the adhesive forces and the surface tension that arises from cohesion produces the characteristic upward curve in a fluid, such as water. Capillarity is the result of cohesion of water molecules and adhesion of those molecules to the solid material forming the void. As the edges of the material are brought closer together, such as in a very narrow path, the interaction causes the liquid to be drawn away from the original source. The more narrow the pathway, the greater the rise of the liquid. Greater surface tension and increased ratio of adhesion to cohesion also result in greater rise. Synthetic materials using conductive polymer as found in polypyrrole to reduce liquid density to a manageable state.

The force with which water is held by capillary action varies with the quantity of water being held. As part of a demonstration conducted by Bright Idea and Webb development: Water entering a natural void, such as a pore within a synthetic mesh material, forms a film on the surface of the material surrounding the pore. The adhesion of the water molecules nearest the solid material is greatest. As water is added to the pore, the thickness of the film increases, the capillary force is reduced in magnitude, and water molecules on the outer portion of the film may begin to flow away from its source. As more water enters the pore the capillary force is reduced to zero when the pore is saturated, unless a hydrophilic body is introduced. The movement of moisture through the mesh is controlled by this capillary action.

Conductive Characteristics within Coated Synthetic Fabrics

Conductive Characteristics with a Coated Synthetic Fabric demonstrates an energy current across a specific woven synthetic material, such energy generation in fabrics coated with a conductive polymer as found in polypyrrole. First validated by D.D.S. developer M.H.Webb, the discovery showed that when PET fabrics are coated by chemical synthesis using four different oxidizing agent–dopant combinations present an increase in energy when a fixed source is applied to the fabric. Several combinations of

blends have proven to be successful in transfer, anthracenedione-2-sulfonic acid (AQSA) sodium salt doped polypyrrole coating was the most effective in generation whereas the sodium perchlorate dopant system was the least effective. The power density per unit area achieved in polypyrrole coated polyester–Lycra fabric with 0.027 mol/l of AQSA acting as dopant was 430 W/m2. The power density per unit area achieved for the sodium perchlorate system, using the same synthesis conditions, was 55 W/m2.

Endohedral hydrogen fullerene

Endohedral hydrogen fullerene or $H_2@C_{60}$ is an endohedral fullerene containing molecular hydrogen. This chemical compound has a potential application in molecular electronics and was synthesized in 2005 at Kyoto University by the group of Koichi Komatsu . Ordinarily the payload of endohedral fullerenes are inserted at the time of the synthesis of the fullerene itself or is introduced to the fullerene at very low yields at high temperatures and high pressure. This particular fullerene was synthesised in an unusual way in three steps starting from pristine C_{60} fullerene: cracking open the carbon framework, insert hydrogen gas and zipping up by organic synthesis methods.

Organic synthesis

Scheme 1 presents an overview of the first step, the creation of a 13 membered ring orifice on the fullerene surface. A 1,2,4-triazine **2** is fitted with two phenyl groups and a pyridine group for reasons of solubility and reacted in 1,2-dichlorobenzene with pristine C_{60} fullerene **2** in a Diels-Alder reaction at high temperature and for an extended reaction time. In this reaction nitrogen is expulsed and an 8-membered ring is formed (**3**). This orifice is further extended by reaction with singlet oxygen in carbon tetrachloride which causes one of the ring alkene groups to oxidize to a ketone. The 12-ring is extended to a 13-ring by reaction with elemental sulfur in presence of tetrakis(dimethylamino)ethylene.

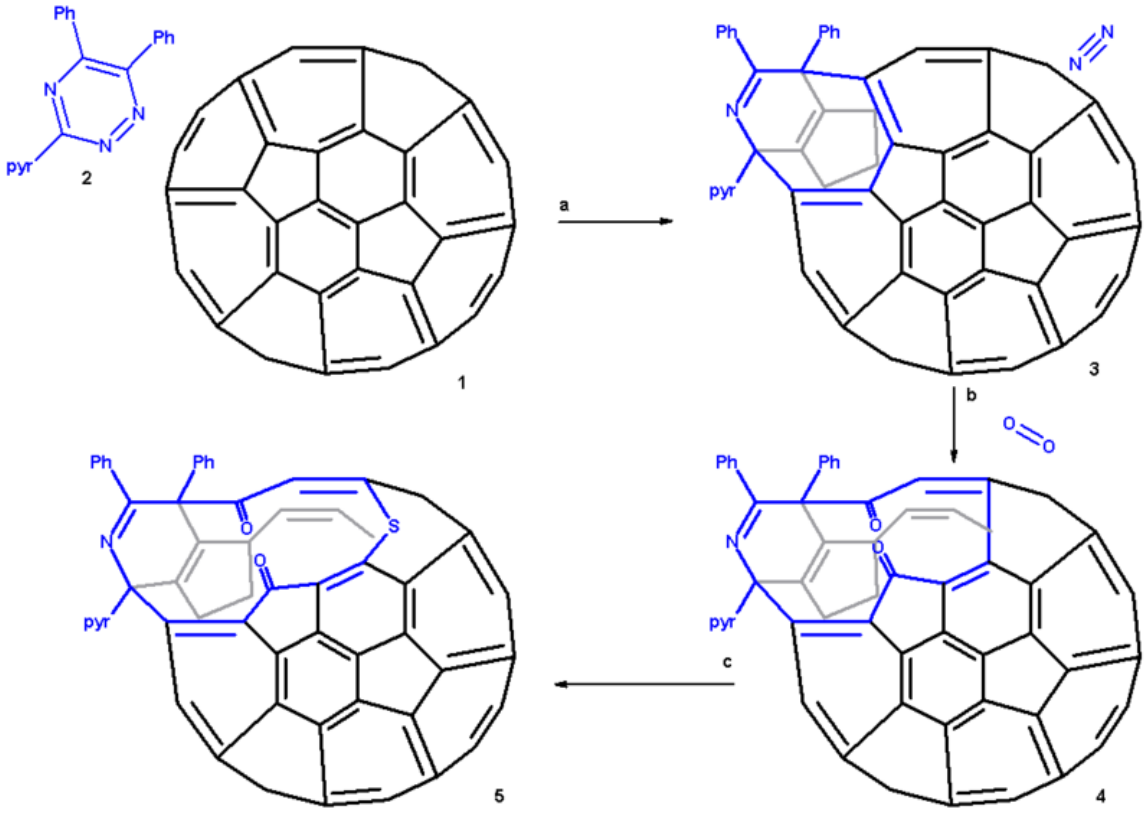

The proposed reaction mechanism is depicted in a plat surface rendition in *scheme 2*. In the first step the triazine reacts with the fullerene in a Diels-Alder reaction. In the second step nitrogen is expulsed from the DA adduct **2** resulting in the formation of a fused aza-cyclohexadiene ring followed by a [4+4]cycloaddition to an intermediate **4** with two cyclopropane rings. This intermediate quickly rearranges in a retro [2+2+2]cycloaddition to the 8 membered ring product **5**. In silico calculations show that the electrons in the HOMO reside primarily in the double bonds of the butadiene part of the ring and indeed singlet oxygen reacts at these positions through the dioxetane intermediate **6** with alkene cleavage to diketone **7** (only one isomer shown). Elemental sulfur S_8 is inserted into the single bond of the diene group leading to the extension of the ring to 13 atoms (structures **8** and **9** are identical). Tetrakis(dimethylamino)ethylene activates this bond for electrophilic sulfur addition either by one-electron reduction or by complexation.

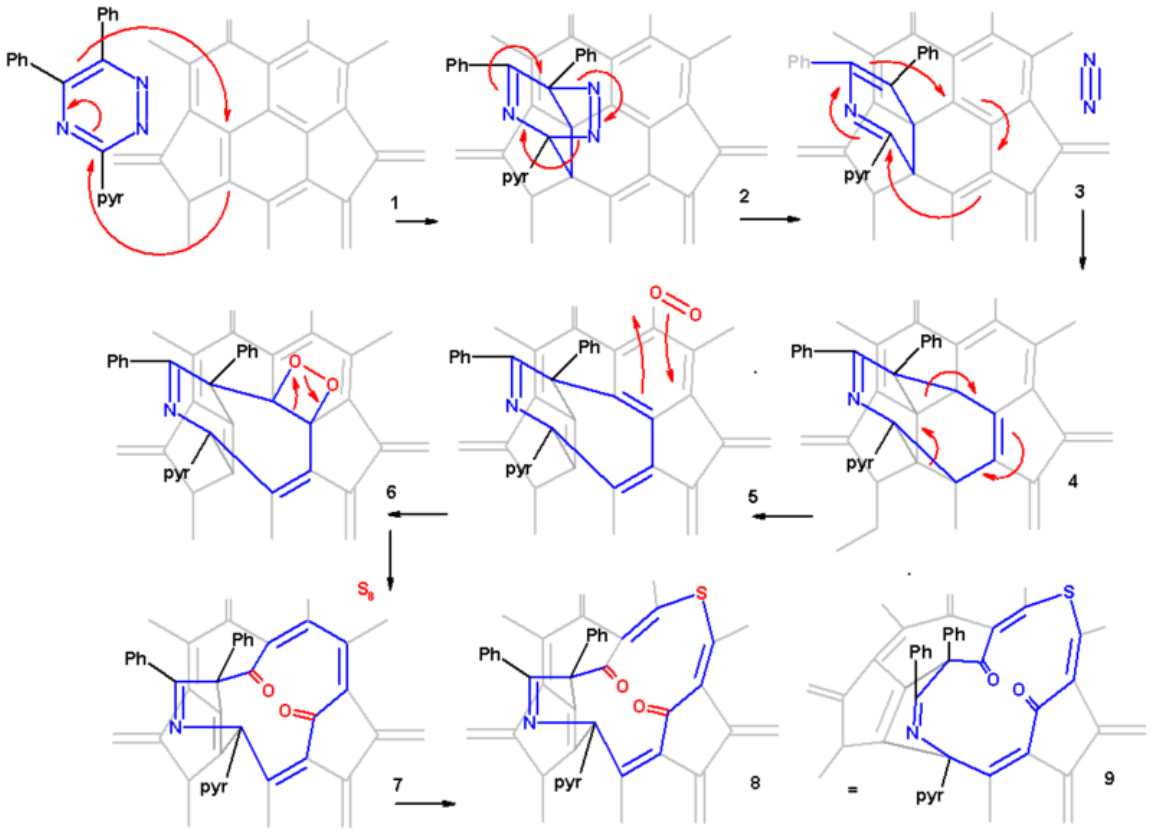

From X-ray crystallography it is determined that the shape of the orifice in the sulfur compound is roughly a circle. Inserting hydrogen in this compound is an easy step taking place with 100% efficiency. Zipping up the orifice is a reversal of the steps required to open the cage. Care must be taken to keep the reaction conditions below 160 °C on order to prevent hydrogen from escaping. m-CPBA oxidizes the sulfur group to a sulfoxide group which can then be extracted from the ring by a photochemical reaction under visible light in toluene. The two ketone groups are re-coupled in a McMurry reaction with titanium tetrachloride and elemental zinc. The reverse cycloadditions take place at 340 °C in a vacuum splitting of 2-cyanopyridine and diphenylacetylene resulting in the formation of $H_2@C_{60}$ at a 40% chemical yield starting from pristine fullerene.

Properties

$H_2@C_{60}$ is found to be a stable molecule. it survives 10 minutes at 500 °C and shows the same chemical reactivity as empty C_{60}. The electronic properties are also largely unaffected.

The process of hydrogen introduction and release can be facilitated by increasing the size of the orifice. This can be done by replacing sulfur by selenium (sodium thiolate, Se_8) exploiting larger C-Se bond length. Filling cracked-open fullerene now takes 8 hours at 190 °C at 760 atmospheres (77 MPa) of hydrogen and release between 150 °C and 180

°C is three times as fast compared to the sulfur analogue. The activation energy for release is lowered by 0.7 kcal/mol to 28.2 kcal/mol (2.9 to 118 kJ/mol).

There is evidence that hydrogen in the fullerene cage is not completely shielded from the outside world as one study found that $H_2@C_{60}$ is more efficient at quenching singlet oxygen than empty C_{60}.

Light-emitting Electrochemical Cell

A **light-emitting electrochemical cell** (**LEC** or **LEEC**) is a solid-state device that generates light from an electric current (electroluminescence). LEC's are usually composed of two metal electrodes connected by (e.g. sandwiching) an organic semiconductor containing mobile ions. Aside from the mobile ions, their structure is very similar to that of an organic light-emitting diode (OLED).

LECs have most of the advantages of OLEDs and as well as additional ones:

- The device does not depend on the difference in work function of the electrodes. Consequently, the electrodes can be made of the same material (e.g. gold). Similarly, the device can still be operated at low voltages.
    - Recently developed materials such as graphene or a blend of carbon nanotubes and polymers have been used as electrodes, eliminating the need for using indium tin oxide for a transparent electrode.
- The thickness of the active electroluminescent layer is not critical for the device to operate. This means that:
    - LECs can be printed with relatively inexpensive printing processes (where control over film thicknesses can be difficult).
    - Internal device operation can be observed directly.

History

While electroluminescence had been seen previously in similar devices , the invention of the polymer LEC is attributed to Pei et al. Since then, numerous research groups, and even a few companies, have worked on improving and commercializing the devices.

Molecular conductance

Molecular Conductance ($G = I / V$), or the conductance of a single molecule, is a physical quantity in molecular electronics. Molecular conductance is dependent on the surrounding conditions (e.g. pH, temperature, pressure), as well as the properties of measuring device. Many experimental techniques have been developed in an attempt to measure this quantity directly, but theorists and experimentalists still face many challenges.

Recently, a great deal of progress has been made in the development of reliable conductance-measuring techniques. These techniques can be divided into two categories: molecular film experiments, which measure groups of tens of molecules, and single-molecule-measuring experiments.

Molecular film experiments

Molecular film experiments generally consist of the sandwiching of a thin layer of molecules between two electrodes which are used to measure the conductance through the layer. Two of the most successful implementations of this concept have been the bulk electrode approach and in the use of nanoelectrodes. In the bulk electrode approach, a molecular film is typically immobilized onto one electrode and an upper electrode is brought into contact with it allowing for a measure of current flow as a function of applied bias voltage. The nanoelectrode class of experiments, in creatively utilizing equipment such as atomic force microscope tips and small-radius wires, are able to perform the same sorts of current versus applied bias measurements but on a much smaller number of molecules as compared to bulk electrode. For instance, the tip of an atomic force microscope can be used as a top electrode and, given the nano-scale radius of curvature of the tip, the number of molecules measured is drastically cut. The difficulties encountered in these experiments have come mainly in dealing with such thin layers of molecules which often results in problems with short-circuiting the electrodes.

Single-molecule-measurement

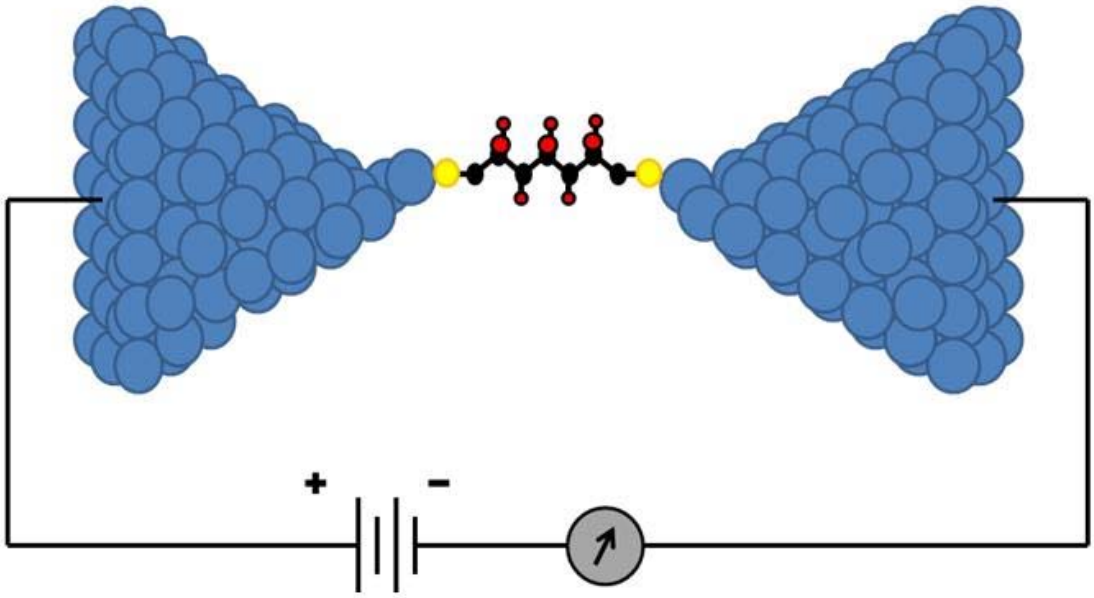

A molecule covalently connected to two electrodes.

More recently, **single-molecule-measurement** experiments have been developed that are bringing experimenters a better look at molecular conductance. These fall under the categories of scanning probe, which involves fixed electrode, and mechanically formed junction techniques. One example of a mechanically formed junction experiment involves using a movable electrode to make contact with and then pull away from an electrode surface coated with a single layer of molecules. As the electrode is removed from the surface the molecules that had bonded between the two electrodes begin to detach until eventually one molecule is connected. The atomic-level geometry of the tip-electrode contact has an effect on the conductance and can change from one run of the experiment to the next so a histogram approach is required. Forming a junction in which the precise contact geometry is known has been one of the main difficulties with this approach.

Applications

An important first step toward the goal of building electronic devices on the molecular level is the ability to measure and control the electrical current through an individual molecule. Based on the anticipated continuation of Moore's Law, which is expected to carry the miniaturization of transistors on integrated circuits into the atomic scale within

the next 10 to 20 years, this goal of single-molecule-level circuit design is likely to become widespread throughout the semiconductor industry.

Other applications focus on the insight provided by these experiments in the area of charge transport, which is a recurrent phenomenon in many chemical and biological processes. This sort of insight gives researchers the ability to read the chemical information stored in a single molecule electronically, which can then be used in a wide variety of chemical and biosensor applications.

Molecular logic gate

A **molecular logic gate** is a molecule that performs a logical operation on one or more logic inputs and produces a single logic output. Much academic research is dedicated to the development of these systems and several prototypes now exist. Because of their potential utility in simple arithmetic these molecular machines are also called **moleculators**.

Molecular logic gates work with input signals based on chemical processes and with output signals based on spectroscopy. One of the earlier water solution-based systems exploits the chemical behavior of compounds **A** and **B** in *scheme 1* .

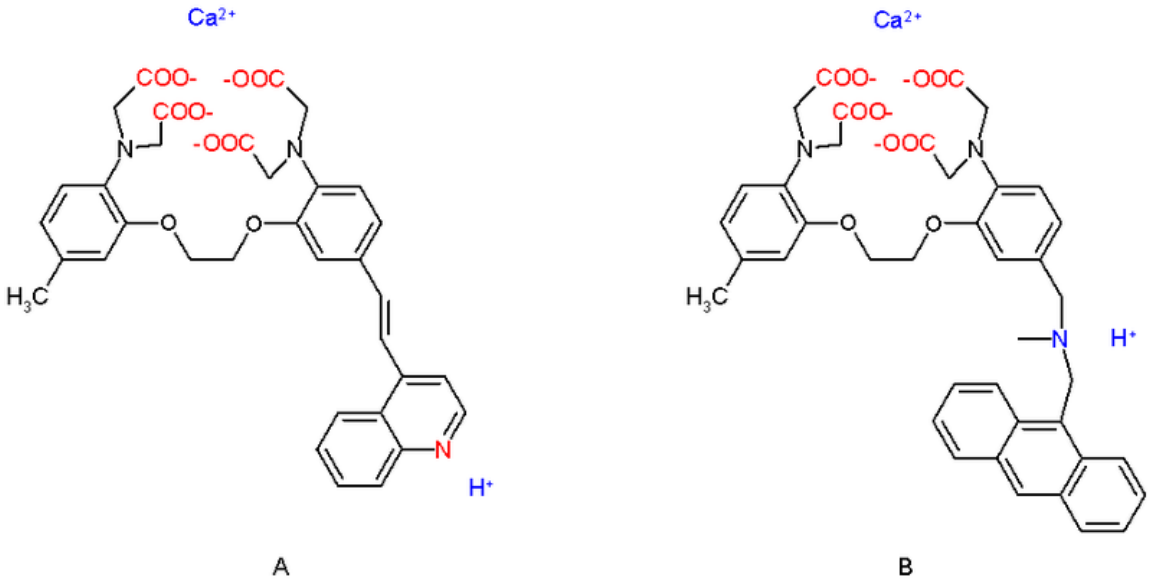

Compound A is a push-pull olefin with the top receptor containing four carboxylic acid anion groups (and non-disclosed counter cations) capable of binding to calcium. The bottom part is a quinoline molecule which is a receptor for hydrogen ions. The logic gate operates as follows.

Without any chemical input of Ca^{2+} or H^{+}, the chromophore shows a maximum absorbance in UV/VIS spectroscopy at 390 nm. When calcium is introduced a blue shift takes place and the absorbance at 390 nm decreases. Likewise addition of protons causes

a red shift and when both cations are in the water the net result is absorption at the original 390 nm. This system represents a XNOR logic gate in absorption and a XOR logic gate in transmittance.

In compound **B** the bottom section now contains a tertiary amino group also capable of binding to protons. In this system fluorescence only takes place when both cations are present and therefore the system represents an AND logic gate.

With both systems run in parallel and with monitoring of transmittance for system A and fluorescence for system B the result is a half-adder capable of reproducing the equation 1+1=2.

In a modification of system B not two but three chemical inputs are simultaneously processed in an AND logic gate . An enhanced fluorescence signal from the compound depicted below is obtained only in the presence of hydrogen, zinc and sodium ions through interaction with respectively the amine, carboxylate and crown ether receptors and this system can be potentially applied in disease screening (lab-on-a-molecule) because these ions are all physiologically relevant.

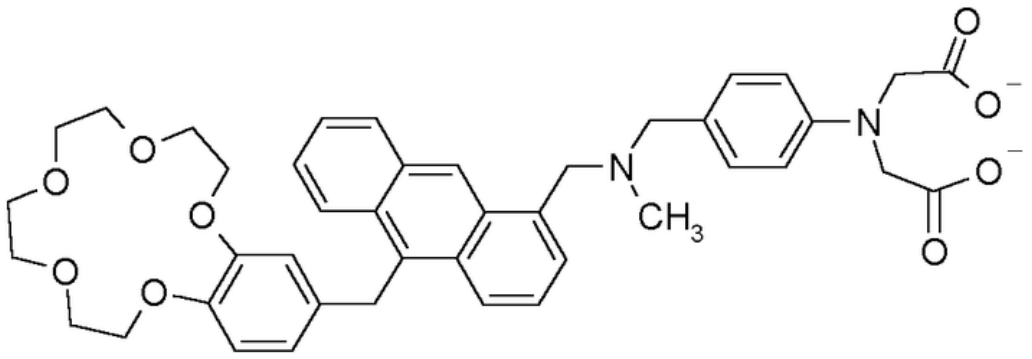

In another XOR logic gate system the chemistry is based on the pseudorotaxane depicted in *scheme 3*. In organic solution the electron deficient diazapyrenium salt (rod) and the electron rich 2,3-dioxynaphthalene units of the crown ether (ring) self-assemble by formation of a charge transfer complex.

An added tertiary amine like tributylamine forms a 1:2 adduct with the diazapyrene and the complex gets dethreaded. This process is accompanied by an increase in emission intensity at 343 nm resulting from freed crown ether. Added trifluoromethanesulfonic acid reacts with the amine and the process is reverted. Excess acid locks the crown ether by protonation and again the complex is dethreaded.

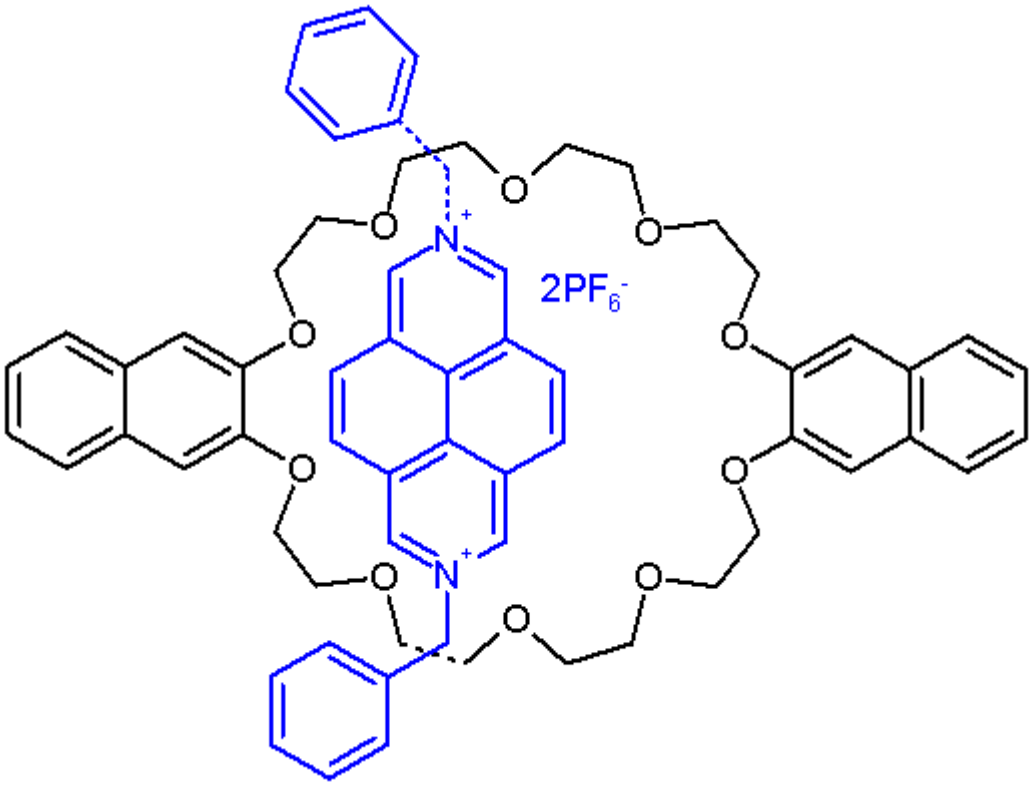

A full adder system based on fluorescein is able to compute 1+1+1=3.

Molecular memory

Molecular memory is a term for data storage technologies that use molecular species as the data storage element, rather than e.g. circuits, magnetics, inorganic materials or physical shapes. The molecular component can be described as a molecular switch, and may perform this function by any of several mechanisms, including charge storage, photochromism, or changes in capacitance. In a perfect molecular memory device, each individual molecule contains a bit of data, leading to massive data capacity. However, practical devices are more likely to use large numbers of molecules for each bit, in the manner of 3D optical data storage (many examples of which can be considered molecular memory devices). The term "molecular memory" is most often used to mean indicate very fast, electronically-addressed solid-state data storage, as is the term computer memory. At present, molecular memories are still found only in laboratories.

Examples

One approach to molecular memories is based on special compounds such as porphyrin-based polymers which are capable of storing electric charge. Once a certain voltage threshold is achieved the material oxidizes, releasing an electric charge. The process is reversible, in effect creating an electric capacitor. The properties of the material allow for

a much greater capacitance per unit area than with conventional DRAM memory, thus potentially leading to smaller and cheaper integrated circuits.

Several universities and a number of companies (Hewlett Packard, ZettaCore) have announced work on molecular memories, which some hope will supplant DRAM memory as the lowest cost technology for high-speed computer memory. NASA is also supporting research on non-volatile molecular memories.

Organic semiconductor

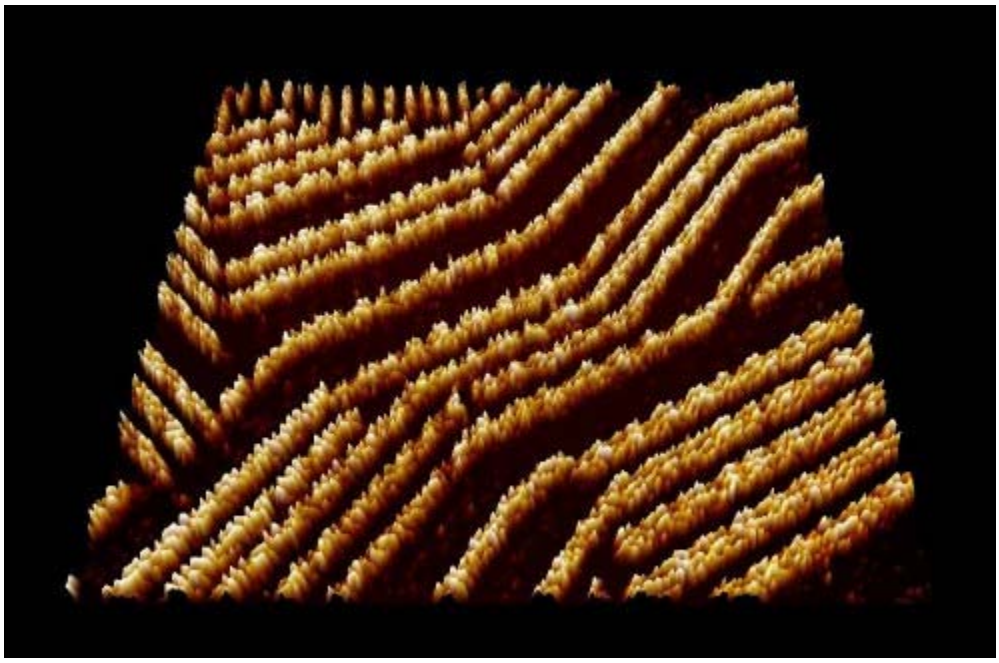

STM image of self-assembled supramolecular chains of the organic semiconductor Quinacridone on Graphite.

An **organic semiconductor** is an organic material with semiconductor properties. Semiconductivity may be exhibited by single molecules, short chain (oligomers) and organic polymers. Semiconducting small molecules (aromatic hydrocarbons) include the polycyclic aromatic compounds pentacene, anthracene, and rubrene. Polymeric organic semiconductors include poly(3-hexylthiophene), poly(p-phenylene vinylene), as well as polyacetylene and its derivatives.

There are two major overlapping classes of organic semiconductors. These are organic charge-transfer complexes and various linear-backbone conductive polymers derived

from polyacetylene. Linear backbone organic semiconductors include polyacetylene itself and its derivatives polypyrrole, and polyaniline. Charge-transfer complexes often exhibit similar conduction mechanisms to inorganic semiconductors, at least locally. Such mechanisms arise from the presence of hole and electron conduction layers separated by a band gap. As with inorganic amorphous semiconductors, tunneling, localized states, mobility gaps, and phonon-assisted hopping also contribute to conduction, particularly in polyacetylenes. Like inorganic semiconductors, organic semiconductors can be doped. Organic semiconductors susceptible to doping such as polyaniline (Ormecon) and PEDOT:PSS are also known as *organic metals*.

Typical current carriers in organic semiconductors are holes and electrons in π-bonds. Almost all organic solids are insulators. But when their constituent molecules have π-conjugate systems, electrons can move via π-electron cloud overlaps, especially by hopping, tunnelling, and related mechanisms. Polycyclic aromatic hydrocarbons and phthalocyanine salt crystals are examples of this type of organic semiconductor.

Mainly due to low mobility, even unpaired electrons may be stable in charge-transfer complexes. Such unpaired electrons can function as current carriers. This type of semiconductor is also obtained by pairing an electron donor molecule and an electron acceptor molecule.

History

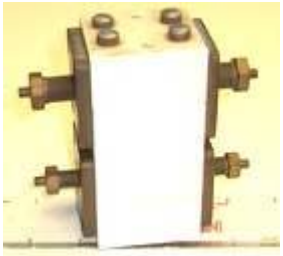

Voltage-controlled switch, an "active" organic polymer electronic device from 1974. Now in the Smithsonian Chip collection.

In 1862, Henry Letheby obtained a partly conductive material by anodic oxidation of aniline in sulfuric acid. The material was probably polyaniline. In the 1950s, researchers discovered that polycyclic aromatic compounds formed semi-conducting charge-transfer complex salts with halogens. In particular, high conductivity of 0.12 S/cm was reported in perylene-iodine complex in 1954. This finding indicated that organic compounds could carry current. In 1972, researchers found metallic conductivity in the charge-transfer complex TTF-TCNQ. Superconductivity in charge-transfer complexes was first reported in the Bechgaard salt $(TMTSF)_2PF_6$ in 1980.

Similar conductivity values in linear backbone polymers (in an iodine-"doped" and oxidized polypyrrole black) were reported in 1963. Highly-conductive polypyrrole was rediscovered in 1979, John McGinness and coworkers subsequently reported a working organic polymer electronic device in 1974.. These investigators reported a high

conductivity "ON" state and hallmark negative differential resistance in melanin, an oxidized copolymer of polyacetylene, polypyrrole, and polyaniline. Melanin is a semiconducting polymer currently of high interest to researchers in the field of organic electronics in both its natural and synthesized forms. This device was a "proof of concept" for their earlier paper in 1972, outlining what is now the classic mechanism for electrical conduction in such materials. In a typical "active" device, a voltage or current controls electron flow. This device is now in the Smithsonian's collection (see figure).

In 1977, Shirakawa *et al.* reported high conductivity in oxidized and iodine-doped polyacetylene. They received the 2000 Nobel prize in Chemistry for "The discovery and development of conductive polymers" . In view of the many previous reports of similar compounds, the "discovery" assignment is contested.

Rigid-backbone organic semiconductors are now-used as active elements in optoelectronic devices such as organic light-emitting diodes (OLED), organic solar cells, organic field-effect transistors (OFET), electrochemical transistors and recently in biosensing applications. Organic semiconductors have many advantages, such as easy fabrication, mechanical flexibility, and low cost.

Processing

There are significant differences between the processing of small molecule organic semiconductors and semiconducting polymers. Thin films of soluble conjugated polymers can be prepared by solution processing methods. On the other hand, small molecules are quite often insoluble and typically require deposition via vacuum sublimation. Both approaches yield amorphous or polycrystalline films with variable degree of disorder. “Wet” coating techniques require polymers to be dissolved in a volatile solvent, filtered and deposited onto a substrate. Common examples of solvent-based coating techniques include drop casting, spin-coating, doctor-blading, inkjet printing and screen printing. Spin-coating is a widely used technique for small area thin film production. It may result in a high material loss. The doctor-blade technique has a minimal material loss and was primarily developed for large area thin film production. Vacuum based thermal deposition of small molecules requires evaporation of molecules from a hot source. The molecules are then transported through vacuum onto a substrate. Condensation of these molecules on the substrate surface results in thin film formation. Wet coating techniques can be applied to small molecules but to a lesser extent depending on material solubility.

Characterization

Organic semiconductors differ from inorganic counterparts in many ways. These include optical, electronic, chemical and structural properties. In order to design and model the organic semiconductors, such optical properties as absorption and photoluminescence need to be characterized. Optical characterization for this class of materials can be done using UV-visible absorption spectrophotometers and photoluminescence spectrometers.

Semiconductor film appearance and morphology can be studied with atomic force microscopy (AFM) and scanning electron microscopy (SEM). Electronic properties such as ionisation potential can be characterized by probing the electronic band structure with ultraviolet photoelectron spectroscopy (UPS). Charge-carrier transport properties of organic semiconductors can be studied by a number of techniques. For example, time-of-flight (TOF) and space charge limited current techniques are used to characterize "bulk" conduction properties of organic films. Organic field effect transistor (OFET) characterization technique is probing "interfacial" properties of semiconductor films and allows to study the charge carrier mobility, transistor threshold voltage and other FET parameters. OFETs development can directly lead to novel device applications such as organic-based flexible circuits, printable radio frequency identification tags (RFID) and active matrix backplanes for displays. Chemical composition and structure of organic semiconductors can be characterized by infrared spectroscopy, secondary ion mass spectrometry (SIMS) and X-ray photoelectron spectroscopy (XPS).

Charge transport in disordered organic semiconductors

Charge transport in organic semiconductors is dependent on π-bonding orbitals and quantum mechanical wave-function overlap. In disordered organic semiconductors, there is limited π-bonding overlapping between molecules and conduction of charge carriers (electrons or holes) is described by quantum mechanical tunnelling. Charge transport depends on the ability of the charge carriers to pass from one molecule to another. Because of the quantum mechanical tunnelling nature of the charge transport, and its subsequent dependence on a probability function, this transport process is commonly referred to as hopping transport. The charge carriers hopping from molecule to molecule are dependent upon the energy gap between HOMO and LUMO levels. Carrier mobility is reliant upon the abundance of similar energy levels for the electrons or holes to move to and hence will experience regions of faster and slower hopping. This can be affected by the temperature and also electric field across the system. A theoretical study has shown that in a low electric field the conductivity of organic semiconductor is proportional to $T^{-1/4}$ and in a high electric field is proportional to $e^{-(E/aT)}$, where *a* is a constant of the material.

Another study showed that the AC conductivity of the organic semiconductor pentacene was frequency-dependent and provided evidence that this behavior was due to its polycrystalline structure and hopping conduction.

Photochemical logic gate

A **photochemical logic gate** is based on the photochemical intersystem crossing and molecular electronic transition between photochemically active molecules, leading to logic gates that can be produced.

The OR gate electron–photon transfer chain

_A* A* = excited state of molecule A
  _B*
    _C*

_A _B _C

The OR gate is based on the activation of molecule A, and thus pass electron / photon to molecule C's excited state orbitals (C*). The electron from molecule A inter system crosses to C* via the excited state orbitals of B, eventually utilised as a signal in the C* $h\upsilon_c$ emission. The 'OR' gate uses two inputs of light (photons) to molecule A in two separate electron transfer chains, both of which are capable of transferring to C* and thus producing the output of an OR gate. Therefore, if either electron transfer chain is activated, molecule C's excitation produces a valid/ output emission.

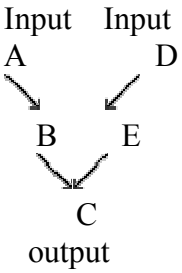

The 'AND' gate

    _C** Second excited state of molecule C
_A*
  _B*
    _C*

_A _B _C

Excitation A⟶A* by $h\upsilon_a$ photon, whereby the promoted electron is passed down to the C* molecular orbital. A second photon applied to the system ($h\upsilon_{c2}$) causes the excitation of the electron in the C* molecular orbital to the C** molecular orbital -analogous pump probe spectroscopy.

_* * Second excited state of molecule C

↑$h\upsilon_{c2}$
_*

↑$h\upsilon_c$

_C

Above, the energy level diagram illustrating the principle of pump probe spectroscopy – the excitation of an excited state. The AND gate is produced by the necessity of both A⟶A* and the C**⟶C excitations occurring at the same time -input hυ and hυ, are simultaneously required. To prevent erroneous emissions of light from a single input to the AND gate, it would be necessary to have an electron transfer series with ability accept any electrons (energy) from C* energy level. The electron transfer series would terminate with a low (non-radiative decay) of the energy The alternatives for producing an AND gate, using molecular photphysics, are two. (1) The emission produced by the electron drop from C*⟶C ($h\upsilon_c$) is not a valid output frequency. The emission from the C** ($h\upsilon_c$ + $h\upsilon_{c2}$, $h\upsilon_{c3}$) molecular orbital is a valid output signal;. to be used in subsequent logic gates -arranged to respond to the C** $\longrightarrow_{c2}$ C emission. The second input of photon(s) to trigger the rapid conversion of a molecule used to complete the electron transfer chain. A very complex molecule like a protein can be engineered to possess high strain energies, so that in the absence of the second light frequency molecule B is inactive (B). The second photon input triggers B⟶B' where the forward rate constant is much smaller than the reverse. If such a molecule is used as molecule B, the transfer chain can be switched on and off.

Creating the NOT gate

To stop the electron transfer chain completing, producing output signals, the input of a photon, $h\upsilon_{c2}$, is used to produce a 'pump probe spectroscopy' effect by promoting an electron in an electron transfer chain. The fall of the pump probe promoted electron produces an output that is quenched down an electron transfer chain.

An alternative is similar to the AND gate alternative; an input causes a change in molecule structure breaking the electron transfer chain by not allowing the smooth energy transfer of electrons.

Poly(*p*-phenylene oxide)

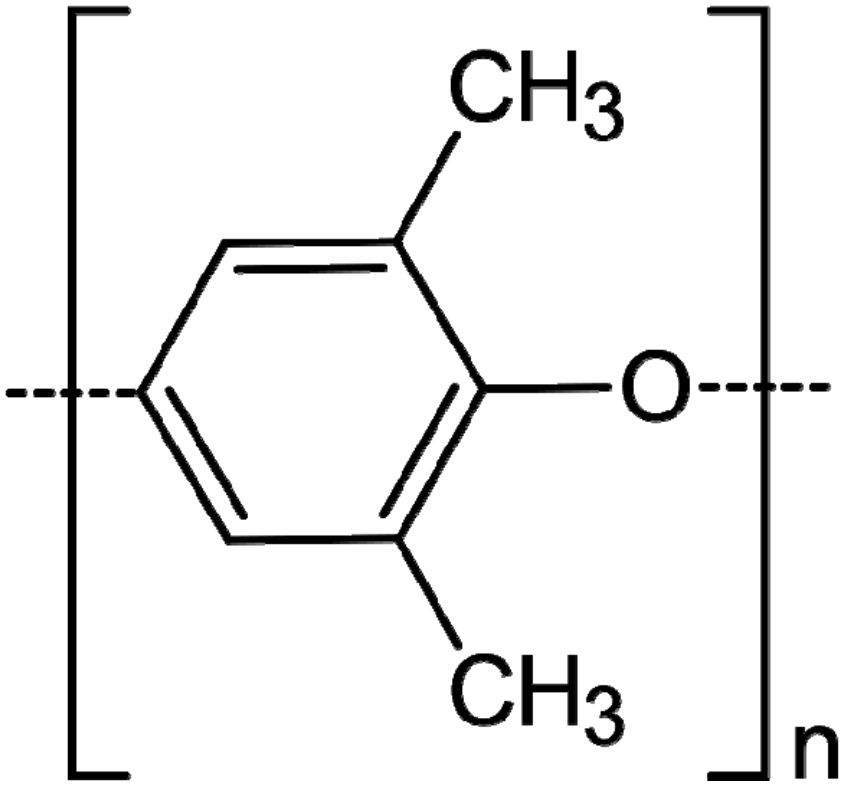

Poly(*p*-phenylene oxide) (**PPO**) or **poly(*p*-phenylene ether)** (**PPE**) is a high-temperature thermoplastic. It is rarely used in its pure form due to difficulties in processing. It is mainly used as blend with polystyrene, high impact styrene-butadiene copolymer or polyamide.

History

Polyphenylene ether was discovered in 1956 by A. S. Hay, and was commercialized by General Electric in 1960. The common name "polyphenylene oxide (PPO)" is incorrect because it is not an oxide but an ether.

While it was one of the cheapest high-temperature resistant plastics, processing was difficult and the impact and heat resistance decreased with time. Mixing it with polystyrene in any ratio could compensate for the disadvantages. In the 1960s, modified PPE came into the market under the trade name Noryl.

Properties

PPE is an amorphous high-performance plastic. The glass transition temperature is 215 °C, but it can be varied by mixing with polystyrene. Through modification and the incorporation of fillers such as glass fibers, the properties can be extensively modified.

Applications

A printer cartridge made of PPE and polystyrene; it is an example of a product which requires good dimensional stability and accuracy to fit

PPE blends are used for structural parts, electronics, household and automotive items that depend on high heat resistance, dimensional stability and accuracy. They are also used in medicine for sterilizable instruments made of plastic.

This plastic is processed by injection molding or extrusion; depending on the type, the processing temperature is 260-300 °C. The surface can be printed, hot-stamped, painted

or metallized. Welds are possible by means of heating element, friction or ultrasonic welding. It can be glued with halogenated solvents or different adhesives.

Super AMOLED

Super Active-Matrix Organic Light-Emitting Diode or **Super AMOLED** is a display technology for use in mobile devices such as mobile phones. It differs from many other display technologies in that the layer which detects touch is integrated into the screen rather than being overlaid on top. The first company known to produce display units of this type is Samsung, when it introduced its Samsung Wave mobile phone on 14 February 2010. The Samsung i9000 Galaxy S series, including the Captivate, Epic 4G, Fascinate, and Vibrant, the Windows Phone 7 Omnia 7 and Focus also use this display. The Nexus S, a smartphone designed by Google and manufactured by Samsung, will be equipped with a 4-inch Super AMOLED screen, and should be available from 16 December 2010.

Compared with the first-generation AMOLED, the Super AMOLED advantages are:

- 20% brighter screen
- 80% less sunlight reflection
- 20% reduced power consumption